



## REVIEW ARTICLE

# Recent progress in MXene and graphene based nanocomposites for microwave absorption and electromagnetic interference shielding



Kishore Chand <sup>a,\*</sup>, Xiao Zhang <sup>a,\*</sup>, Yujin Chen <sup>a,b,\*</sup>

<sup>a</sup> Key Laboratory of In-Fiber Integrated Optics, College of Physics and Optoelectronic Engineering, Harbin Engineering University, Harbin 150001, China

<sup>b</sup> School of Materials Science and Engineering, Zhengzhou University, Zhengzhou 450001, China

Received 12 May 2022; accepted 19 July 2022

Available online 25 July 2022

## KEYWORDS

Electromagnetic interference shielding;  
Microwave absorption;  
Intrinsic conducting polymers (ICPs);  
Graphene;  
MXenes

**Abstract** There is widespread use of telecommunication and microwave technology in modern society, and raised the electromagnetic interference (EMI) issue to alarming situation due to apprehensive demand and growth of 5G technology undesirably disturbing the human health. The two dimensional (2D) materials including graphene and MXenes are already been used for variety of electronic devices due to their exceptional electrical, mechanical, optical, chemical, and thermal properties. MXene is composed of metal carbides, in which mainly metals are the building blocks for dielectrics, semiconductors, or semimetals. However, the strong interfaces with electromagnetic waves (EM) are variable from terahertz (THz) to gigahertz (GHz) frequency levels and are widely used in EMI and Microwave absorption (MA) for mobile networks and communication technologies. The use of different organic materials with metal, organic, inorganic fillers, polymers nanocomposite and MXene as a novel material has been studied to address the recent advancement and challenges in the microwave absorption mechanism of 2D materials and their nanocomposites. In this concern, various techniques and materials has been reported for the improvement of shielding effectiveness (SE), and theoretical aspects of EMI shielding performance, as well stability of 2D materials particularly MXene, graphene and its nanocomposites. Consequently, various materials including polymers, conducting polymers, and metal-organic frameworks (MOF) have also been discussed by introducing various strategies for improved MA and control of EMI shielding. Here in this comprehensive review, we summarized the recent developments on material synthesis and fabrication of MXene based nanocomposites for EMI shielding and MA. This research work is a

\* Corresponding authors.

E-mail addresses: [kishor.vallasai@gmail.com](mailto:kishor.vallasai@gmail.com) (K. Chand), [zhangxiaoch@hrbeu.edu.cn](mailto:zhangxiaoch@hrbeu.edu.cn) (X. Zhang), [chenyujin@hrbeu.edu.cn](mailto:chenyujin@hrbeu.edu.cn) (Y. Chen).  
Peer review under responsibility of King Saud University.



comprehensive review majorly focuses on the fundamentals of EMI/MA. The recent developments and challenges of the MXene and graphene based various structures with different polymeric composites are described in a broader perspective.

© 2022 The Author(s). Published by Elsevier B.V. on behalf of King Saud University. This is an open access article under the CC BY-NC-ND license (<http://creativecommons.org/licenses/by-nc-nd/4.0/>).

## 1. Introduction

The revolution of science and technology impressively enhanced the daily lives and altered their way of living standards. Fast-growing technology and recent advancements resulted in the spread of microwave and radio frequency (RF) communications systems during the last few years led to massive growth and increased the use of electronic devices in everyday life (Zhi et al., 2017). The larger intensity and huge amount of electromagnetic waves are released in the form of radiation and heat energy in the environment and become a great challenge of the new world (Zhang et al., 2016; Cao, 2022). During the last several decades, the recent progress in wireless mobiles communication and other electronic devices including (mobile phones, laptops) wireless antennas increased pollution and are the major source of microwave and other radiation (Russell, 2018). The rapid development of technology and growth of wireless technologies resulted in the continuous release of harmful microwaves, electromagnetic signals and heat dissipation (Zamanian, 2005; Cao, 2021). The excessive use of different electronic devices influence our daily life and may also cause severe health problems/issues. The electromagnetic waves are the major cause of typical indoor and outdoor environment pollution, which adversely influencing the life of common peoples due to which the human life and health are at higher risk. The use of such electronic devices requires special care to protect from the electromagnetic waves and should be capable to shield effectively to protect life and reduce the risk to the environment (Li, 2019). The harmful effect placed life of common people on tip of the sword; due to the excessive use of e-appliances in different fields of everyday life for example medical devices, home appliances, satellites, radar, automobiles, and military purposes (Li, 2019). Conventional metallic materials are suitable due to their high EMI shielding performance, electrical and thermal conductivity (Hao et al., 2020). Although due to recent technological development there is an increasing demand of lightweight, highly durable and flexible device for microwave and EMI shielding. Metal organic framework (MOF) based shielding materials are being gradually replaced by some organic materials and various polymers to develop microwave and EMI shielding nanocomposites (Shu et al., 2021). Nonetheless, the polymer composites have certain limitations; as EMI shielding materials require significant proportions of fillers required to be used for the development of such nanocomposites; which can retain EM waves and demonstrate EMI shielding efficiency (SE) (Wanasinghe et al., 2020; Guo et al., 2020). Several studies has been performed to produce such nanocomposites and to understand and estimate the impact of fillers on mechanical durability; fragility of the highly flexible and low permeable films by using simple hot pressing method (Kim, 2021; Li, 2021).

Hence, the two-dimensional (2D) materials are not only solving these problems, but also provide a possible breakthrough by solving the higher loading of different (MOF) and organic fillers in the polymer based composite assemblies. Generally, the metal organic framework based composites are more rigid and less flexible; whereas the developed polymer based films, foams and fibrous assemblies are an alternative solution, which could reduced the mixing of metals as a shielding materials (Wang et al., 2021; Qu et al., 2016). Consequently, the use of such polymeric composites containing different organic materials; for example carbon black (CB) and graphene and MXene have been used for the development of shielding materials with enhanced mechanical, electrical and thermal properties towards an improved EMI shielding efficiency (SE) (Chen, et al., 2021).

Therefore, the use of 2D materials has been increased in recent years due to their increasing demand for flexible wearable electronic devices. The 2D materials are considered as potential candidate for microwave and EMI shielding; due to their several attributes including, chemical, physical and mechanical properties (Hong et al., 2020). Even though, the synthesis of 2D materials is made through chemical, mechanical and physical etching; whereas the chemical exfoliation is strongly recommended for separation of graphite and MXene (Metal Carbides) solid layers as presented in Fig. 1a, b and c respectively (Li, 2021). Beyond graphene, MXene is well known and a new material in the family of 2D materials, and composed of favorable structural composition; due to its special features including higher electrical conductivity and specific surface areas and sufficient reactive functional groups; which makes it an appropriated and suitable material for MAs and EMI devices (Ma et al., 2021; Oliveira and Gusmão, 2020).

MXene is considered as a suitable material due to its diverse structural composition and bringing groups; with in and out of plane order of the metal carbides (MXene) (Hong et al., 2020). Thus the fabrication methods and synthesis graphene and MXene for flexible polymer based composites are revealed suitable for EMI shielding and MA as well as other enormous potential applications in aerospace and wireless communications. Recently several research efforts have been made to overcome the effect of electromagnetic and microwave radiations on human life. Therefore, new materials have been introduced to improve the MA and EMI shielding effectiveness (SE). The 2D materials have been proved as highly efficient and potential candidate for several applications including energy storage, harvesting; effective EMI and MA shielding effectiveness (Ren, 2021). Predominantly, the 2D materials exhibit significant performance against EMI shielding and MA shielding effectiveness is attribute to interfacial polarization and surface polarization due to the induced reactive functional groups on the surface. The mixing of different MOF with graphene and MXene films varying in size, thickness of the films and single to few layered structure (Zhang, 2021). Although, in the case of multiple layered hetero-structures including the first outermost layer and the second layer may be designed in such a way that could potentially absorb microwaves and reflect the EM waves. The designing of such porous assemblies for example 3D porous and polymeric composite structures intensively dissipate the microwaves and electromagnetic waves over wider range of frequency ranging from 12 to 20 GHz (Pan et al., 2021). Conversely, in the composite layered assemblies the inner (core) layer is designed with highly conductive porous compounds, whereas on the other hand the upper and bottom layers are made up of conductive polymeric metallic compounds for example silver and copper; which assists in conduction and reflection loss in the designed composite assemblies (Zhang and Gu, 2022; Liang et al., 2021). Even though, the layer by layer (LbL) approach and self assemblies with organic fillers have been used to improve the MA and EMI (SE). The carbonous compounds include carbon nanotubes (CNTs), graphene, MXene and boron nitride (hBN) to significantly retain the EM waves released from the second absorbing layer in such a way that, substantial SE is attained (Zhang, 2022). Nonetheless, the MXene and 2D materials with MOF and filler based heterostructures in combination with various polymers are designed for self-assembly made from aqueous solution by using vacuum filtration, heat pressing are most widely used and most exciting methods. On the other hand, the large-scale environmentally friendly synthesis of MXene and graphene is facing several challenges and are still under investigation for the potential use in various technologies (Ma et al., 2021). Nevertheless, during the synthesis

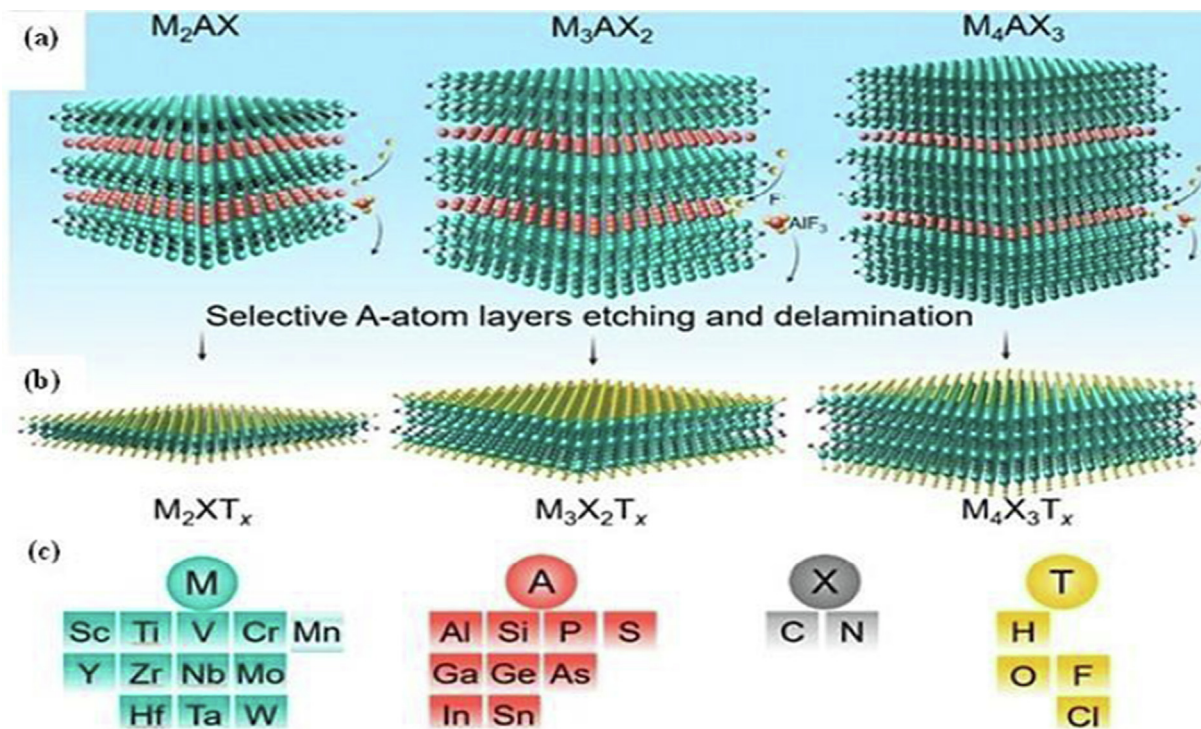


**Fig. 1** Presentation of various metal Carbides (MAX)-Phase (a) into 2D MXenes (b) showing metal carbides M–A–X–T in (c); reproduced with copy right material Springer, 2020 (Hong et al., 2020).

of 2D materials for the development of the various structural assemblies and surface modification may include resulting defects induced polarization, which could pave the new ways to predict the conductive loss, magnetic loss in conductive, semi-conductive, insulating, and ferromagnetic materials of the developed nanocomposites (Miao, 2022). However, the MXene and its derivatives are mechanically strong, environmentally stable and highly conductive; which significantly influences the performance of highly flexible and wearable electronics devices against various applications including supercapacitors, batteries, filtration as well as microwave MA and EMI-SE (Khan, et al., 2020). The progress in the synthesis of 2D materials including preparation of metal carbide (MXene), and graphene by using various approaches for example vacuum filtration (Raagulan et al., 2020), freeze drying (Rajavel et al., 2020), vapor phase polymerization (VPP) (Khan, et al., 2020), chemical exfoliation (Zhang, 2020), and chemical vapor deposition (CVD) (Zhang et al., 2019). However, these methods still needs some improvements for the fabrication and integration of MXene, graphene and other 2D materials for the development of such wearable electronic devices by using recent techniques made on micro to nano scale (Xu, et al., 2021). The polymer-based nanocomposites of 2D materials could improve the EMI shielding and are highly efficient materials; which could potentially overcome or reduce the shortcomings of traditional shielding materials; due to their unique and superior performance (Zhang et al., 2019).

## 2. Working principle

Multiple relaxation are promising and systematic approach for broad band and strong electromagnetic wave (EMW) absorption behaviour; which is based on interphase, defects induced, and surface charge with controlled EM attenuation. According to theory of Schelkunoff; the SE mechanism of EM waves are based on conduction, dielectric, absorption, reflection,

magnetic and eddy current losses (Verger et al., 2019). The tuning of electrical, thermal conductivity and magnetic properties are related to shielding materials to enhance shielding performance. The other factors including the variable size, shape and porosity of the material assembly towards abortion, reflection and diffraction of the incident waves (Geng and Yang, 2018).

### 2.1. EMI shielding mechanism

Several studies have been made in recent years on the theoretical hypothesis and computational models towards the prediction of EMI shielding attributes of such complex multiphase composites. These structures are still challenging for the improvements of films, 2D and 3D foams, majorly concerned to the structural processing and fabrication of the nanocomposites towards maximizing the EMI shielding and MA efficiency (Cheng, 2022). Therefore, it is important to control both of the interferences i.e MA and EMI from common electronic devices, home appliances, industrial equipment, and medical care instruments to make necessary strategic systems to develop such novel and efficient materials; which not only protect from the released EM waves but should be cost-effective as well as flexible, light weight, user friendly, and eco-friendly (Liang et al., 2021).

As the Fig. 2 (a) shows an absorbed and multiple reflected microwaves with interfacial polarization, conduction, dielectric and magnetic loss as a principle and mechanism factors influencing EMI & MA mechanism. Moreover, the future trends in the design and development of 2D materials for microwave and EMI shielding could replace the metal-based

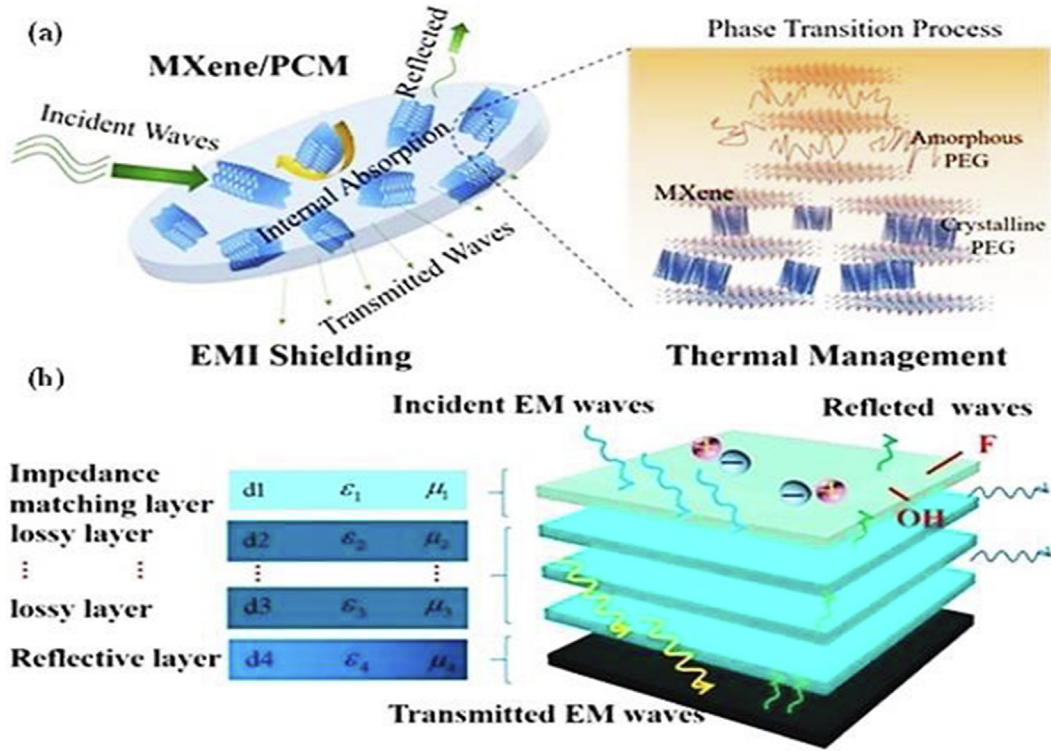


**Fig. 2** In-situ-synthesized graphene and MXene based phase change Materials (PCM) segregated films for EMI Shielding mechanism (a); reproduced with permission copy right material Elsevier, (2021) (Ji, 2021), layered structure for microwave absorption (MA) mechanism (b); reproduced with permission of copy right material, Elsevier (2021) (Ji et al., 2021).

shielding materials, with low reflection and high absorption. The microwave and EMI shielding are generally related to higher electrical and thermal conductivity; which results in strong EMI-SE through conduction and reflection of EM waves as presented in Fig. 2 (a & b) respectively (Wang et al., 2021; Ji, 2021). Eventhough, the microwave and EMI pollution can be significantly reduced by improving the shielding performance through absorption and reflection of electromagnetic waves; but still there is a huge research and there is an urgent need of such novel materials that could have low-reflection and high-absorption properties (Liu, 2021). These attributes may be assigned to novel 2D materials; with enhanced shielding effectiveness as compared to common metal such as MOF based polymeric nanomaterials (Zhao, 2021). Furthermore, the properties of the 2D materials including MXene may also be improved through the addition of different inorganic fillers on the cellular level to design and develop less permeable hetero-structures (Bhuvanesh Kumar and Sathiya, 2021). Keeping, in view these considerations; new systematic approaches are still required to develop such composite assembly, that could have better-shielding performance, for example in 3D assembly the graphene and MXene sheets can be sandwiched inside the polymeric films to improve the shielding performance of the resultant nanocomposite (Iqbal et al., 2020). In brief, the next-generation 2D materials and their nanocomposites made of various orientations including segregated, sandwiched and porous assemblies loaded with fillers in the polymeric films may enhance the shielding (SE) performance of the nanocomposites. In, such assemblies, the first layer is designed by layer by layer (LbL) structure of poly-

meric materials to avoid the microwaves propagation and reflection respectively (Chen et al., 2021).

The electrical conductivity of the material in the polymer-based nanocomposites is an important factor; that significantly influence the overall SE of the materials (Chen et al., 2021). The structural assembly significantly improve the electromagnetic waves absorption as a shielding structure. The second foremost factor is the high cost that restricts the broader use of EMI shielding and MA absorption materials (Abdolhosseinzadeh et al., 2021). The current status and development of the 2D nanomaterials showed significant improvements in recent years by introducing several special properties, such as magnetic, electrical, thermal and tremendously strong mechanical attributes towards an improved MA or reflection (Gunda, 2021). The free space technique is used to restrain the reflection loss ( $R_L$ ) of the microwave. The  $R_L$  value is generally measured by continuous sweeping of the frequency range from 2 to 18 GHz. The reflectivity is given by Eq. (1);

$$R_L = 10 \log \frac{P_1(f)}{P_0(f)} \quad (1)$$

Whereas, the “f” is the frequency,  $P_1(f)$  and  $P_0(f)$  are presented as power reflected by the metallic plate as base material and sample placed on the metallic base plate, respectively.

The shielding performance (SE) is measured in terms of reflection loss and transmission loads by using the Eq. (1) and Eq. (2) respectively (Yuan et al., 2018; Quan, 2018).

$$R_L = 20 \log \left| \frac{Z_{in}(N) - Z_0}{Z_{in}(N) + Z_0} \right| \quad (2)$$

Where;  $Z_0$  is free space impedance level,  $Z_{in}(N)$  is input impedance value of the RAMs can be expressed by Eq. (3);

$$Z_{in}(N) = Z_c(N) \frac{Z_n(N-1) + Z_c(N) \tan_h \gamma(N) d(N)}{Z_c(N) + Z_{in}(N-1) \tan_h \gamma(N) d(N)} \quad (3)$$

Where  $Z_c(N)$ ,  $g(N)$  and  $d(N)$  are the three different characteristics i.e impedance, propagation constant and width for number of layers ( $N$ -layer), respectively.

According to the metal back model and line theory used for transmittance or reflectance in which, the  $R_C$  can be achieved by using Eq. (1–4). However, for two or more than two layered composite assembly; consider the upper layer as open to air and second layer lying between the metal back plate and the first layer can be expressed as following Eq. (4) (Yuan et al., 2018).

$$R = 20 \log_{10} \left( \frac{Z_1 - 1}{Z_1 + 1} \right) \quad (4)$$

Where  $R$  is reflection and  $R_C$  is reflection of proposed material and expressed in dB; and  $Z_1$  is the normalized impedance level for the first layer, and calculated by Eq. (5–8).

$$Z_2 = \eta_1 + \left[ Z_2 + \frac{\eta_1 \tanh(\gamma_1 d_1)}{\eta_{1+Z_1} \tanh(\gamma_1 d_1)} \right] \quad (5)$$

$$Z_2 = \eta_2 \tanh(\gamma_2 d_2) \quad (6)$$

$$\eta_i = \sqrt{\frac{\mu_i}{\epsilon_i}} \quad (7)$$

$$\gamma_i = \frac{j2\pi f}{c} \sqrt{\mu_{ri} \epsilon_{ri}} \quad (8)$$

Where;  $Z_2$  is normalized impedance level of the second layer,  $\eta_i$  is the intrinsic level of impedance of second layer  $i$ ;  $\gamma_i$  is the propagation constant of layer  $i$ ; and  $d_i$  is the thickness of layer  $i$ ; similarly  $f$  is the frequency of the EM waves;  $\epsilon_i$  and  $\mu_i$  are the relative complex permittivity and permeability of the layer  $i$ , respectively; and  $c$  is the speed of light in vacuum free space (Yan, 2018; Yan, 2018).

## 2.2. Microwave absorption mechanism

However, the microwave absorption mechanism is defined under the alternating electromagnetic fields. Whereas, the microwave energy cannot be stored but also can be changed or converted into heat energy during the energy conversion and the amount of energy to be absorbed represented as ( $E$ ). The process may be further divided into two components one is stored energy ( $E_1$ ), and the other is converted energy ( $E_2$ ) respectively. These energies can also be transformed to thermal energy and electrical energy (Yan, 2018). The storage efficiency is presented as ( $W_s$ ) and calculated by using following formula i.e ( $W_s = E_1/E$ ). In which, the  $W_s$  value of an absorbents ranges over 2–18 GHz, which indicates the high energy storage ability of the microwaves by the shielding material or system. Secondly, the ratios of both of the energies i.e  $E_1$  to  $E_2$  ( $W_r = E_1/E_2$ ) is used for presentation of energy storage capacity, which is better, than that of the conversion capacities. Thirdly, the microwave energy conversion efficiency is presented and calculated from the following equation which is also the ratio of both of energies ( $W_d = E_2/E$ ) which demonstrate that, the most of the microwave energy is converted into

heat energy (Yan, 2018). The Debye theory describe, that the converted microwave energy is achieved from the conduction ( $E_c$ ), polarization ( $E_p$ ) and magnetic losses ( $E_m$ ) can be calculated from the following Eq. (9).

$$E_2 = E_c + E_p + E_m \quad (9)$$

The overall efficiency of the system can be calculated from the converted microwave energy which is obtained from the conduction ( $W_c$ ), polarization ( $W_p$ ) and magnetic losses ( $W_m$ ). The efficiency can be expressed as: in Eq. (10–12).

$$W_c = \frac{E_c}{E_2} = \frac{P_c}{P_2} = \frac{P_c}{P_c + P_p + P_m} \quad (10)$$

$$W_p = \frac{E_p}{E_2} = \frac{P_p}{P_2} = \frac{P_p}{P_c + P_p + P_m} \quad (11)$$

$$W_m = \frac{E_m}{E_2} = \frac{P_m}{P_2} = \frac{P_m}{P_c + P_p + P_m} \quad (12)$$

Whereas;  $P_2$ ,  $P_c$ ,  $P_p$  and  $P_m$  describes, the different powers of the converted, conduction, polarization and magnetic losses, respectively and can be calculated from the Eq. (13–15).

$$P_c = \frac{\omega}{2} \epsilon_c E_0^2 \quad (13)$$

$$P_p = \frac{\omega}{2} \epsilon_p E_0^2 \quad (14)$$

$$P_m = \frac{\omega}{2} \mu H_0^2 \quad (15)$$

Whereas, the Greek word omega ( $\omega$ ) is used to present the angular frequency,  $E_0$  and  $H_0$  are the electric and magnetic field intensity or amplitude of microwave.

### 2.2.1. Magnetic–Dielectric synergy

The magnetic and dielectric synergetic effects are critical factors and components for EMI shielding and microwave absorpton. The combination of dielectric as well as magnetic attributes of the developed composite could be attained by the impedance matching. The reduction in surface reflection of electromagnetic wave absorption with strong attenuation capacity of an incident waves which contributes an excellent absorption effectiveness (Saini and Aror, 2012). The study can be made on impedance matching; and calculated through Eq. (13) and Eq. (14).

**Impedance Matching:** The EMI shielding and microwave absorption can be indicated through “ $\mu_r$ ” value to the “ $\epsilon_r$ ” the values for the higher reflection loss ( $R_L$ ) response. Therefore, the complementary example lies between dielectric and magnetic loss; which has been previously reported, showing that, the moderate EM parameters of Carbon and nickel C–Ni composites resulted as  $Z$  value over a wide range of bandwidth. The results are corresponds to a broadband EMI and MA absorption. It has been revealed that enhanced EM wave absorption of Co/ZnO/C based composites was attained by the metal–organic framework (MOF) primarily beneficial and satisfactory balance between the dielectric and magnetic attributes of each component as counter part of the composite (Saini and Aror, 2012). The second and foremost common factor is attenuation capacity of the composites for betterment of the shielding performance amongst the magnetic and dielectric loss as synergetic effect.

**Attenuation Capacity:** The property is measured by using the Equation the attenuation capability of a magnetic–dielectric based composite shows a stronger effect than the dielectric and magnetic constituents. However, a critical component among the core and shell composites is excessively higher with dielectric loss. Despite of that, the developed nanocomposite showed a reasonable attenuation capability and their impedance matching can barely studied, leading to a narrow EAB. Whereas, according to the design of EM wave absorbent materials in the nanocomposite assembly certainly requires rational dielectric retention to accomplish the reasonable steadiness and stability between the frequency dispersion (Fd) properties of dielectric and magnetic spectra. Furthermore, several new strategies has been practiced and used for enhancing the magnetic loss tangent; whereas, improvements made in the dielectric attributes to the metal organic framework, which are remarkably anticipated for the better impedance matching (Saini and Aror, 2012). Within microwave frequency bands, dielectric polarization includes both interfacial and dipolar mechanisms. The dielectric properties are based on polarization and conduction attributes. Within a microwave frequency bands are related to dielectric polarization which comprising the interfacial, dipolar, and defects induced polarization mechanism. However, the polarization is raised with interfacial charge, when heterostructured assemblies consisting of dielectric attributes with reorganization of the dipoles. However, the conduction loss in low-dimensional materials are responsible for the transport mechanism with more conductive paths and the electron hopping effect as defects induced barriers, and can be determined from the increase or decrease of the filler contents and carrier mobility.

Additionally, the dipolar polarization and dielectric mechanisms are correlated to the several induced defects on the surface of low dimensional materials and which is quite interesting where as the functional groups works as work function due to the presence of these reactive species on the surface of two dimensional materials may improve interfacial bonding between two different counterparts. However, on the other-side, the large specific surface area may also assists in the enhancement of polarization of electromagnetic wave with exceptional electrical conductivity in low dimensional and two dimensional materials. Therefore, due to excellent conductivity the 2D materials, such as graphene and MXene, can introduce a great impact on the dielectric attributes and the conduction loss. The geometrical shapes could also influence these polarization effects, such as in 1D materials with higher anisotropy aspect ratio, chirality, and plasma resonance resulting in multiple scattering. However, the polarization is greatly influence by the propagation behavior of the incident EM waves, which leads to an additional EM energy loss. Keeping in view these factors in consideration the 2D materials showed an exceptional behavior which resulted as increased demand and potential use of dielectric materials in the field of EM shielding and microwaves absorption (Saini and Aror, 2012).

### 2.2.2. Magnetic loss

The magnetic loss in the 2D, and 3D nanocomposites structures are totally dependent and based on the size confinement. Whereas, the frequency dispersion includes, the complex permeability in the low dimensional materials containing the magnetic attributes. The properties are generally characterized by

four main mechanisms: domain-wall motion, natural resonance, exchange resonance, and eddy current. In which, the magnetic domains are based on geometrical and morphological arrangement, size, shape, crystal size, crystal, structure and growth; which work as external magnetic field. Whereas, the higher electrical conductivity of such low dimensional MOF and metal complexes containing magnetic characteristics could enables the cohort of eddy currents and can potentially reduce the magnetic loss capacity. The such contrivancies among the 2D and low dimensional materials demonstrates that the low dimensional materials in terms of surface morphology, size, and crystalline nature could greatly be used to fine tune the magnetic loss capacity. Subsequently, the optimistic impedance matching and attenuation capacity are also considered as key factors for improved MA and EMI shielding effectiveness (Saini and Aror, 2012).

### 2.2.3. Dielectric loss

Furthermore, to clarify the mechanism, the electromagnetic parameters including the real ( $\epsilon'$  and  $\mu'$ ) and imaginary parts ( $\epsilon''$  and  $\mu''$ ); wherein  $\epsilon'$  and  $\mu'$  represent the storage capability of electric and magnetic energies, respectively. However, the values " $\epsilon''$ " and " $\mu''$ " denote the dissipation capability of electric and magnetic energies, respectively. Generally, the dielectric loss of the aerogels materials is attributed to polarization relaxation and conduction losses ( $\epsilon_p''$  and  $i''$ , respectively), because of the uniform incorporation of a ferromagnetic component from the dielectric rGO aerogels. The negative  $\mu''$  value indicates that the magnetic energy from the induced magnetic field of the materials is transformed into the electric energy (Saini and Aror, 2012).

Generally, the magnetic loss is attributed to the eddy current and magnetic resonance loss (natural and exchange resonance). The eddy current loss is evaluated using Eq. (16) and Eq. (17).

$$\mu'' \approx \frac{2}{3\pi\mu_0\mu'2\sigma d^2 f} \quad (16)$$

$$C_0 = \mu''\mu' - 2f - 1 = 23\pi\mu_0\sigma d^2 \quad (17)$$

Whereas; " $\mu_0$ " denotes the vacuum permeability; " $C_0$ " is positively correlated with " $d^2$ " and " $\sigma$ " (conductivity). The " $C_0$ " value is almost stable in the range of 14–18 GHz in the  $C_0 - f$  curves, indicating a magnetic loss from the eddy current loss. In contrast, magnetic loss will be generated from natural resonance loss.

While; the eddy current loss is the dominant factor at frequencies of 9–18 GHz. Therefore, a good impedance matching means that more incident microwaves penetrate into the materials rather than being reflected, thus guaranteeing ultra-efficient MA properties. The impedance matching characteristic can be described as the Eq. (18) and Eq. (19) (Saini and Aror, 2012).

$$Z_{in} = Z_0 \mu_r \epsilon_r \sqrt{\tanh [j(2\pi f d c) \sqrt{\mu_r \epsilon_r}]} \quad (18)$$

$$Z_{in} = Z_0 \mu_r \epsilon_r \tanh j2\pi f d c \mu_r \epsilon_r \quad (19)$$

Where  $Z_{in}$  represents normalized input impedance of the absorbers,  $Z_0$  refers the free space impedance,  $f$ ,  $d$ ,  $c$ ,  $\mu_r$ , and  $\epsilon_r$  are the frequency, thickness, velocity of electromagnetic waves in free space, complex permeability, and complex per-

mittivity of the absorber, respectively. The attenuation constant “ $\alpha$ ” is another vital factor for excellent MA performance and reflects synergetic dielectric and magnetic loss capacity. The value of  $\alpha$  can be expressed as the following Eq. (20).

$$\begin{aligned} \alpha &= 2\sqrt{\pi f c} \times (\mu \varepsilon'' - \mu' \varepsilon') + (\mu'' \varepsilon'' - \mu' \varepsilon')^2 \\ &\quad + (\mu' \varepsilon'' + \mu'' \varepsilon') 2\sqrt{\alpha} \\ &= 2\pi f c \times \mu'' \varepsilon'' - \mu' \varepsilon' + \mu'' \varepsilon'' - \mu' \varepsilon'^2 + \mu' \varepsilon'' + \mu'' \varepsilon'^2 \end{aligned} \quad (20)$$

Where “ $f$ ” and “ $c$ ” are the frequency and electromagnetic waves in free space, respectively. The “ $\alpha$ ” values is increased by increasing the frequency levels. Noticeably, the “ $\alpha$ ” values of the composites films are much higher than those of pristine films in the entire frequency range, demonstrating their stronger dissipation capacity to electromagnetic waves. The higher “ $\alpha$ ” values are attributed to enhancement of dielectric loss and magnetic loss in composites. Among them, the dielectric loss plays an important role for increasing attenuation ability of the developed composites. It should be pointed that the high  $\alpha$  values and excellent  $Z$  are mutually exclusive and difficult to obtain simultaneously for single carbon-based materials (Saini and Aror, 2012).

### 2.3. Development of composite structures

The study made on carbonous aggregates, porous foamed 3D architectures with magnetic ferric oxide  $\text{Fe}_2\text{O}_4$  components were made-up by using a solvothermal method and has been used as an alternative and cost effective microwave absorbing material. The porous composites were developed through carbonization approach, at variable temperature range and etching agent potassium hydroxide. The established porous assembly distinctly enhanced the (MA performance. It is revealed from the studies, that the  $\text{Fe}_2\text{O}_4$  particles were found to be evenly distributed and attached to the porous carbonous framework as an aggregate. The lightweight highly conductive bio-char-like permeable network showed an improved dielectric loss. The ferric oxide ( $\text{Fe}_3\text{O}_4$ ) nanoparticles have higher magnetic loss properties when fabricated as spongy like carbonous complexes showed an exceptional (MA) performance (Quan, 2018; Zhang, 2022). The designed uniform, segregated and foam/porous structures are demonstrated in Fig. 3 (a). The developed framework had a reasonable dielectric and magnetic loss attributes; and owned the better microwave absorption performance with a RL of  $-51.6$  dB over a frequency of  $13.6$  GHz. The highly efficient microwave absorption was observed (below  $-10$  dB) with a bandwidth of  $5.8$  GHz (ranging from  $11.9$  to  $17.7$  GHz) with a thickness of  $2$  mm.

#### 2.3.1. Uniform layered structure

The layered structure favors multiple reflected and scattered waves among contiguous sheets due to the absorption caused by reflection, conduction and interface/dipole polarization loss at the material surface, and the resulting composite films have excellent performance at  $8.2$ – $12.4$  GHz demonstrating the high EMI-SE of  $37.1$  dB over the frequency range of  $8.0$ – $18.0$  demonstrated in Fig. 3 (b) (Liu, 2021). Additional the EMI shielding ability is sound preservation in extreme situations for example high temperature, acid/salt based solution, with long-term sturdiness. In addition, the parameters are generally based on its stable and excellent electrical conductivity, & exhi-

bits fast, stable joule heating performance, which shows that, the higher thermal stability and deicing effect are required under practical working conditions (Liu, 2021).

#### 2.3.2. Segregated structure

The designing of layered structures for electromagnetic and shielding materials is easier and highly flexible assemblies as compared to segregated and foam structures. Therefore, the use of developed such multiple to few layered structures on flexible, sheets films of polymeric materials and fibrous materials is highly anticipated for shielding against the different wearable electronic devices. These 2D material based composite assemblies have unique properties and suitable for shielding effectiveness due to their multiple layers as a dual functionality, in which each layer works its own real time functionality, for example reflection, absorption, conductivity, and EMI shielding performance as demonstrate in Fig. 3 (c). The absorption and reflection loss are key factors being considered as dual nature of the materials toward an improved or reduced electrical, and thermal conductivity; which results an enhanced SE value. The shielding materials with different assemblies varying shape and size from 0D to 3D, these structure shows great impact on EMI shielding performance, the structural shapes are demonstrated in Fig. 3 (c), reflection and transmission of an incident waves; which is caused by the conduction and reflection loss mechanism between different layers of the segregated nanocomposite structures (Liu, 2021).

#### 2.3.3. Foam structure

Likewise, the segregated structural arrangements, the establishment of highly conductive porous assemblies are needed to be designed from various 2D materials, with heterogeneous structures when mixed together with polymers, conductive polymers and metal organic frameworks. In, such assemblies, the polymer loaded with different content percent of 2D materials and MOF work as filler in the form of multidimensional gradients ranging to 0D, 1D, 2D and 3D in a foam structure as demonstrated in Fig. 3 (c). The properties of each nanocomposite in the assembly can be fine tuned and optimized by variation in parameters for example, shape, size and conductive paths, with variable loading of fillers as demonstrated in Fig. 3 (c). However, higher electrical conductivity is attained by varying the filler content percent, to reduce or overcome the limitation of the forces of interaction between conductive polymers and filler (Liu, 2021). The composition of different nanocomposite and polymer matrix with variable filler content percent is demonstrated in Table 1.

The required parameter are achieved by dispersion of CNT and other fillers which comprise several available reactive sites. Secondly, the higher conductive paths are introduced with strong adhesion and interfacial bonding; which is due to the presence of reactive functional groups on the surface of GO and the “ $\pi$ - $\pi$ ” conjugation between polymer and carbon based materials as filler. The designed syntactic foam structure showed an average EMI shielding efficiency (SE) of  $28.2$  dB, with a density of  $0.02$  g  $\text{cm}^{-3}$ . Whereas, in the developed multilayered assembly each individual porous unit cell has a higher interfacial interaction between each other, resulting as strong mechanical compressibility and higher absorption of EM waves at available cavities as well as the deflection of the incident waves as presented in Fig. 4 (a-e) respectively (Liu, 2010).

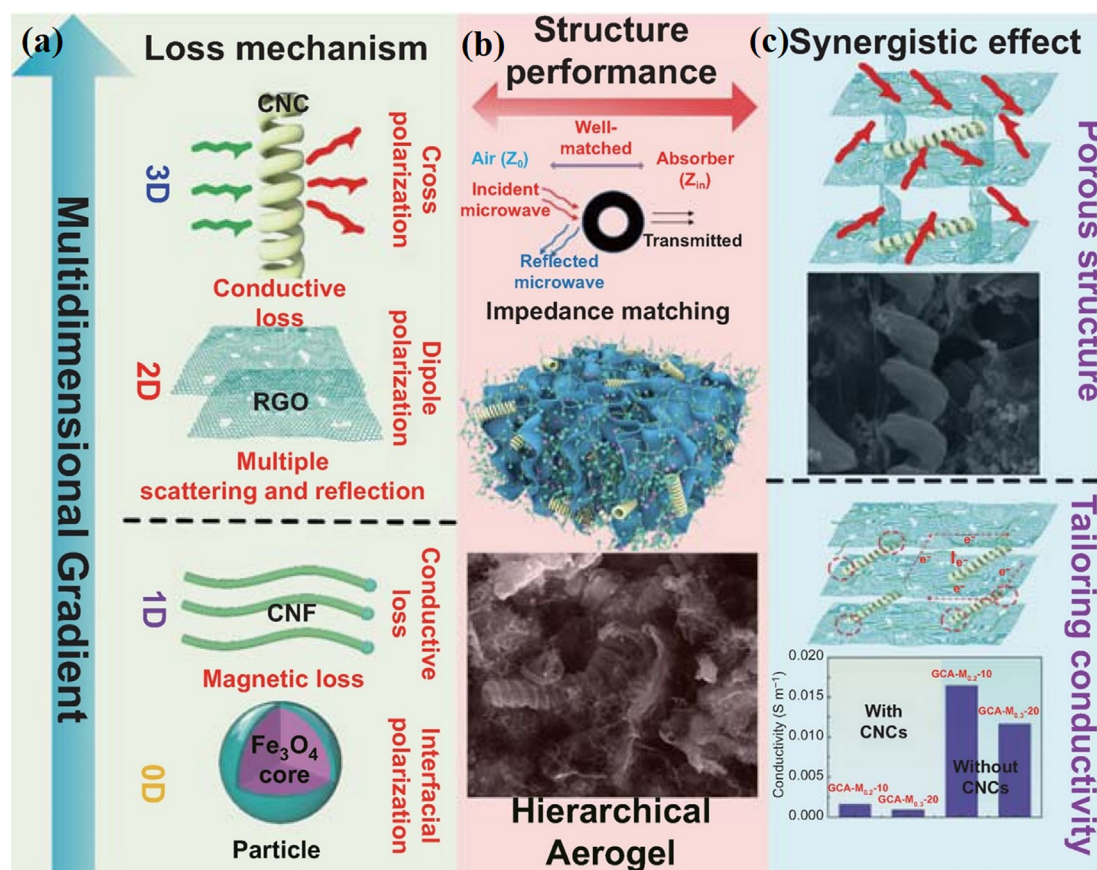


**Fig. 3** EMI shielding loss mechanism in development of multifunctional 3D composite aerogel structure (a), structural performance of herarchical aerogel structure (b), synergistic effect in 0D-3D porous structure showing conductivity for multifunctional gradient (c), reproduced with copyright materials from the Springer Nature (Zhao et al., 2021).

**Table 1** Different composite network structures with variable filler content percent and shielding performance (H, 2021).

Structure	Composite network	Filler Content W%	EMI SE <sub>T</sub> [dB] dB cm <sup>3</sup> g <sup>-1</sup>
Uniform	PVDF/MWCNT	5.0	35.0
	MWCNT/Fe <sub>3</sub> O <sub>4</sub> /PLA	15 0.0	22.0
Segregated	CEMS/SnBi58	50.5	72.0
	CNT/PE	5.5	46.6
	Ag/PLA	5.99	50.0
Layered	TPU/FRs/CNTs	4.0	38.5
	MXene/PU	7.5	20.0
Foam	TPU/rGO	3.17	21.8
	EP/NCCFs	5.03	77.0

In present work proposed for the microwave frequency 2–18 GHz x-band, to overcome such broader challenge, a high-efficient material has been reported so far and the absorption mechanism was attained over a band of (greater than 7 GHz). The size dependency of the composite exhibited an improved microwave absorption with a thickness (<3 mm). The proposed work demonstrates a new strategy to accomplish lightweight and highly efficient microwave absorption materials in the form of porous foam structures. The three-

dimensional (3D) carbon foam (BNA/3dCF) was prepared from carbon loaded cobalt in organic solvent and water by using simple hydrothermal technique (Wei, 2022). A hollow carbonous spheres were made from Nb<sub>2</sub>O<sub>5</sub>@SHCs with unique attributes and morphological structure. The Nb<sub>2</sub>O<sub>5</sub>@SHCs with rambutan-like morphology were synthesized using a simple hydrothermal method. The electromagnetic wave absorption performance of Nb<sub>2</sub>O<sub>5</sub>@SHCs was significantly improved due to high reflection losses (R<sub>L</sub>) and effective absorption bandwidths (EAB, R<sub>L</sub> < -10 dB). The minimum reflection loss (R<sub>Lmin</sub>) of a 3.25 mm substrate is 52 dB, while the maximum EAB of a 2.8 5 mm substrate is 5.28 GHz. Multiple reflections and scattering were increased in Nb<sub>2</sub>O<sub>5</sub>@SHCs as their interface polarization is enhanced, and their impedance matching was also improved, which increased their EMW absorption capacity. Rambutan-like Nb<sub>2</sub>O<sub>5</sub>@SHCs nanoarrays showed a great potential toward the absorption of high-performance electromagnetic radiation (Chen et al., 2022; Yu et al., 2021).

Carbon foam, a novel and new type of material for microwave absorbing is capable to greatly retain the electromagnetic wave by using melamine based highly efficient porous micro-structure foam as a template. The designed porous structure showed significant improvements due to the high electrical and thermal conductivity of micro cavities to restrain the wave propagation and currents. As a result a large number of waves has been scattered with more number of available sites towards

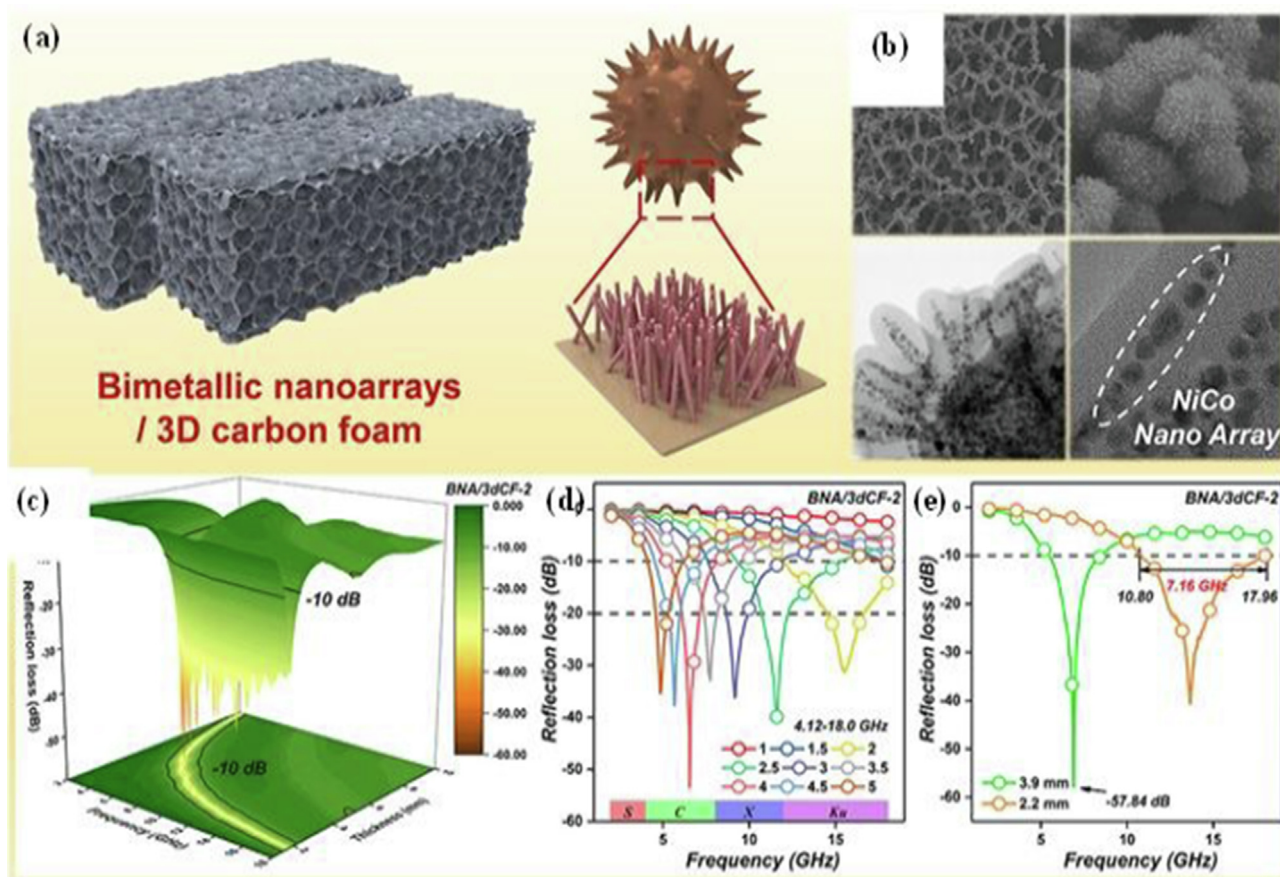


**Fig. 4** Shielding mechanism of bimetallic polymer based 3D porous structure (a), SEM images of segregated structure of nanocomposite porous films (b), shielding performance of developed nanoarrays of 3D carbon foam (c-e). The image is reproduced with permission to copyright materials Wiley Online, 2020 reproduced with permission to copyright materials Elsevier, 2022 (Wei et al., 2022).

improved electromagnetic absorption through conduction and convection (Zheng, 2022). More interestingly, the shielding performance is attributed towards greater sustainability and protection from the electromagnetic waves by carbon layers without affecting the structural assembly; which is attributed to low oxidation of MOF. So that, the composite had capability to retain the dielectric properties of carbon foam with an exceptional SE and an excellent magnetic behavior and higher impedance matching as well as magnetic loss attributes (Sankaran et al., 2018).

### 3. Microwave absorption and Electromagnetic interference shielding material

The most common and widely used traditional EMI shielding materials are based of metals alloys. In recent years, the increasing demand of electronic items increased the demand of new materials for EMI shielding and MA with higher flexibility, lightweight, excellent mechanical stability and higher SE. So far, several studies have been reported on the design and development of lightweight and flexible EMI shielding materials. Numerous polymer composites have been explored for EMI shielding materials instead of metals due to their low density and poor stability. Preparation of different nanocomposites assemblies with CNT@graphene and rGO-Fe<sub>3</sub>O<sub>4</sub> coated fibers respectively have been presented in

the previous studies. The surface of fibrous assembly has been coated with conductive polymers metals and metal oxides including ZnO, Fe<sub>3</sub>O<sub>4</sub>, and AgNPs/TiO<sub>2</sub> and AgNWs/CuO with coral/flower like structure micro to nano-spheres (Yu et al., 2021). The similar work presented on CNF coated fiber with graphene/polymer wires loaded with MnS<sub>2</sub>-Fe<sub>3</sub>O<sub>4</sub> core and MoS<sub>2</sub> shell structures with enhanced shielding performance efficiency; due to the reflection loss, dielectric loss, and magnetic loss under variable thickness and size respectively (Wu, 2022; Kumar et al., 2019). The designed carbon based composites could be derived from such MOF and can potentially be used as herarchical core and shell structures. The well dispersion of carbon compounds in the structural arrangements may comprising of metals and metal oxides as core and 2D graphene as shell. In such architectures the core and shell works as function are loosely packed with polyhydron, micro and nanospheres resulting as hollow spheres with numerous pores inside. The distinctive assembly based on various components; in which their properties could enhance the dielectric loss, electrical conductivity dielectric polarization, and magnetic properties to attain the remarkable EM shielding and MA performance (Liu, 2018; Chen et al., 2012). The direct conversion of these metal complexes is generally attained through carbonization of MOF into metal ions, and metal oxide for example ferric oxides (Fe), cobalt (Co), nickel (Ni), manganese dioxide (MnO<sub>2</sub>), zinc oxide (ZnO), and zirconium

dioxide (ZrO<sub>2</sub>) as a porous carbon with reserved morphology. The multiplicity of the components of the carbonized MOFs has enthused the dedication towards the exploration of their probable retreats for microwave and EM absorption or retention. Notably, the component content of MOF derivatives is unmanageable due to certain limitation. The use of various metal organic frameworks (MOF) is reported in Table 2 (Xu et al., 2020).

It is revealed from previous works the carbonization over high temperature as a key factor, which is used to develop carbonous compounds and are used to the EM and shielding properties. The studies shows that, the mecahism of EMI shielding and Microwave absorption are based on porosity of material, graphitic degree, the number of defect induced, electric conductivity, thermal and megnatic attributes of the complex materials; which requires in depth analysis and further studies. Similiarly, the oxidation, reduction, vulcanization and phosphating techniques are widely used to produce semi-conductive structures from the metals, metal oxide and highly conductive metal sulphates, and phashides for potential application in different fields. Therefore, such approaches require certain research work and critical care for hyberdizaiton of MOF and their derivatives of low dimensional materials, which are dominated and could open new dimension for EM shielding materials (Wu, 2022). Therefore, the studies has been made on development of such structures, for example core and shealth assemblies of Zn-Co dopped carbon as shell comprising of Fe<sub>3</sub>O<sub>4</sub> nanoparticles as demonstrated in Fig. 5 (a & b) (Yang et al., 2022). Whereas, the interfacial polarization is also significantly enhanced with CNT, carbon nanosheets, and metal complex towards enriched dipolar polarization of N—O—containing polar reactive groups with enhanced dielectric loss ability. The internsic electromegnatic properties may also be improved by increasing the interfacial polarizaiton for the interfaces; which jointly contributes to improve the EM waves absorption properties (Liu, 2019). Further, the greater orientation and alignment of CNT in the polymeric compounds could improve the dielectric loss and enhanced EM shielding effectiveness towards MA properties. The work

presented on intercalated MOF to drive the Co/C and Ni/C into Ti<sub>3</sub>C<sub>2</sub>T<sub>x</sub> ML-MXene showed a greater R<sub>L</sub> value of − 60.1 dB with a mild thickness of 2.7 mm. Upto date, several low-dimensional with other carbon compounds as 2D materials for example CNTs, CNFs, CNCs, rGO, MXene, and MoS<sub>2</sub>, been put into practices by incorporation of MOF and their nano-composites to further strengthen the EM shielding and MA capabilities (Sankaran et al., 2018). In brief, the dielectric and magnetic loss attribues are highly efficient to enrich the interface between metal oxides and carbon based 2D materials, with variable geometrical arragments, which could beneficial for EM sheiding with their hybrids. These characters of microwave shielding towards impedance matcing could efficiently optimized by changing the arrangements of low dimensional and 2D materials as two different components (Sankaran et al., 2018; Zhang et al., 2022).

The particular mechanism of their configuration and morphology is predictable to expand the EM shielding and microwave characteristics in the functional field to attain more refined concert. The well-organized core and shell structure of ferric oxide and silica oxide (SiO<sub>2</sub>) over polypropylene coated microsphere were developed for better microwave and electromagnetic shielding, the composites assemblies have been developed by commonly used micro-emulsion polymerization method (Cao, 2021). The morphological crystal structures having highly reactive functional group and demonstrated an enhanced electro-magnetism and MA properties. The designed core-shell structure with a thickness of (2 um) which is tuned 20 to 60 nm (SiO<sub>2</sub> layer) by variation in the molar ratio of Fe<sub>3</sub>O<sub>4</sub>@SiO<sub>2</sub> to Poly Pyrrole. The results demonstrate that, the absorption peaks gradually move to low frequency with an increment striking the coating with lower thicknesses. The lowest R<sub>L</sub> value was about to reached − 40.9 dB over 6 GHz for a mild thickness of 5 mm. The efficient microwaves absorption over a wider bandwidth of 6.88 GHz from 12 to 18 GHz, due to completely covering the incident waves for (12–18 GHz) bands as demonstrated in Fig. 5 (c & d) respectively (Huang et al., 2021). However, the results also demonstrated an excellent microwaves and electromagnetic waves absorption

**Table 2** The EM loss mechanism of magnetic nanomaterials (Huang et al., 2021).

Classify	Magnetic Materials	Microstructure	Electromagnetic Loss Mechanism
Ferrite	Fe <sub>3</sub> O <sub>4</sub>	Nanocrystal	Natural resonance
	Fe <sub>3</sub> O <sub>4</sub>	Nanoring	Orientation/interface polarization, dielectric loss, oscillation resonance absorption
	BaFe <sub>12</sub> O <sub>19</sub> / CoFe <sub>2</sub> O <sub>4</sub>	Hollow microrod	High saturation magnetization
Magnetic metal	Ni	Chain	Natural resonance, micro eddy current, interfacial polarization
	Fe	Microplates	Magnetic loss, conduction loss
	Ni	Nanoparticle	More interfacial polarization
Magnetic alloy	Fe <sub>x</sub> Co <sub>3</sub>	Layer	Magnetic loss is domain, impedance matching
	CoNi	Flower	Interfacial magnetic dipole interaction, multiple scattering in the space woven
	Co <sub>20</sub> Ni <sub>80</sub>	Urchin	Eddy-current loss, magnetic hysteresis loss
MOF-derived material	Co/C	Porous	highly porous structure, dielectric loss, magnetic loss
	Fe-Co/graphene	Dodecahedrons	Dielectric loss, magnetic loss
	Ni/C	Hollow	Electronic dipole polarization, multiple reflection, interfacial polarization, conduction loss
	Co-C/MWCNT	Hollow	Orientation-enhanced dielectric and magnetic loss, impedance matching
	Ni@C@ZnO	Yolk-shell	Interfacial polarization, magnetic-dielectric synergistic effect
	CoFe@carbon	Fiber	Interfacial polarization, multi-scattering, magnetic loss
	Co@NC@rGO	Nanosheets	Magnetic loss, interfacial polarization

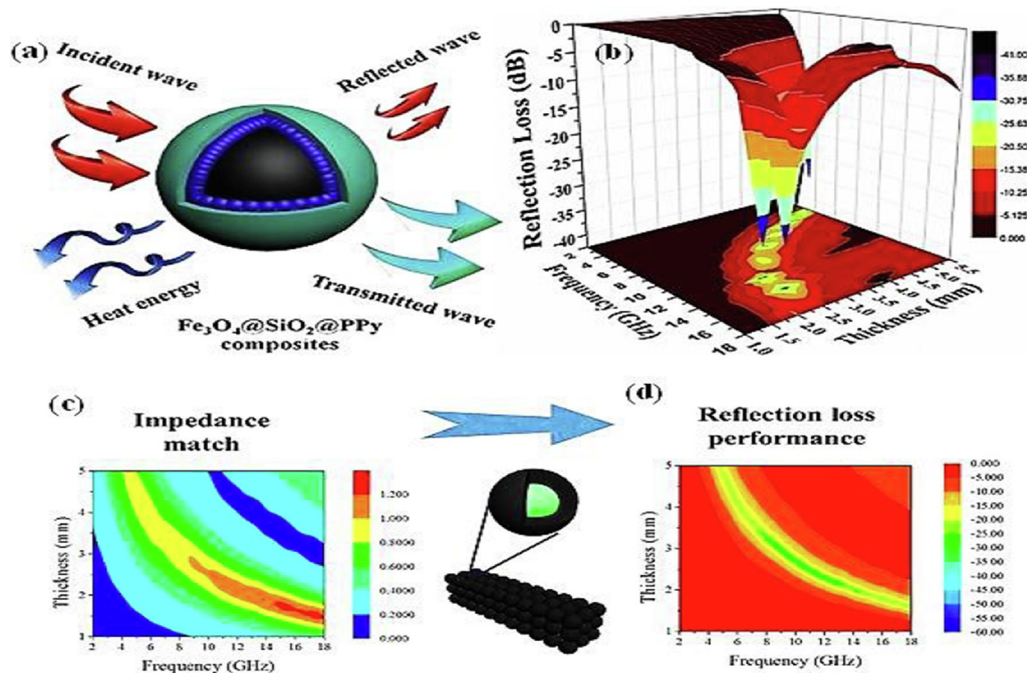


**Fig. 5** Schematic diagram of different MOF structures  $\text{Fe}_3\text{O}_2\text{-SiO}_2/\text{PPy}-\text{Fe}^{3+}$  ferric oxide (NPs) loaded polymer (PPy presented core-shell model for microwave and Electromagnetic shielding response of nanomaterials (a & b) (Liu et al., 2019), impedance matching with variable thickness (c), reflection loss performance with variable thickness (mm) (d). Figure reproduced with copyright permission from Elsevier 2019.

over a broader range of 4.4–18 GHz with different coating layers and thickness. The perfect EMI and MA absorption properties are attributed to different attributes including the dielectric loss due to the special core and shell structure, which is highly suitable and efficient assembly as microstructure of the  $\text{Fe}_3\text{O}_4$  microspheres. The newly prepared  $\text{Fe}_3\text{O}_4@/\text{SiO}_2@/\text{PPy}$  microspheres are considered as prospective candidates for highly efficient microwave absorption materials with tailored nanostructure respectively (Tong, 2021). In other work, a hierarchical structure of ferric oxide decorated carbon and molybdenum sulphide ( $\text{Fe}_3\text{O}_4/\text{Fe}@/\text{C}@/\text{MoS}_2$ ) as core and shell structured. The newly developed nanofibers introduced by using a simple three-step process. The ternary assembly containing of  $\text{Fe}_3\text{O}_4/\text{Fe}@/\text{C}$  over carbon based nanofibers, followed by in-situ polymerization attained via carbonization and reduction in hydrogen and nitrogen ( $\text{H}_2/\text{N}_2$ ) inert gaseous atmosphere Fig. 6 (a & b) respectively (Huang et al., 2021; Huan, 2022). Herein,  $\text{MoS}_2$  nanosheets were grown in irregular manner on the surface of nanofibers; which is transformed into flower like assembly. The surface morphology of the developed composite and an electro-magnetism property of the each sample was thoroughly explored. Additionally, the EMI and MA properties of  $\text{Fe}_3\text{O}_4/\text{Fe}@/\text{C}$  nanofibers and  $\text{Fe}_3\text{O}_4/\text{Fe}@/\text{C}@/\text{MoS}_2$  were compared to previously reported works. The designed structure showed a ( $R_{L\min}$ ) of  $\text{Fe}_3\text{O}_4/\text{Fe}@/\text{C}@/\text{MoS}_2$  was nearly about to  $-53.79$  dB at 11.12 GHz and on the other side the variable thickness analysis was made for different bandwidth ( $R_L < -10$  dB) at 4.4 GHz by using a film thickness of 2.24 mm as demonstrated in Fig. 6 (c & d). Carbon nanotube microspheres (CNTsM) were prepared using a facile method of ultrasonic atomization and heat treatment. Between 2 and 18 GHz, CNTsM were studied for their dielectric properties and electromagnetic wave absorption

properties. Enhanced interfacial polarization, multiple reflections/scattering, and optimized impedance matching resulted in good EMW absorption for CNTsM,  $R_L$  is 35 dB at 1.5 mm thickness, and effective absorption bandwidth (EAB,  $R_L < -10$  dB) is 4.4 GHz. CNTsM can be considered a brand-new candidate for EMW absorption materials (He et al., 2021; Zhang et al., 2021).

The freezing drying is the most common and widely used technique for the development of various 2D and 3D aerogels, porous structures for EMI and MA. The developed structure is highly organized and well-aligned/oriented cell structure and heterogeneous assembly in which the dielectric/magnetic interfaces and porous structure benefits the superior absorption (Yu et al., 2022; Sharma, 2022). Meanwhile, the broad band absorption over a wide range of bandwidth is significantly influenced by the size, shape and thickness of the nanocomposites having low filling levels towards strong absorption properties. The impedance and shielding performance are achieved by variable thickness, size forming and greater filler content percent with an improved impedance matching as well as variable polarizations and magnetic-coupling belongings. Furthermore, the high decomposition over a temperature of 630.9 °C; the developed composites exhibited a great competitive advantage as reported for polymer based various composites. These features confirm the potential of CNT/graphene/PI foams as lightweight, compressible, heat-resistant materials that can effectively shield and absorb electromagnetic waves. Similar studies have been made on highly porous, light weight graphene-PU sponge/foams based multi-layered polymer (PU) aerogels (Wang et al., 2020).

The porous assembly and films showed an improved mechanical compressibility and heat resistant and worked as highly suitable structural design assembly for EMI-SE and

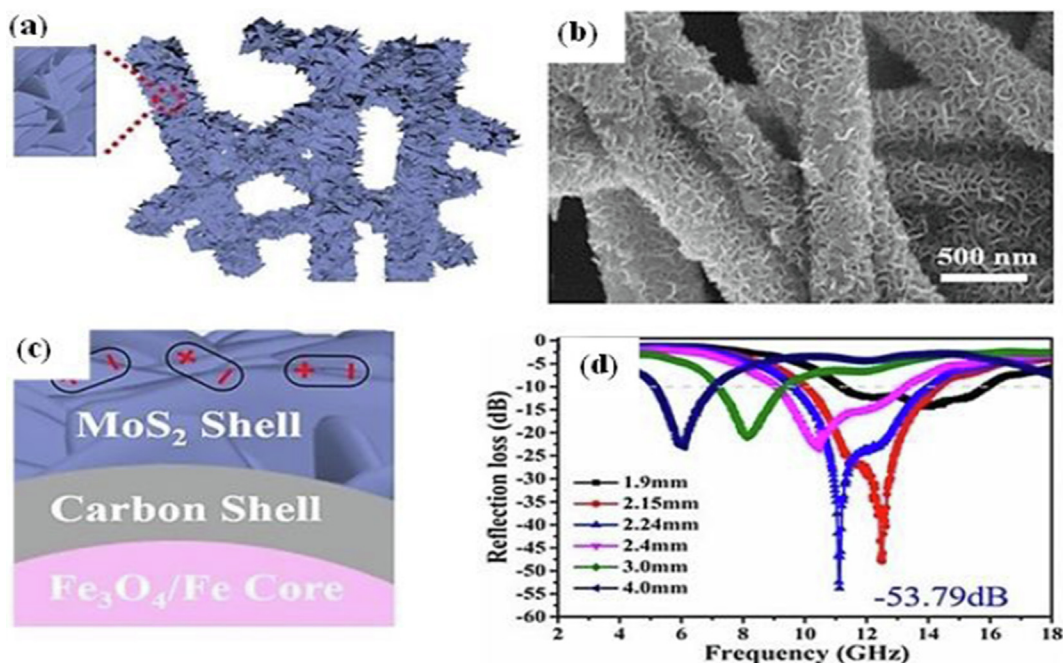


**Fig. 6** Development of flexible carbon/MoS<sub>2</sub>/Fe<sub>3</sub>O<sub>4</sub> composites (a), unit cell Structure design (b), carbon fibers arrangement in developed 2D fibrous assembly nanocomposites for Microwave absorption (c), shielding effectiveness showing (RL) of designed structure with different thickness (d), Reproduced with permission Copyright material from Elsevier, 2021 (Tong et al., 2021).

MA. The aerogels of 2D graphene sheets and 3D-helical/helix based nanocomposite structure has been developed and used for electromagnetic shielding mechanism. Herein, another systematic approach is applied to formulate a thermoplastic polyurethane (TPU) and carbon nanotube loaded with silver nanoparticles as segregated assembly shown in Fig. 7 (a & b) (Wang et al., 2021).

The developed composite containing silver layer, which worked as highly efficient towards electrical, thermal properties, finely tuned with electrostatic absorption. The designed structure was produced via thermal annealing, vacuum filtration and hot pressing as well as baldd coating techniques (Sun, 2021). Similar works has been reported so far, the production of nanocomposites using high speed stirring of CNT in TPU, PU followed by sequential vacuum assisted filtration and compressing molding techniques. As segregated composite made of TPU and CNT layered structure having CNT as conductive channels, which provided significant improvements in the EMI and MA properties. Further, the addition of the silver in the developed nanocomposites, exhibited good impedance matching and able to absorb or reflect the electromagnetic waves in a more systematic way. The systematic effect resulted, as an outstanding shielding performance of 79.4 dB and SE<sub>A</sub> of 74.8 dB against the X-band at extremely low filler content (3.7 wt% CNTs and 0.04 wt% Ag) in the nanocomposite. The synergistic effect result shows, that the around 99.9 % EM waves are attenuated in the proliferation with a shielding efficiency SE<sub>A</sub> of 94.2 % to the total SE as shown in Fig. 7 (c & d) (Wang et al., 2021). Additionally, R<sub>L</sub>-value of 0.54 is extended since of the critical intervention amongst the reflected and incident EM waves. However, the performance and reflection loss of -20 dB of such nanocomposites is ranging from 7.0 to 17.5 GHz by refining the Debye relaxation. The graphene and epoxy resin demonstrates the replication loss of

-14.5 dB over a frequency of 18.9 GHz; which may attribute to the change in multiple poles for the polarization of interfaces inside the nanocomposite material (Ameri et al., 2022).

Therefore, overcome the use of metal complexes by using 2D materials with different polymers and their nanocomposites due to higher flexibility, light weight, low processing cost and corrosion resistance against water and mist. Though, the existing problems are still under investigation and considered as it becomes a very important and critical global challenge; and being studied for further improvements toward fabrication and development of (electromagnetic/dielectric) materials composites. The newly developed nanomaterials and meta materials could effectively work under a versatile range of microwave and electromagnetic shielding with satisfactory shielding performance. Since, PDMS/PI with MXene as 2D materials in various forms for example films, foams, fibers and aerogels are typically much more efficient to absorb in-plane polarized waves than out-of-plane polarized waves (Zhu et al., 2019). A very fine and ultra-light weight as well as bendable carbon nano tubes (CNT) Bucky paper improved with MXene (Ti<sub>3</sub>C<sub>2</sub>T<sub>x</sub>) was synthesized. Furthermore, the mechanical tensile test results showed that the addition of 10 % rGO in the PS matrix increased the mechanical performance of developed nanocomposite of rGO/PS about to 13.8 % which is several orders of magnitude higher as compared to pristine rGO and PS polymers as presented in Fig. 8 (a & b) (Shi, 2022).

A very fine and ultra-light weight as well as bendable carbon nano tubes (CNT) Bucky paper improved with MXene (Ti<sub>3</sub>C<sub>2</sub>T<sub>x</sub>) was synthesized. The developed composite Bucky paper showed highly efficient shielding (SE) performance through a simple electro deposition approach. The designed composite buckypaper represented an outstanding shielding efficiency of 60–65.5 dB in X-band with minimum thickness

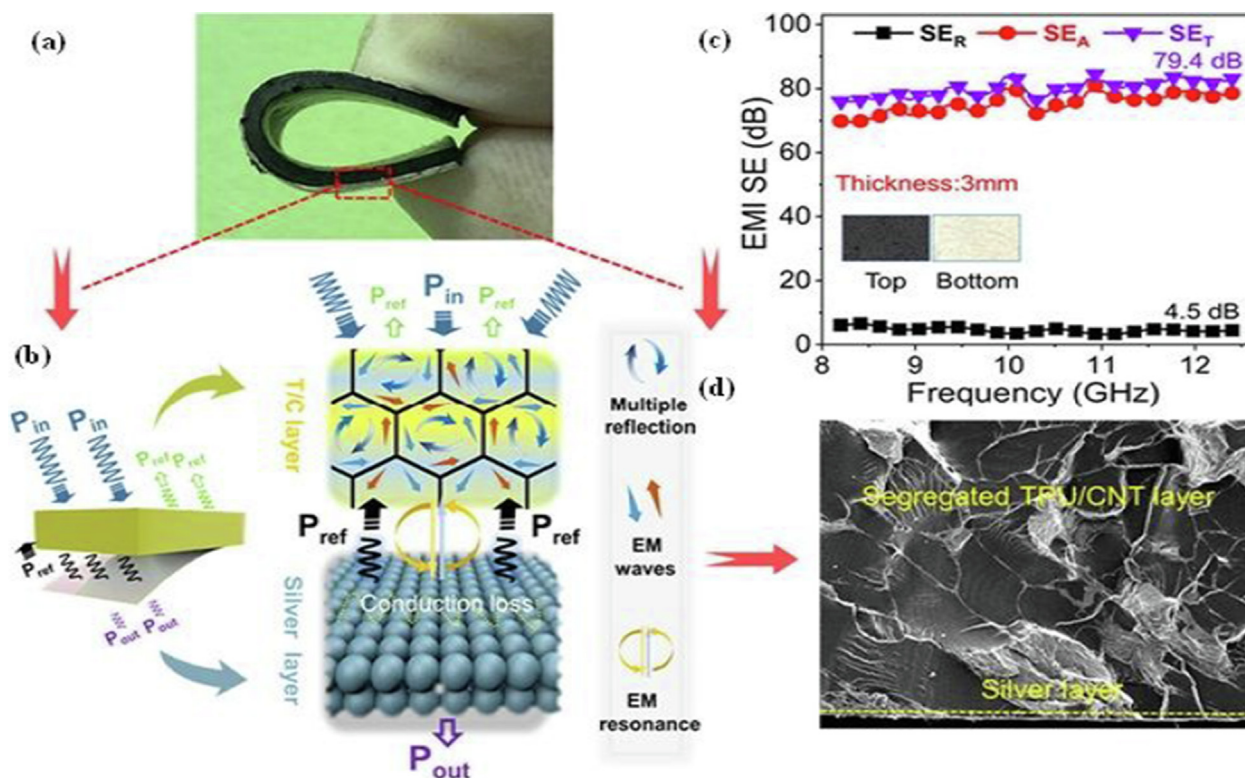


**Fig. 7** Development of segregated thermoplastic polyurethane/carbon nanotubes porous nanocomposites layered sample (a), simulated designed model for microwaves absorption (b), EMI shielding responses of composites (c), and SEM images of TPU/CNT (d). Copyright permission granted; Elsevier 2021 Sun et al., 2021.

of 100  $\mu\text{m}$ , which is best ever as compared to previously reported findings for MXene and CNT based composites as presented in Fig. 8 (c & d) (Shi, 2022). The hybrid structure was designed from a variable range of content percent of CNT as filler, and attained a value of 50–54.5 dB for the X-band. The performance was greatly enhanced by increasing the filler content percent and by increasing or decreasing the film thickness up to 15  $\mu\text{m}$ , which several orders higher as compared with pristine MXene and CNT Bucky papers. Additionally, the average specific shielding efficiency (SE) of  $5.7 \times 10^4$   $\text{dB cm}^2 \text{g}^{-1}$  was achieved, which is exhibited by the film thickness of 5- $\mu\text{m}$  for the hybrid buckypaper Fig. 9 (a-f) (Shi, 2022).

Herein, a segregated assembly of (CNT)/ with Poly(lactic acid) (PLA) has been developed with the newly designed composite was originally subjected to progress in height machine-driven possessions; while accomplishing upright presentation for EMI and MA as demonstrated in Fig. 10 (a-d). The 3D printed model of PLA based porous scaffold has been developed subsequently dipping in CNT dispersion the loading of CNT was hot pressed to design 3D CNT/PLA assembly for EMI and MA. The developed assembly is demonstrated with various profiles including cross profile Fig. 10 (b). Local 3D view of CNT loaded PLA scaffold before heat pressing as shown in the Fig. 10 (c) and cross profile of 2D sheet made of 3D-CNT/PLA scaffold after heating pressing as mentioned in the Fig. 10 (d) as layered assembly.. The final 3D-printed CNT/PLA compounds deposited on scaffold were interpreted to consistent conductive frame work afterwards the mechanical compression. Hence, the SE of resultant composite was as high as 67.5 dB at 5.0 wt% CNTs was incorporated in the

assembly (Ma et al., 2021; Yang, 2021). The fine tuning of 3D printed PLA composite leads to make it more promising CNT/PLA composites for controlled EMI SE as shown in Fig. 10 (e & f).

The study results reveals, that 3D printing technology is more cost-effective and modest method to achieving the outstanding shielding performance of under variable range of different radiation source from the electronic devices. The mechanical strength is nearly reached to 40 % and 45 % higher as compared to pristine polymeric scaffolds with tensile strength of 43.7 MPa and 3.08 GPa of PLA. The polymer based composites various assemblies' performance to EMI effectiveness (Shi, 2022; Yang, 2021). In addition, the 2D materials have multiple layered skins; for example MXene and graphene have better shielding performance, MA capability, enhanced electrical conductivity and thermal stability at high temperature ( $\sim 500$   $^{\circ}\text{C}$ ). The 2D MXene and polymer based aerogels material has received great attention in recent works, as MX-phase to MXene been developed using chemical exfoliation. The MX-Phase sheets are delaminated with strong acids for example HF and in-situ synthesized with PVA to develop aerogels. In which MXene showed stacked several layered micro-macro level permeable structure as demonstrated in SEM images of developed nanocomposites (Yu et al., 2022). The other carbide structures have been developed so far, to be used for microwave absorption properties. The developed assembly and layered Structure had large specific surface area, and rich natural defects with particular metallic attributes. The designed polymeric composites have been broadly premeditated for MA and EMI shielding. The major

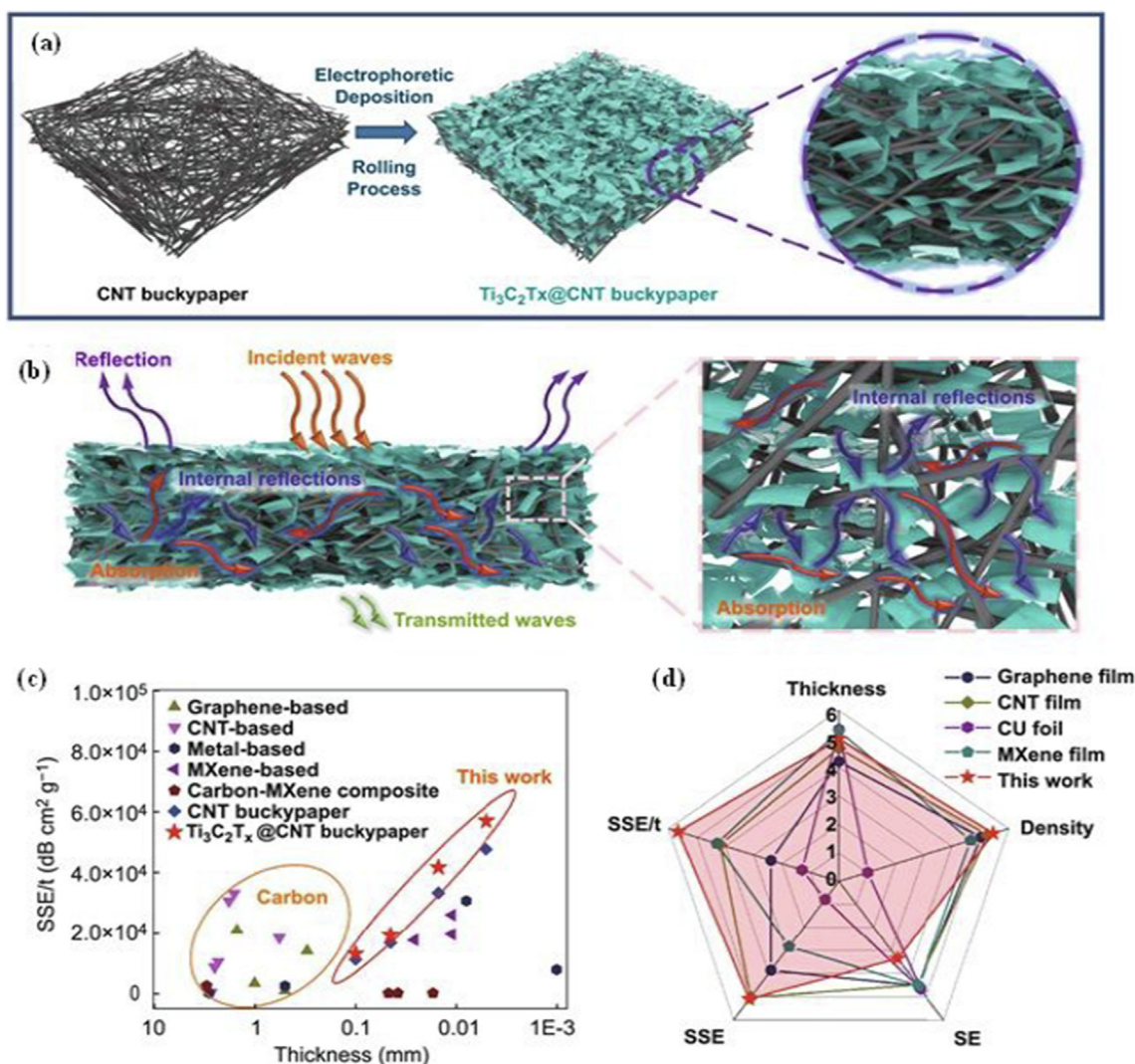


**Fig. 8** Morphological assembly of MXene and CNT bucky paper composites shielding mechanism with multiple reflection from the composite film, inside view of the absorption of EM waves (a & b), EMI shielding performance of MXene based composite with variable size and thickness (c), simulation SE performance of Graphene films, CNT films, copper foil Cu, and MXene based composite (d). Reproduced with permission of copyright material Springer Nature 2021 (Yang et al., 2021).

work focused on novelty of MXene based polymeric compounds specifically focusing on the incorporation of defects, and synthesis progress as well as introducing various metal organic frameworks, organic and inorganic compounds to attain higher SE and particular emphasis on effects formation during the synthesis process. Secondly, the structural design attained through different structural assemblies of these composites for electromagnetic properties (EMI) shielding effectiveness of  $\text{Ti}_3\text{C}_2\text{T}_x$  MXene as demonstrated in Fig. 11 (a-d) (Sharma, 2022).

### 3.1. Graphene

Recently, various materials have been globally studied as EMI shielding or/and EM wave absorbing materials, including 0D, 1D, and 2D materials. Among them, 2D materials are the materials of choice as they are lightweight, have large aspect ratios, and offer distinguished electronic properties. For example, Cao's group reported that chemically graphitized r-GOs

exhibited high-efficiency EMI-SE) at elevated temperatures. The EMI SE of the composites with 20 wt% r-GOs reached a maximum at  $\sim 38$  dB (Wang, 2021). Zhang et al. prepared 2D  $\text{WS}_2$ -rGO heterostructure nanosheets. The composite containing 40 wt%  $\text{WS}_2$ -rGO showed a minimum reflection loss ( $R_L$ ) of  $-41.5$  dB, with the absorption bandwidth reaching up to 13.62 GHz (Zhan, 2021).

Graphene is a single atomic layer of 2D material with a hexagonal structure on the nanoscale level. The hexagonal carbon atom rings are self-attenuated and bonded with each other, with less permeability of water and air molecules on a single layer too few-layered graphene 2D sheet. The material has exceptional electrical, thermal, mechanical and electronic properties with higher electron mobility of  $\mu = 230,000 \text{ cm}^2 \cdot \text{V}^{-1} \cdot \text{s}^{-1}$ , the electrical conductivity of  $400\text{--}5000 \text{ S cm}^{-1}$  for single layer and  $\sigma = 5 \times 10^{-6} \text{ S m}^{-1}$  in a thin layer, and thermal conductivity of  $K = 3000 \text{ } \mu\text{W/K}$  (Yang, 2013). The graphene-based nanocomposites showed a microwave reflection loss of  $-6.9$  dB obtained a frequency range at

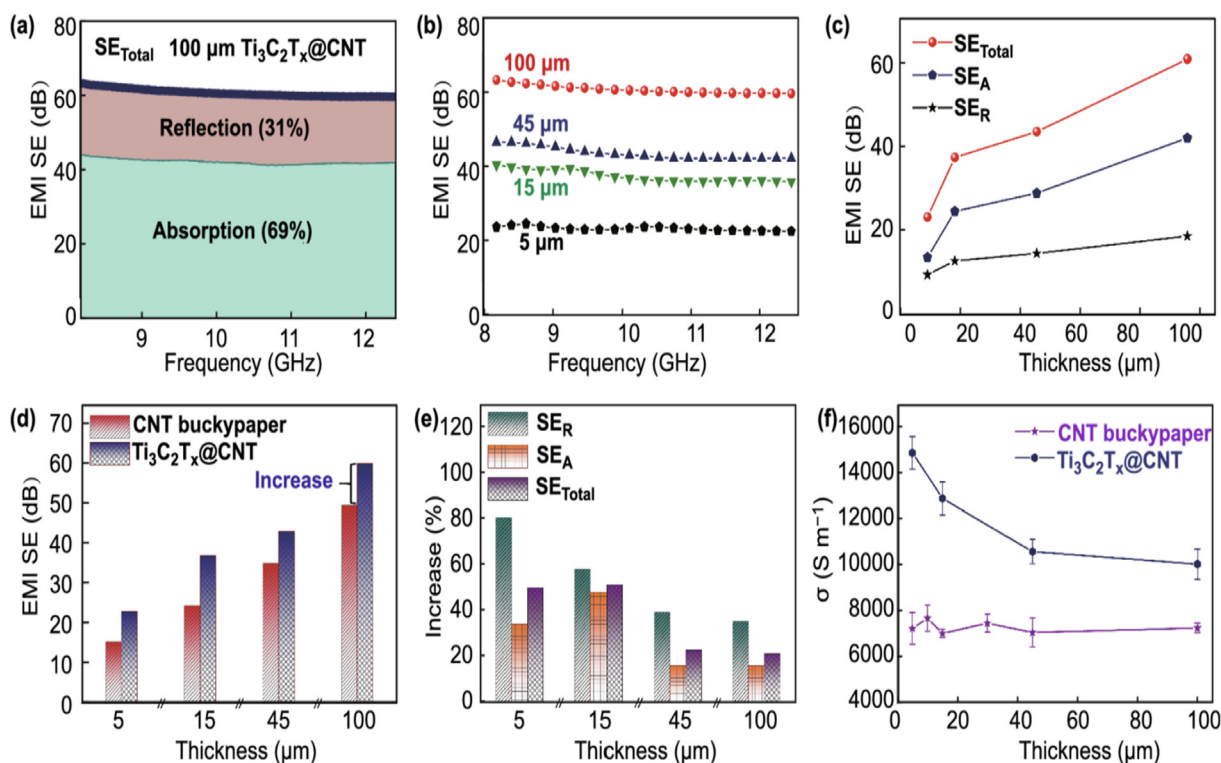


**Fig. 9** Preparation of novel high-performance carbon CNT buckypaper and MXene @CNT for EMI (SE) performance reflection and absorption response (a), EMI (SE) report with different size (b), total shielding response (SE) (c), comparison of CNT buckypaper and MXene loaded with CNT (d), SE reflection and absorption total performance (e), electrical conductivity of CNT buckypaper and MXene@CNT (f). Reproduced with permission of copyright material Springer Nature 2021 (Yang et al., 2021).

7–18 GHz &  $R_L$  value of 50.0 dB. Graphene is one of the leading materials due to its exceptional, mechanical, electrical, thermal and electronic properties. Among all the inorganics and organic materials, graphene has some distinctive behavior and attributes which makes it different from others and unique features; which make it suitable 2D material for EMI shielding and MA as demonstrated in Fig. 12 (a-e) respectively (Zhu et al., 2022). The use of pure graphene is not suitable for microwave absorption, therefore it requires certain modification on its surface functionalization to introduce the defects induced polarization. However, the graphene consisting of zero band gaps, which is favorable for various remarkable advantages, for several potential end use applications. These attributes are assigned to its, light weight higher, flexibility, excellent chemical and mechanical properties. Somehow, on the other side, graphene is suitable for mechanical strength, electrical conductivity and carrier mobility at room temperatures. Therefore, the use of graphene in the form of reduced (rGO) is highly capable and suitable for EM and MA SE performance. These features are dedicated to  $Sp^3$  hybridization toward enhanced dielectric properties, interfacial polarization and defects induced polarization as grafted functional reactive sites, or defects on the surface of graphene sheets (Zhu et al., 2022; Zang, 2015).

Similarly, on the other hand the reduced graphene oxide (rGO) is acknowledged as a simple type of material having lightweight; conductive, and insulation attributes towards EM shielding and microwaves absorption attributes. Furthermore, the attenuation of the EM waves with enhanced absorption is

attained with high dielectric loss capacity. Due to its conductive and dielectric behavior, the microwave absorption thresholds are nearly about to 0.52 and with a very slight 0.31 vol%. These values are also fine tuned and can be altered thresholds with more smaller range through organization and orientation of graphene films in the segregated composite structures. In a microwave field, the dielectric loss of rGO can be separated into two typical processes, i.e., dipolar polarization and charge transport. For instance, the former values of microwave absorption and shielding effectiveness are correlated with defects induced in the films with few missing carbon atoms and accompanied by the dangling bonds; which may work as a function of attenuation of microwaves and can cause charge redistribution. However, the dipoles could alternatively work as in-plane dipole polarization for a single vacancy and out-plane dipoles with surface functional reactive groups for example hydroxyl, carbonyl and carboxy -OH and C-O-C more apparently. Whereas, the dipolar polarization may also contribute towards the microwave and EM energy absorption. The mechanism is totally based on interfacial, surface charge, in-plane vibrational movement of the EM waves, and could jump among the atomic level graphene sheets as a carrier that can consume EM energy which is related to electrical and thermal conductivity (Zang, 2015).

### 3.1.1. Graphene-CNT/polymer-based composites

The multi-walled carbon nanotubes (MWCNT) with reinforced polypropylene (PP) nanocomposites was prepared by melt processing technology through a twin-screw extruder.

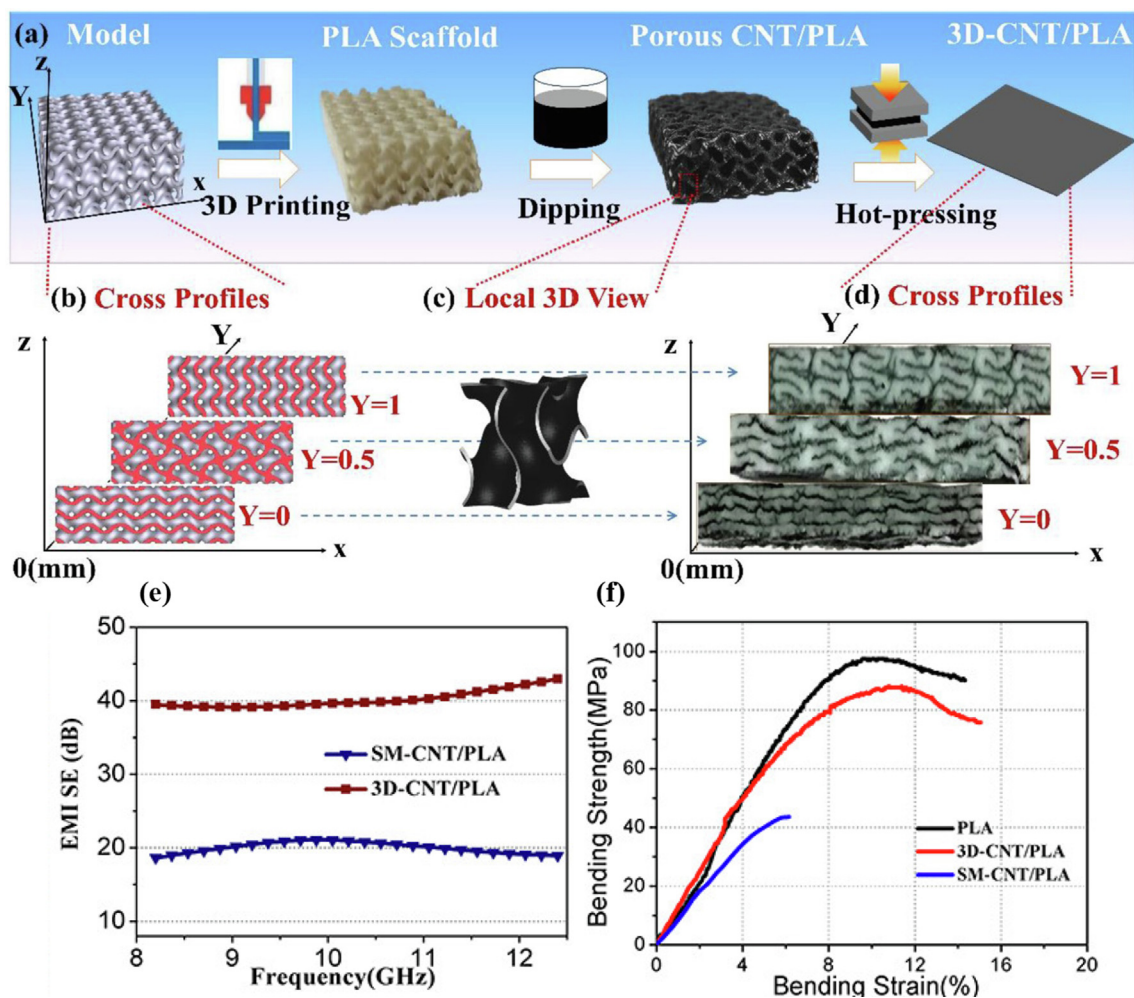


**Fig. 10** Development of CNT-PLA based 3D porous nanocomposites model (a), cross profile (b), local 3D view (c), cross profiles (d), EMI shielding (e), and mechanical bending strength (f) of developed 3D printed PLA scaffold for microwave & EMI shielding. Copyright materials from Elsevier 2021 have been used to reproduce this Figure (Wang et al., 2021).

Compared with the sample without filler (PCN), the tensile strength of the nanocomposite is increased by 27 %. The introduction of MWCNT increases the conductivity from  $2.07 \times 10^{-10}$  to  $4.21 \times 10^{-6}$  S/cm (Wang et al., 2021; Lai et al., 2020; Xie, 2021). The frequency range of X band (8.2–12.4 GHz) was measured with a vector network analyzer; when aqueous solution of GO was loaded at 5.0–10.0 wt% of the CNT showed significant improvements in electrical conductivity as well as microwave and EMI shielding effectiveness as compared to pristine rGO films a loaded with  $\text{Fe}_3\text{O}_4$  nanoparticles showed an incident waves reflected from the surface of graphene films and ferric oxide nanoparticles for EMI shielding performance with higher reflection as demonstrated in Fig. 13 (a). Similarly; in another work presented on 2D materials MXene was for microwave and EMI shielding. The MXene films were decorated with  $\text{Fe}^+$  and were processed via solvothermal approach, The Fig. 13 (b) demonstrate the compact MXene sheets towards improved EMI shielding with magnetic loss, conductive loss, dipolar polarization and interfacial polarization of the MXene sheets after widening of MXene stacked layers for enhanced EMI shielding (Wang et al., 2021; Lai et al., 2020; Xie, 2021). However, the high per-

formance materials for better EMI shielding effectiveness (EMI) with improved shielding efficiency (SE) is achieved with enhanced electrical and thermal properties due to the increasing the conductive fillers, which results as a high stiffness and increased compressibility of the composite foam structures (Li, 2021).

In which, the agglomerations results an enhanced polymer to filler interaction with stronger bonding forces between conductive filler and PI polymer matrix as demonstrated in Fig. 13 (b). Another, study made on carbon nano tubes CNT dispersion was achieved in the polymer matrix, due to the chemical surface functionalization of reactive sites as chemical groups on graphene oxide (GO) films, which resulted as improved “ $\pi$ - $\pi$ ” conjugated bonds between GO films and CNT as demonstrated in Fig. 13 (c). The developed nanocomposite foam demonstrated an average EMI performance of 28.2 dB and specific (SSE) of  $70\text{--}50$  dB  $\text{cm}^2 \text{g}^{-1}$  with very little density of  $0.02 \text{ g cm}^{-3}$ . For the time being, the multiple layered structures developed on graphene films and showed strong chemical bonding between PI matrix and graphene films (Yang, 2018; Zhang, 2019). The designed composite foam structure showed a better cycling loading and unloading during the compression

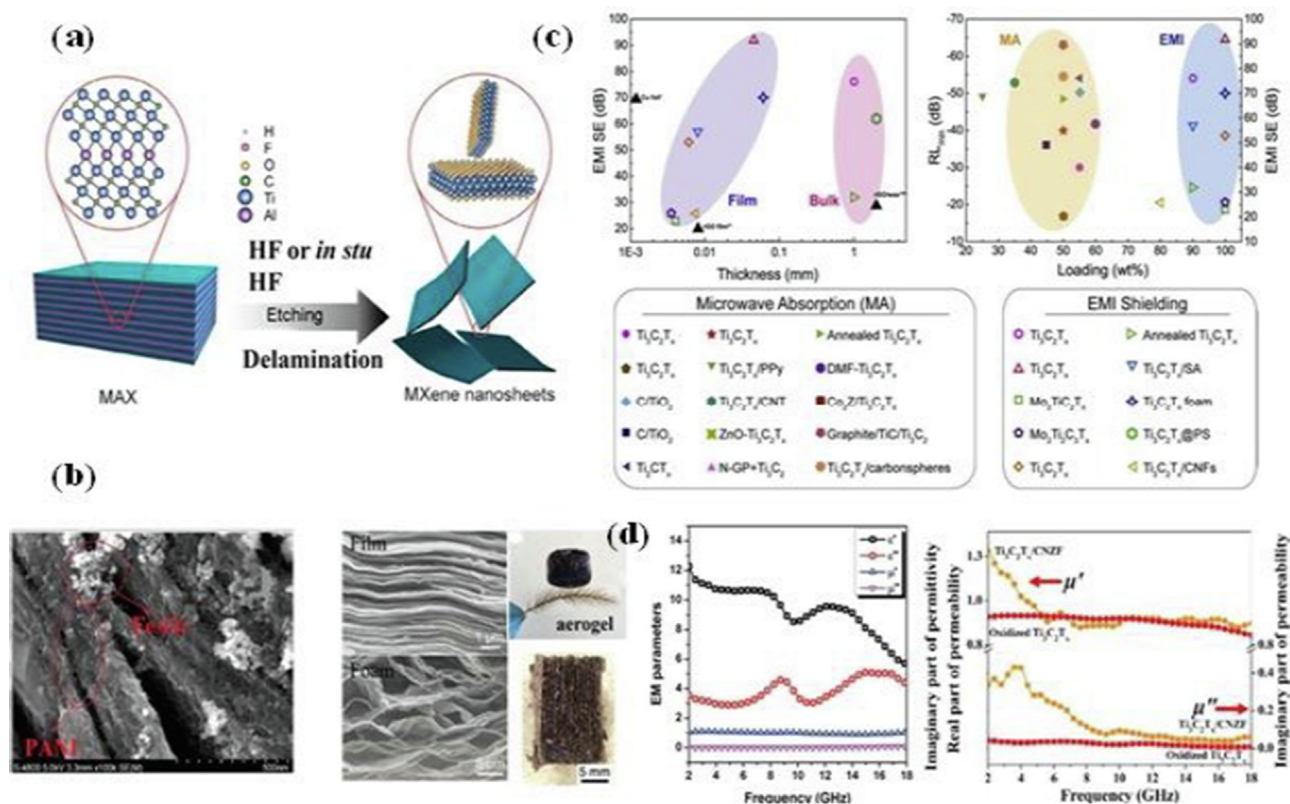


**Fig. 11** Chemical delamination etching of MXenes sheets using HF etchant (a), FESEM images of MXene decorated Fe<sub>3</sub>O<sub>4</sub> (b), EMI shielding effect of different forms of MXene (c), and shielding performance of MXene films (d), reproduced with copyright materials Elsevier, 2020 Wang et al., 2020.

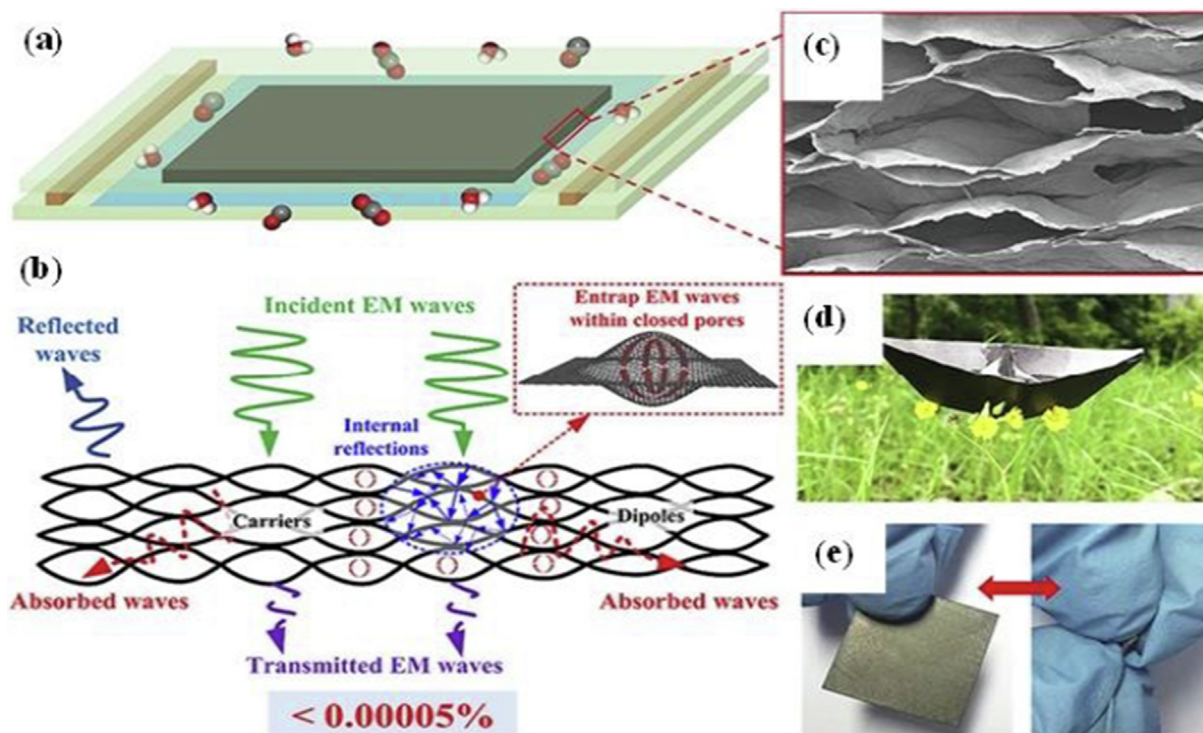


**Fig. 12** Development of rGO films via blade coating (a), shielding mechanism model for Multiple layered rGO films (b), SEM images of rGO films (c), and developed coated substrate foldable films (d & e), reproduced with copyright permission by Elsevier 2020 (Lai et al., 2020).

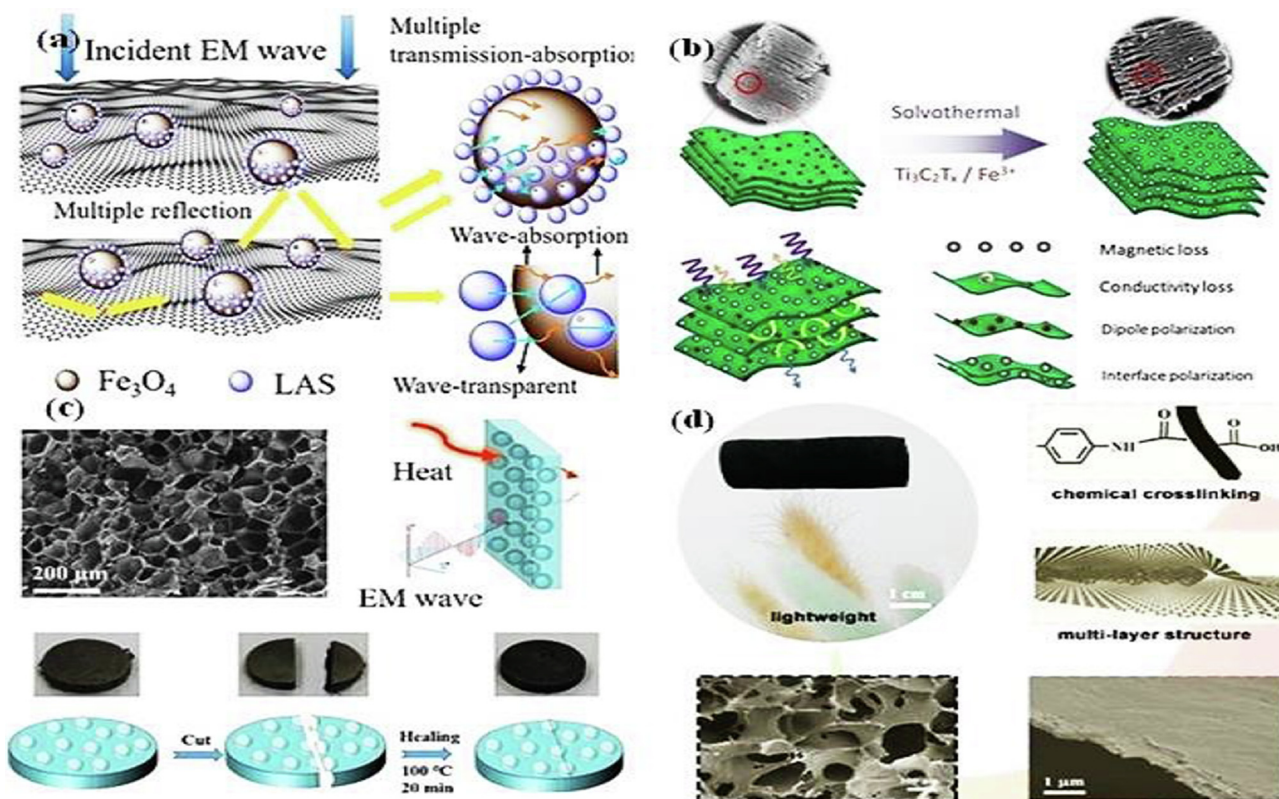


**Fig. 13** (a) Development of GO & Fe<sub>3</sub>O<sub>4</sub> based composites reproduced with permission of copyright material Elsevier; 2018 (Yang et al., 2018), (b) MXene and Fe<sub>3</sub>O<sub>4</sub> composites, reproduced with copyright permission by Elsevier; 2019 (Zhang et al., 2019), (c) self healing carbon nanotubes/arylic polymer composites. This figure has been reproduced with the copyright materials by Elsevier (2021) (Zhan et al., 2021); and (d) ultra light and ultra thin carbon nanotube/polyimide foam and graphene nanocomposites for microwave absorption. Reproduced with permission of copyright material Elsevier; 2021 (Wang et al., 2021).

stability analysis. These topographies endorse the probable use of the CNT/graphene/PI foam as lightweight, compressive, heat-resistant toward an improved EMI shielding and electromagnetic wave absorption as demonstrated in Fig. 13 (d). The maximum EMI shielding effect of  $-21.07$  dB was attained, which is effective value for EMI shielding. The results also demonstrate, that \as prepared nanocomposite material is highly effective and suitable for EMI shielding to meet the requirements of the industry. The newly developed a lightweight, highly flexible, conductive and efficient EMI shielding (Wang et al., 2020). Similarly, the graphene loaded with silver (Ag)/and other metallic nanoparticles, instead of magnetic carbon nanotube (mCNT) composite loaded on polypropylene (PP) fabrics by a facile spray deposition technique (Yang, 2013) The nonwoven PP fibers coated with MCNTs after plasma modifications and Polydopamine (PDA) assists in the development of hydrogen bonds between Fe<sub>3</sub>O<sub>4</sub> on polymer surface towards an improved adhesion properties as compared to untreated nonwoven pp fibers. The introduction of mCNTs significantly improved the electrical conductivity and EMI shielding performance of the Ag/mCNTs composite coating was nearly about to 8.2–12.4 GHz (Zhan, 2021). Thus, the Ag/mCNTs composite coating exhibits excellent EMI shielding effectiveness (SE) of 61.1 dB and a specific SE (SSE/t) of 2811.78 dB cm<sup>2</sup>/g, and reveals a good stability, maintained over 91.6 %, 80.2 % and 69.8 % enhanced EMI SE after washing tests. Therefore, Ag/mCNTs-coated PP fabrics can be a

reliable candidate for exploring flexible electronics for high-performance EMI shielding fabrics and porous assemblies with better stability (Liang, 2020; Bai, 2022). Another work based on silica carbide (SiC) loaded with graphene also showed improved SE performance over different thicknesses ( $\sim 10$ , and  $\sim 15$  nm) and developed by using freeze drying method. The effect of SiC shell and nanoparticles with variable size and thickness greatly influence on the overall MA and EMI shielding properties of the resulting GO-polymer nanocomposite. The as coated SiC shell effectively promotes the dispersion of CNTs in the geopolymer matrix due to the chemical reaction between SiC and polymer composites as presented in Fig. 14 (a & b) (Li, 2022).

In another work, made on the development and designing of a lightweight spongy structure looks a like bone-like made of graphene@silicon carbide (SiC). These aerogels were fabricated by the simple available method i.e freeze-casting of GO coated SiC whiskers made from the slurry through thermal reduction of GO@SiC to produce highly flexible and porous aerogels (Jiang et al., 2018). The developed sponge like structure showed exclusive hierarchical assembly with well oriented and good ordered structure of graphene@SiC. These aerogels were formed by graphene wrapped SiC whiskers, which hold pronounced benefits for example, having a low density (72 mg/cm<sup>3</sup>) with a higher MA performance. The developed assembly showed a minimum reflection loss and attained EMI performance of  $-47.3$  dB at 10.52 GHz for a very small-

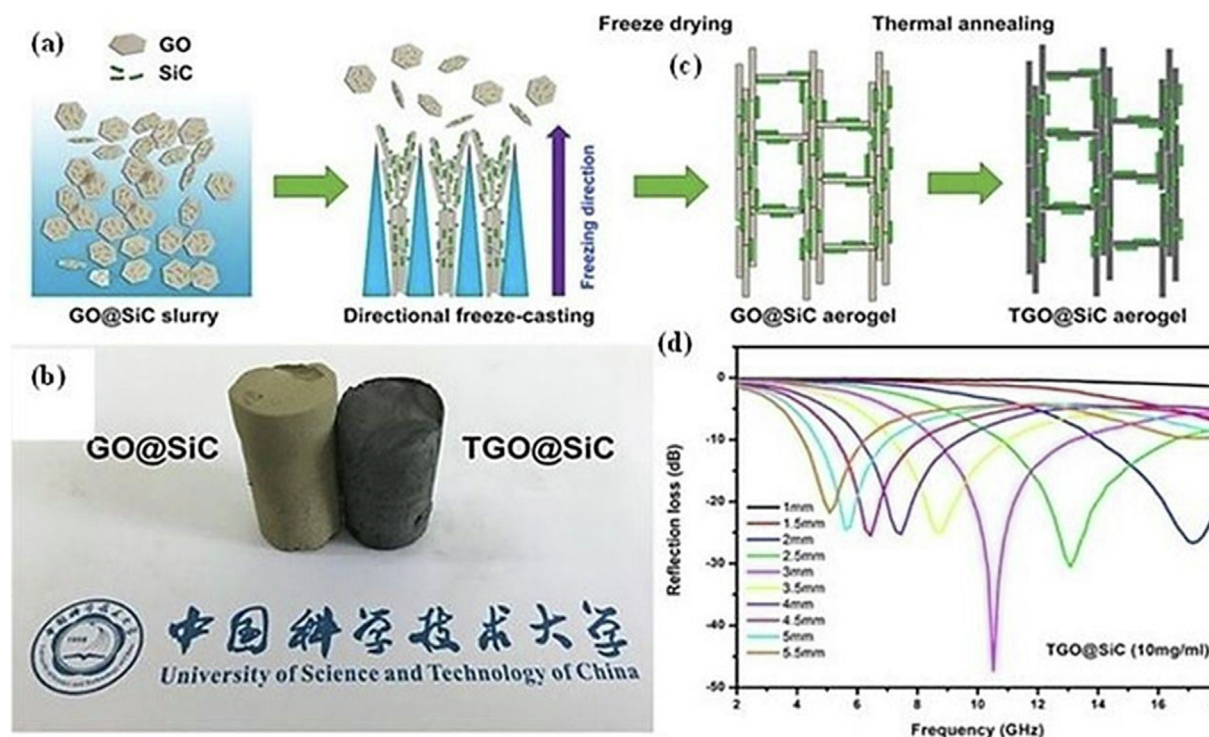


**Fig. 14** Development of GO and SiC slurry into as a directional free standing porous films (a) orientation of as prepared foams/aerogels, (b) GO and rGO with SiC aerogels, (c) developed aerogels with freeze drying and thermal annealing, and (d) Microwave reflection loss ( $R_L$ ) response of aerogels, reproduced with permission of copyright material, Elsevier 2018 (Jiang et al., 2018).

ler thickness of 3 nm. The effective bandwidth of reflection loss was reached to  $\leq -10$  dB for 4.7 GHz. These out performance, demonstrates that the developed composite is a novel graphene@SiC aerogels and highly efficient material for high-performance microwave absorption application. The dispersive core and shell of the altered CNTs can be more improved by growing the thickness of SiC. However, the insulating SiC shell may restrain or hindered delocalization of electrons and reduced when the SiO<sub>2</sub> shell is thin; the conduction of CNTs was disintegrated. The electrical properties are also recovered during the polymerization process, which may attribute to the higher interfacial bonding and more interaction on molecular level (Jiang et al., 2018). A high EMI shielding efficiency (SE) of 24.2 dB is achieved for the geopolymer nanocomposite containing 5 vol% S-CNT and thin SiC shell as demonstrated in Fig. 14 (c & d). The obtained values are more competitive than reported composites; when sample thickness and filler content are taken into account. To address the overheating and EMI problems of integrated electronic device is more important and essential towards the design of multifunctional materials with enhances EMI shielding effect (Chen, 2021).

In this concern, the anisotropic graphene and MWCNT were used to develop a continuous 3D continuous networks via KOH-induced hydrothermal and chemical reaction. Subsequently the graphitization was attained at 2800 °C, where the ratio of GO: mWCNT was kept 1:3, which is favorable for electrical and heat transport. The optimal thermal conductivity of the composite can reach  $1.30 \text{ W m}^{-1} \text{ K}^{-1}$  at a low load of 2.77 wt%, which is 465 % higher than that of pure silicone rubber ( $0.23 \text{ W m}^{-1} \text{ K}^{-1}$ ) (Chen, 2021; Fu, 2020). However,

the developed composite reveals a higher electrical conductivity with EMI shielding of  $-42$  dB in K-band. Also, it still retains the flexibility of the matrix. This work provides the better understanding of lightweight functional materials for potential end use of microwave and EMI shielding as presented in Fig. 15 (a & b). The work reported on graphene/epoxy nanocomposites and aerogels with highly conductive polymer; i.e polyaniline nano structured (NWs) has been developed in the paraffin matrix. The loading percent of the graphene with CNT was varied to produce segregated composite films produced on simple filtration technique, on PET, and PVDF filter papers. Similarly some other works are also been reviewed in previous studies with continuously increased EMIS SE performance with variable size, thickness and filler content percent with and epoxy resins as presented in Fig. 15 (c & d) (Chen, 2021; Liao, 2022).

Similarly, another Inspired work presented by successful manufacture of porous structure amongst the graphene film-strip and the other 2D structures of MXene Ti<sub>3</sub>C<sub>2</sub>T<sub>x</sub> as porous hetro structure made for superior performance towards EMI shielding. The composite films were prepared by using ion-induced and vacuum filtration of MXene and rGO porous composites for enriched microwave and EMI shielding. The developed porous structure of Ti<sub>3</sub>C<sub>2</sub>T<sub>x</sub>/rGO films prevailing a compact surface and highly porous assembly inside. The resultant assembly showed higher electrical conductivity in which the mass fraction of GO and Ti<sub>3</sub>C<sub>2</sub>T<sub>x</sub> was varied from 2:2. The maximum EMI shielding efficiency (SE) composite assembly including the rGO and MXene films extended up to (59 dB), and obtained a specific SE (SSE/t) of  $37619 \text{ dB cm}^2 \text{ g}^{-1}$  which is almost high performance achieved with similar

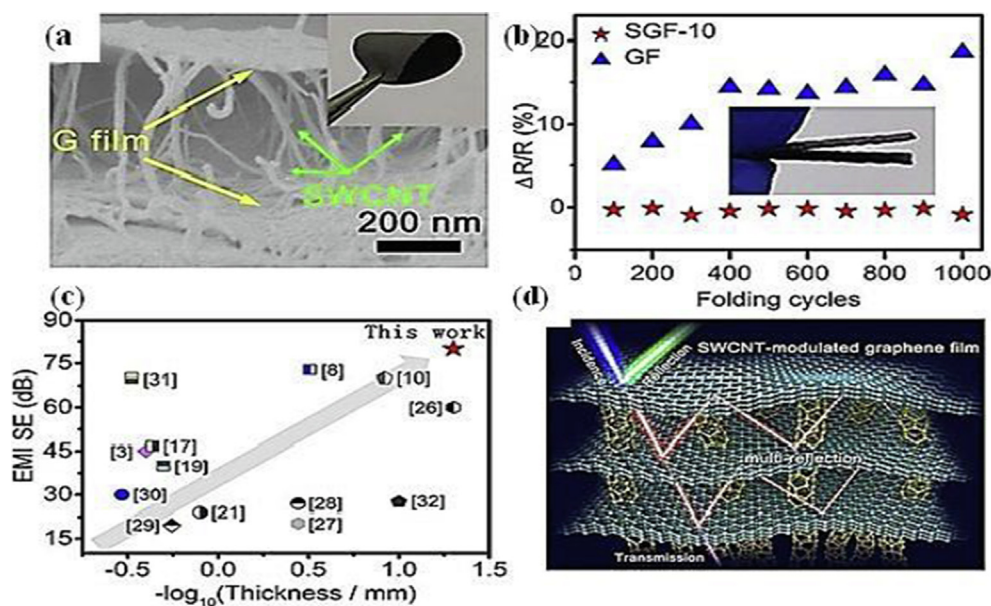


**Fig. 15** CNT-graphene oxide (GO) based porous aerogel converted into rGO-CNT based 3D structures of nanocomposites via sequential hydrothermal reduction (a), rGO-CNT decorated graphene films; conductivity (b), and EMI shielding effect (c), and computerized simulated image for rGO based layered assembly loaded CNT (d). Reproduced with copyright permission by Elsevier 2020 (Fu et al., 2020).

materials as reported in previous studies (Huang et al., 2021; Duan, 2022).

Whereas, the resultant composite were also find to be highly water repellent and flame proof ability of rGO and MXene as compared to barely used materials. The synergistic effect is attributed to MXene and rGO films with similar behavior before reduction as (GO) and MXene are composed of similar chemical nature i.e hydrophilic behavior; which is due to the reduction of GO into rGO via elimination of oxygenated reactive functional (OH) groups from the surface of GO (Zhang, 2021; Cai et al., 2021). The attributes, are highly beneficent for resultant admixture and development of such composites for EMI shielding and other broader range of applications (Yan, 2018). The newly developed  $Ti_3C_2T_x/rGO$  porous assembly in the form of composite films generosity longer lasting thermal stability, improved electrical conductivity ( $\sigma$ ) & EMI shielding performance (SE) (Yan, 2018; Cui, 2022). The environmental steadiness was greatly improved, which indicates a pronounced and probable use in various fields as ultra-thin, light and highly flexible EMI (SE also development of highly flexible instruments as presented in Fig. 16 (a & b).

Hence, the use of different 2D nano-materials in the form of 3D aerogels, hydrogels and porous hybrids is an alternative and effective method being used to fabricate the high-performance MA materials. The developed hetero structure in the matrix of the composite has higher interfaces and propels the magnetic loss mechanisms to overcome the problems of the 2D material by attenuating the electromagnetic energy as presented in Fig. 16 (c) (Duan, 2022; Zhang, et al., 2021).

However, the performance and reflection loss of  $-20$  dB of such nanocomposites is ranging from 7.0 to 17.5 GHz by refining the Debye relaxation. The graphene and epoxy resin

demonstrates the replication loss of  $-14.5$  dB over a frequency of 18.9 GHz; which may attribute to the change in multiple poles for the polarization of interfaces inside the nanocomposite material (Lan, 2022; Zeng, 2022). The production of GO based assembly of hybrid lamellar membranes has been developed with controllable layered structures to accomplish high performance microwave and EMI (SE). The interlayer spacing of the GO films in the membranes is controlled by using  $TiO_2$  interpolate by different sizes and shape, while the stability of rGO membranes is improved by compressing with Polyethylenimine (PEI); as presented in Fig. 17 (a & b) (Saini and Aror, 2012; Lan, 2022; Liu et al., 2021; Luo, 2021).

The graphene and other 2D materials have such attributes as compared with traditional metal-based materials against the shielding effectiveness. Therefore, due to the limited use of metal complexes; which can only be reduced by using various conductive polymers, and their nanocomposites with different two-dimensional materials; and are considered as high flexibility, light weight, low cost and corrosion resistance due to the water and mist Fig. 17 (c-f) (Lan, 2022; Zhang, 2019). Though, the existing problems are still under investigation and considered as it become a global challenge; and being studied towards further improvements in the synthesis, fabrication and development of (electromagnetic/dielectric) materials composites. The developed nanomaterials and meta materials could effectively work under a versatile range of microwave and electromagnetic shielding with satisfactory shielding performance (Xu, 2021). Since, CNT and graphene with PDMS/PI as 2D material foams, fibers and aerogels are typically much more efficient to absorb in-plane than out-of-plane polarized waves. Keeping the polarized light and wave's in-plane in 2D material foams as a critical factor other than coupling for the enhancement of MA (Zhang, 2022). The systems are

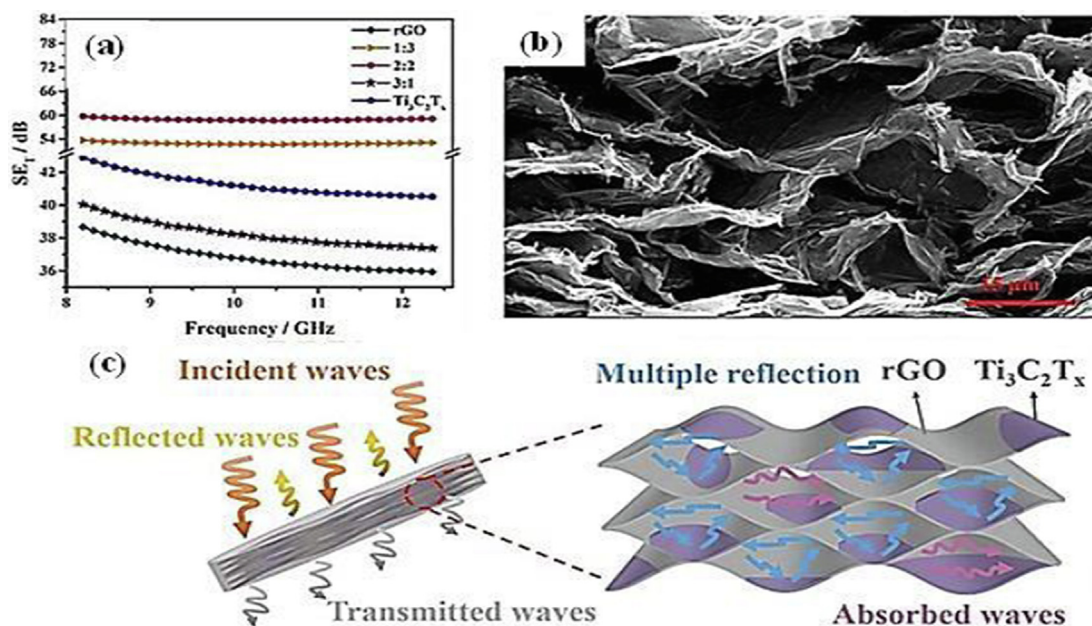


**Fig. 16** EMI shielding performance of Graphene films loaded with MXenes films (a), SEM Images of segregated multiple layers (b), and EMI shielding design with simulated image of rGO and simulated image of MXene films (c). Reproduced with copyright permission by Elsevier 2021 (Zhang et al., 2021).

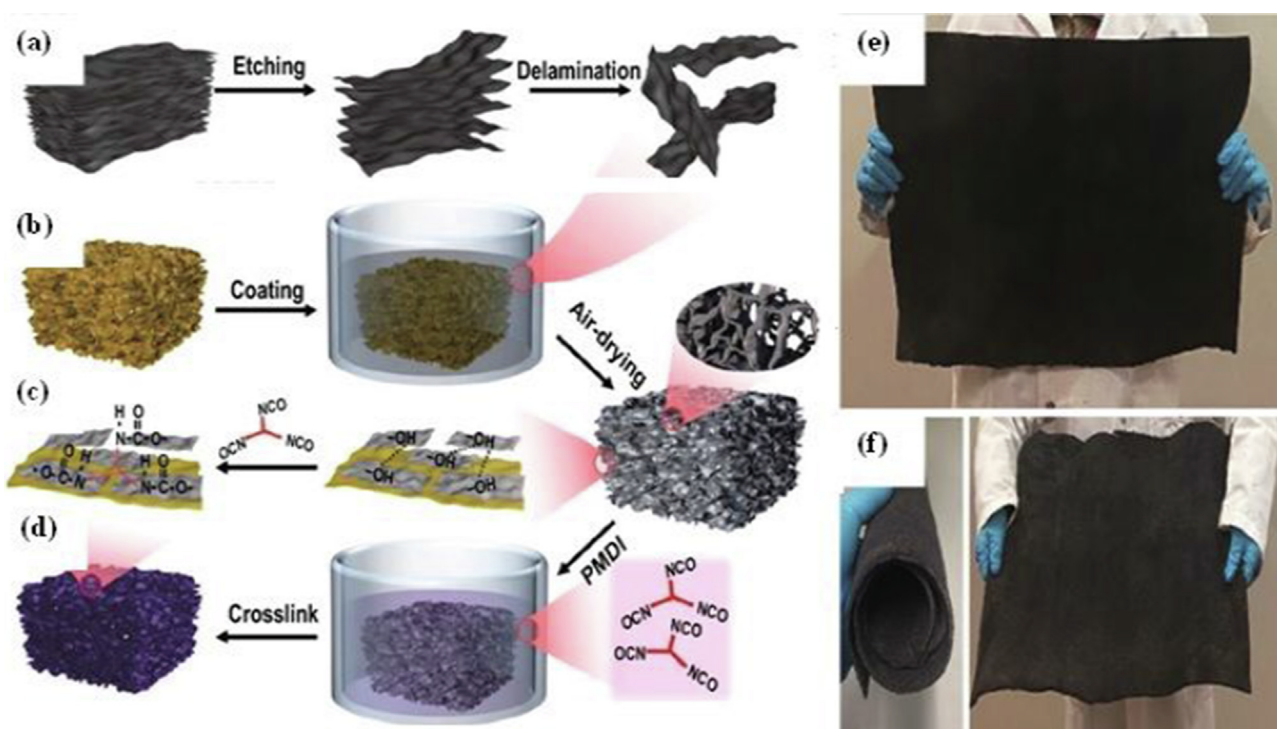


**Fig. 17** Scalable synthesis and fabrication of carbon coated MXene over PI composite (a), MXene films coated via air drying approach (b), Carbon and MXene/PI composite foam(c), Carbon and MXenes with reactive functional groups present on the modified surface mixed with PMDI (d), MXenes and PI coated fabric surface before (e), and after rolling and stretching of fabric (f). Reproduced with copyright material Springer 2022 (Zeng et al., 2022).

integrated with variable architecture and structural assemblies' i.e foam, fibers, modified with dopamine and poly dopamine (PDA) as shown in Table 3.

### 3.1.2. Graphene/metal-non-metal polymer-based composites

Metal-organic framework (MOF) during the construction of this item, the method of layering carbon fiber (CF) on the sur-

**Table 3** Comparison EMI shielding effectiveness of different polymer composite with rGO as a filler material (Zeng et al., 2022).

Materials	EMI SE (dB)	Density (mg cm <sup>-3</sup> )	Thickness (mm)	SSE (dB cm <sup>3</sup> g <sup>-1</sup> )	SSE/d (dB cm <sup>2</sup> g <sup>-1</sup> )
C-MXene@PI foam	43.7	41.0	0.5	1066	21,317
Ag NWs/PI foam	17–23.5	22	5	1068–772	2136–1544
CNT/PI foam	41.1	32.1	2	1280	6402
MWCNT/PI	13.0–14.3	470	0.5	28–30	553–609
rGO/PI foam	13.7–15.1	460	0.5	30–33	596–657
MWCNT-CNT/rGO/PI foam	16.6–18.2	440	0.5	38–41	755–823
CNT/graphene/PI foam	28.2	20	2	1410	7050
Graphene/PI foam	22	280	0.8	78.6	982
Anisotropic graphene/PI foam	26.1–28.8	76	2.5	343–379	1373–1518
Graphene/PI foam	13.7–14.9	430	0.5	32–35	637–693
Graphene/PI film	31.3	~ 1200	0.151	26	1727
Carbon nanofiber/PI film	12	~ 1200	0.07	10	1429
Carbon nanofiber/carbon black/PI film	23.9	~ 1200	0.35	20	571
PI derived carbon foam	54	91	2	593	2965
Graphene/PI-derived carbon foam	24	720	0.024	33	13,888
MXene/PI porous film	54.5	390	0.09	140	15,527
MXene/nanocellulose film	24	2000	0.047	12	2647
MXene/CNF film	33	2477	0.0009	37	148,000
MXene/CNF foam	75	0.008	2	9320	46,600
MXene/PVA porous film	26	~ 545	0.1	48	4770
MXene/PVA foam	28	0.0108	5	2586	5136
MXene/ANF	28	1250	0.02	22	11,200
MXene/SA film	57	~ 2317	0.008	25	30,830

face is a MOF. MOF loaded on the surface of the rice fragmentary structure homogeneous structure. MOF opposite interface shear strength (IFSS) with a surface energy of 70.30 % Sum 69.75 %. After the MOF, the effective CNF showed the interfacial ability, and the primary effect rate of 97.01 %. In the future, effective CNF is possible (Zhang, 2019). In the rGO-Ns-like rings made of oxide solution is vaporized and melted in parallel at 180 °C, and solidified at 0.6 MPa. The developed nanocomposite rGO-Ns-epoxy, in which the graphene (Nitrogen) *n*-doped rGO-N is reduced with hydrazine via vapor phase method. The developed composite with different weight percent of rGO-Ns are attributed with improved mechanical and the effective performance (EMI) coverage (Shi et al., 2021). Consequently expression of the given rGO, the flexure performance is encountered by the addition rGO-Ns possible improvement in EMI suppression effect performance. GO has lower oxygen content as compared to rGO; showed an improved interfacial performance; which is caused by rGO-N doped porous like films (Deng, et al., 2021; Du, 2022).

In another work, MXene aramid fiber decorated 2D fibrous composites aerogel assembly was developed using simple dipping and solution casting method. The developed composite assembly with thickness of 2 mm and showed 80 % (SE) with reflection loss of 21.5 dB/mm (Wang et al., 2020). Typically carbon coated PVA fibers showed an efficiency of composite materials have higher reflection loss and main electromagnetic interference. It is possible to move freely in the inner layer of the composite material, and the ability to cover the electromagnetic interference. (Yu et al., 2022). The rGO/PI-CNT composites were prepared by incorporating rGO into the PS polymer matrix as demonstrated in Fig. 18 (a & b). Similarly, the CNT-PU based paper was developed via electrodeposition method. The developed nano composites showed and efficient

EMI (SE) of 60.0-65.5 dB. The developed composite Bucky paper showed highly efficient shielding (SE) performance through a simple electro deposition approach. The designed composite Foam represented an outstanding shielding efficiency of 60–65.5 dB in X-band with minimum thickness of 100  $\mu$ m, which is best ever as compared to previously reported findings for MXene, CNT-PU and graphene-PI-Adamine based porous foam composites Fig. 18 (c & d) (Liu et al., 2021; Fan, 2021; Lu et al., 2021; Amini et al., 2021).

Conductive polymer nanocomposites (PNCs) were prepared by adding Cu NSs to rGO/PS composites. The results also demonstrate that these PNCs have EMI shielding; the shielding efficiency of 36.0 dB at 8.0 GHz and 29.5 dB at 12.0 GHz. In the frequency range and percentage of fillers studied, the dominant protection mechanism was reflective. Eventhough, the distance between rGO membranes can be prolonged by using intercalation to improve the permeability (Thadathil et al., 2022). Achieving a uniform intercalation without the addition of fillers for porous media is under investigation, to increase the proliferation of EMI waves. The preparation of elastic porous films with high compressibility and facile fabrication processes is one of the most popular hot-pots especially for electromagnetic shielding and microwave absorption is under investigation and still facing great challenges (Sang, 2022). Similarly, graphene and silver nanocomposites (rGO-AgNWs) as solgels and PU-hydrogels has been developed and used for improved EMI shielding. The developed nanocomposites are highly conductive, flexible, bendable, and are stretchable with improved tensile strength (Xu, 2021). The microwave and shielding performance (SE) of the graphene-based nanocomposites is also improved with the addition of different metal-organic frame works (MOF), with graphene oxide and reduced graphene oxide as shown in Fig. 19 (a-e). A novel and green one-step (In-Situ) thermal

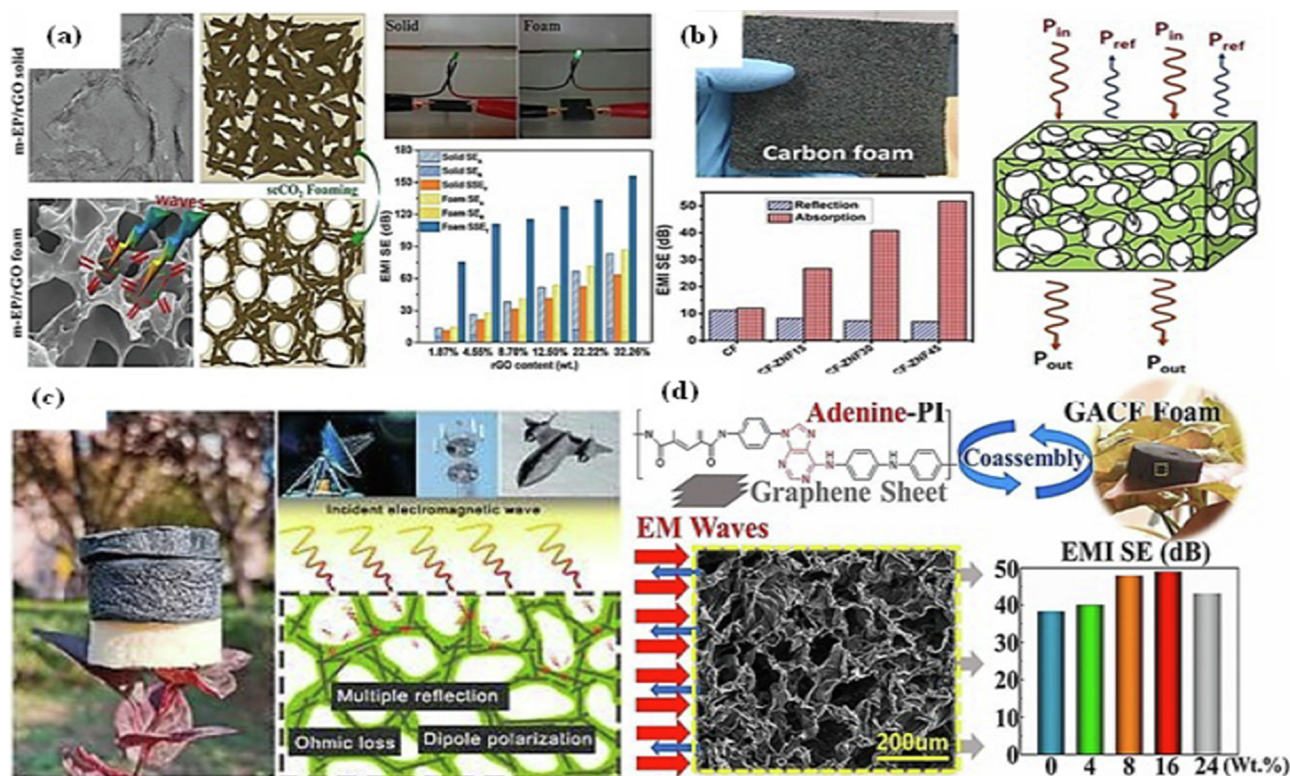


**Fig. 18** (a) Graphene based rGO/PVA aerogels nanocomposites aerogels foam structure reproduced with permission Elsevier 2021 (Fan et al., 2021), (b) carbon foam via PU impregnation method; reproduced with the copyright permission of Elsevier (2022) (Sharma et al., 2022), (c) MXene and aramid nanofibers aerogels; reproduced with copyright permission by Elsevier 2021 Lu et al., 2021 and (d) Adenine-PI polymer and graphene foam for EMI (SE). Elsevier 2021 has granted permission to reproduce this Figure (Luo et al., 2021).

treatment approach have been used to fabricate the lightweight silver/rGO-coated melamine carbide (NFC/rGO/PU-PDMS) films and porous foams with superior mechanical properties and excellent EMI shielding effect (SE) (Wei, 2022). The NFC/rGO/PU-PDMS based MXene and graphene based polymer composites (MGP) foam exhibits excellent structural stability after 1000 load-unload compression test cycles; due to the enhanced interface of rGO between the NFC framework and silver nano particles showed better stability against mechanical detrition (Xin et al., 2021). However, graphene oxide (GO/MXene-PU) and rGO-MXenes based aerogels are encouraging materials for advanced applications for example; batteries, supercapacitors, filtration and electronic devices for microwave and EMI shielding; but still there is a great demand to improve the performance stability (Bai et al., 2020). Although; the interlayer distance of rGO-MXene-PU aerogels can be expanded by using intercalation to increase permeability, achieving uniform intercalation without the addition of fillers and removal from the porous media to improve the propagation of electromagnetic waves (Cao, 2019). The preparation of elastic porous films with high compressibility and facile fabrication processes is one of the most popular hotspots especially for EMI and MA is under exploration and facing great challenges. Similarly, graphene and silver nanocomposites (rGO-AgNWs) as solgels and PU-hydrogels has been developed and used for improved EMI shielding. The developed nanocomposites are highly conductive, flexible, bendable, and are stretchable with improved tensile strength. The micro-

wave and shielding performance (SE) of the graphene-based nanocomposites is also improved with the addition of different metal-organic frame works (MOF), with GO and rGO (Sun, 2021; Srivastava and Manna, 2022). Another work was used to determine by practicing a novel method for the construction of graphene on micro-cellular level with epoxy and attained the long-lasting performance in the designing of the nanocomposites with dispersion of CNT in GO and epoxy resin to develop nanocomposites structures as shown in the Fig. 19 (a). The designed nanocomposite has been developed by utilizing a supercritical CO<sub>2</sub> foaming approach; in which the epoxy based composite was modified nanocomposite was effervesced showed a multiple boundaries and finely tunable cellular structures (Song, 2017; Zheng, 2021). Furthermore, the re-organization of nano filler during formation of foam structure which is reasonable with more intense conductive framework, and leading to improved microwave attenuation with higher dielectric loss and repeated reflection loss to improve the microwave absorption. The optimistic combination of electrical conductivity of 314 S m<sup>-1</sup> and effective shielding of 86.6 dB and 156.3 dB/(g/cm<sup>3</sup>) was attained with mechanical performance of (27.5–30 MPa) and density of (0.55 g cm<sup>-3</sup>) has been achieved for the foam structure of the resultant composite containing 30–32 % wt% of graphene as filler (Liu et al., 2016).

The research was used to develop a novel and lightweight carbon foam (CF) adorned with ZnO nanofibers (NF) for highly stable and improved EMI shielding. Initially, the car-

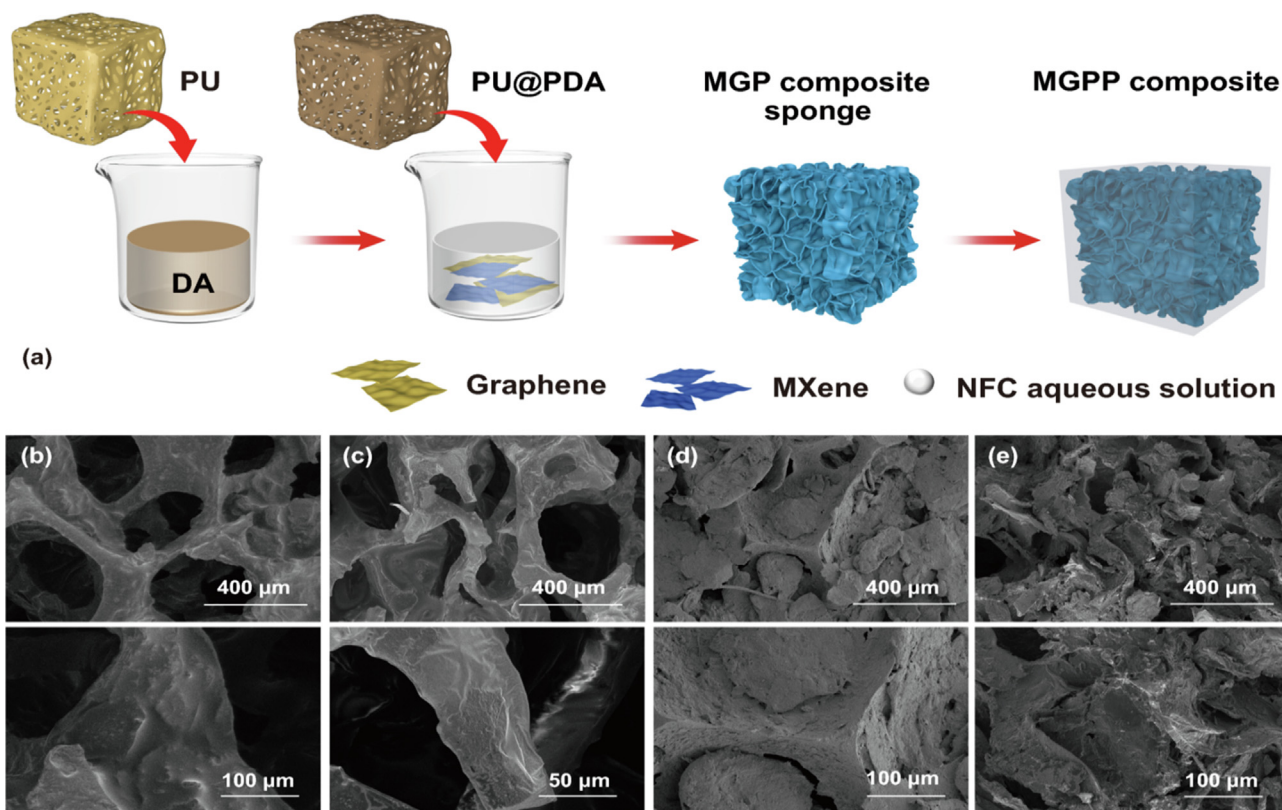


**Fig. 19** Process for fabricating MGPP composites (a), surface SEM images of PU (b), PU@PDA (c), MGPP100 composite sponges (d), and MGPP100-3 composite sponges and their corresponding magnification images (e), reproduced with copyright materials by Springer (2022) (Jin et al., 2022).

bon fibers (CF) were synthesized from a phenolic based resin using the polymer polyurethane (PU) to develop foam through an simple mixing method trailed by carbonization, and finally the CF were decorated with an electrospinning method (Jin et al., 2022). The (SE) and comparative multifaceted permittivity of the ornamented froths were studied by vector network analyzer in X band over a frequency range of (8.2–12.4 GHz) for a minimum thickness of 2.0 mm. It is revealed from the findings of experimental analysis, that the porous assembly of ZnO-NF can significantly improve overall EMI shielding effectiveness, with enhanced microwave absorption. The impedance matching and interfacial polarization delivered by the porous structure and ZnO nanofibers which leads to improve the EM wave absorption performance in CFs due to the decoration of ZnO on the surface of NF. The resultant CF exhibited excellent absorption-dominant with an EMI SE of 58.6 dB and a specific EMI SE of  $1046 \text{ dB cm}^2 \text{ g}^{-1}$  at only  $0.28 \text{ g/cm}^3$  density (Li, 2022; Liang, 2016).

Thus, the lightweight ZnO decorated CF is a promising material for aerospace and next-generation smart devices. Similarly, the work made on the production of porous carbon based foam structure showing an improved EMI performance was successfully designed from graphene oxide (GO) and adenine-polyamide fibers (Zhu et al., 2017). The development of graphene with conductive framework; which showed higher retention of EM waves with regulated conversion of nitrogen doped films to enhance the films porosity. Whereas, the graphitization was successfully made by the carbon layers; which resulted as an improved electrical conductivity of (0.22–0.55

$\text{S/}C\text{m}$ ). the x-band valued to (8.5–12.5 GHz) as out performance shielding (SE) performance increased to 48.5 dB as well SSE to 8375.6 dB SSE ( $8370.8 \text{ dB cm}^3/\text{g}$ ), and SSE/d ( $19789 \text{ dB cm}^2/\text{g}$ ) (Gao, 2020). Moreover, the carbon based foams exhibited firmness towards cyclic retention and recover ability against the MA and EMI shielding capability in the organic solvents. The overall performance (SE) and microwave shielding enhanced with higher aspect ratio and filler content percent of 2D materials including (MXene), boron nitride (hBN), and graphene with epoxy resin as a binder (Wan et al., 2018; Wu et al., 2020). The significant effect of epoxy assists in self-assemble nanowires and developed nanocomposites decorated glass fibers could help in self-bridging and more conductive paths, towards improved, electrical, mechanical and shielding performance. More significantly, the developed aerogel retains a high EMI-shielding presentation of up to  $\sim 45.2\text{--}65.0 \text{ dB}$ , which may attribute to its unique assembly showing better electrical and thermal properties. Additionally, the EMI SE of the designed foam reaches up to 50.6 dB only at a density of  $16 \text{ mg cm}^{-3}$ . The resultant composite has a stabilized specific surface area (SE) with as high as EMI shielding outperformance of  $76.16 \text{ dB cm}^2 \text{ g}^{-1}$  over a very lower content percent (Zhang, 2021; Nazir, 2018). In addition, the high disintegration temperature ( $T_d$ , 10 %) of  $600 \text{ }^\circ\text{C}$  showed a great advantage as compared to previously reported PI-based composite materials. These characteristics endorse the prospective of CNT/graphene/PI foam as a lightweight, compact, and heat-resistant material, which can effectively shield EMI and absorb electromagnetic waves (Zhang, 2019, 2020; Zhang,

2020). Similarly, in previous studies a new method for high-performance shielding materials; by MWCNT homogeneously in-situ synthesis with conductive polymers and pristine graphene. Whereas, the rGO sheets are connected with  $Ti_3C_2Tx$  films and loaded nanoparticles on the catalysis of nickel, copper, aluminum or silver layered; which can be directly covered into aerogels and can be applied on the carbon cloth as a binder-free approach as shown in Table 4.

### 3.1.3. Graphene polymer-based Aerogels/Hydrogels composites

Herein, acrylonitrile butadiene styrene (ABS) porous materials foamed by etching and post-etching supercritical  $CO_2$  (SC- $CO_2$ ) was prepared and proposed for shielding effective utilization for electronic applications. The newly designed ABS porous and conductive composites were synthesized via addition of conductive filler of carbon black (CB) (Wu et al., 2017). The outcomes showed that, as the content percent of polyethylene oxide (PEO) was varied in the composite the overall SE performance was increased to 50 hrs. stability. As prepared ABS materials with a SC- $CO_2$  an open-cell with wider spacer structures after foaming and chemical etching. When the CB content reaches 6 %, the conductivity of the ABS porous material prepared by the etching method is  $25.6 \text{ Sm}^{-1}$  after etching. The electrical performance of the ABS porous material foam/films was further improved to  $150 \text{ Sm}^{-1}$  with EMI shielding performance of 23 dB. In brief, the electrical conductivity was greatly influenced and improved when the filler content percent was increased more than 6 %. The electrical conductivity of the ABS aperture materials prepared by the two folds of magnitude by using both of the methods reached to 150–650  $\text{Sm}^{-1}$ , and the highest EMI shielding was reached 32–65 dB (Yang, 2021; Luo, 2022). The developed foam has great potential in electronic and EMI shielding presentations. A lightweight melamine-formaldehyde-based materials showing substantial EMI shielding properties; developed through a facile and green synthesis of conductive electroless silver (Ag)

plating and Polydimethylsiloxane/ $SiO_2$ (PDMS/ $SiO_2$ ) coating method composite ( $SiO_2@Ag@MF$ ) foam. The results show that  $SiO_2@Ag@MF$  foam has excellent EMI shielding performance with an extreme shielding efficiency (SET) of 65 dB, with a lower density ( $0.014\text{--}0.019 \text{ g/cm}^3$ ), and higher SP efficiency (due to the open-cell having more wider space and porous structure). The resultant composite demonstrated a higher conductivity for a silver-plated skeleton, (SSE  $\tau$ ) of  $34.39 \text{ dB cm}^3 \text{ g}^{-1}$ . At the same time, the syntactic foam is superhydrophobic, anti-corrosion and anti-fatigue properties due to PDMS and  $SiO_2$  coating (Wu et al., 2017). The combination of carbon nanotubes and reduced graphene oxide as a lightweight and higher electrical conductivity with improved mechanical performance is acquiring higher demand for macro-micro scale graphene based composites, films, foam and aerogels. Therefore, the carbon nanotubes and graphene oxide as demonstrated in Fig. 20(a), are prepared by simple and cost effective method freeze-drying and in-situ catalytic growth methods (Gao et al., 2021; Luo, 2021). The carbon nanotubes and graphene based foams comprising of higher interconnection of rGO sheets with each other through CNT as bridging groups to develop 3D structure, showing significant growth towards EM and MA performance. Whereas, the graphene sheets has been grown on metallic and polymeric substrates. The in-situ progress containing graphene films loaded CNT leading to an enhanced EMI, shielding through conductive paths, and defect induced polarization loss. The designed nanocomposite made from CNT/rGO showed greater interaction with rGO nanocomposite as 3D heterostructure developed via in-situ growth of CNT on rGO films (Zhang, 2019; Xu et al., 2022).

The composites foams made of CNTs/rGO with variable filler content percent of CNT in rGO are prepared to study the effect on EMI shielding properties over a variable range in X-Band. The effective shielding (SE) performance of composite was nearly 31.5–23.5 dB with minimum thickness of

**Table 4** Effect of thickness of various polymer based nanocomposites for EMI shielding and EM loss mechanisms of different dimensional carbon nanomaterials (Huang et al., 2021).

Dimension	Carbon Materials	Microstructure	Electromagnetic Loss Mechanism
1D carbonaceous materials	CNT/cellulose	Film	Dielectric loss, multiple reflection
	Cds-CNT	Core-shell	Dielectric loss, interfacial polarization
	ZnO@MWCNT	Hybrid	Interfacial polarization, impedance matching, and dielectric loss
	Ag nanowire/Carbon fiber	Fabric	Conduction loss, multiple reflection and scattering
	Carbon fiber/SiC	Hybrid	Conduction loss, reflection at various surface or interface
	Carbon fiber/ $Si_3N_4$ Carbon fiber	Hybrid Hollow	Electronic relax polarization, conductive loss, impedance Hollow structure accelerates the increasing rate part while lowering that of the imaginary part
2D carbonaceous materials	rGO/cellulose	Film	Multiple reflection loss, dielectric loss
	rGO	Film	Dipole polarization originate from few defects, better alignment of the large area
3D carbonaceous materials	rGO	Nanosheet	Dielectric loss, impedance matching
	Polyetherimide/rGO	Sponge	Multiple interface reflection, dielectric loss
	MWCNT/WPU	Foam	Multiple reflection loss at various surface and interface, conduction loss, dielectric loss
	Epoxy/carbon nanotube	Sponge	Conduction loss, abundant interfaces that multiply the reflection
	MWCNT/Graphene PANI/GO	Foam Aerogel	High loss multilevel network architecture Impedance matching, multiple reflection, electron polarization

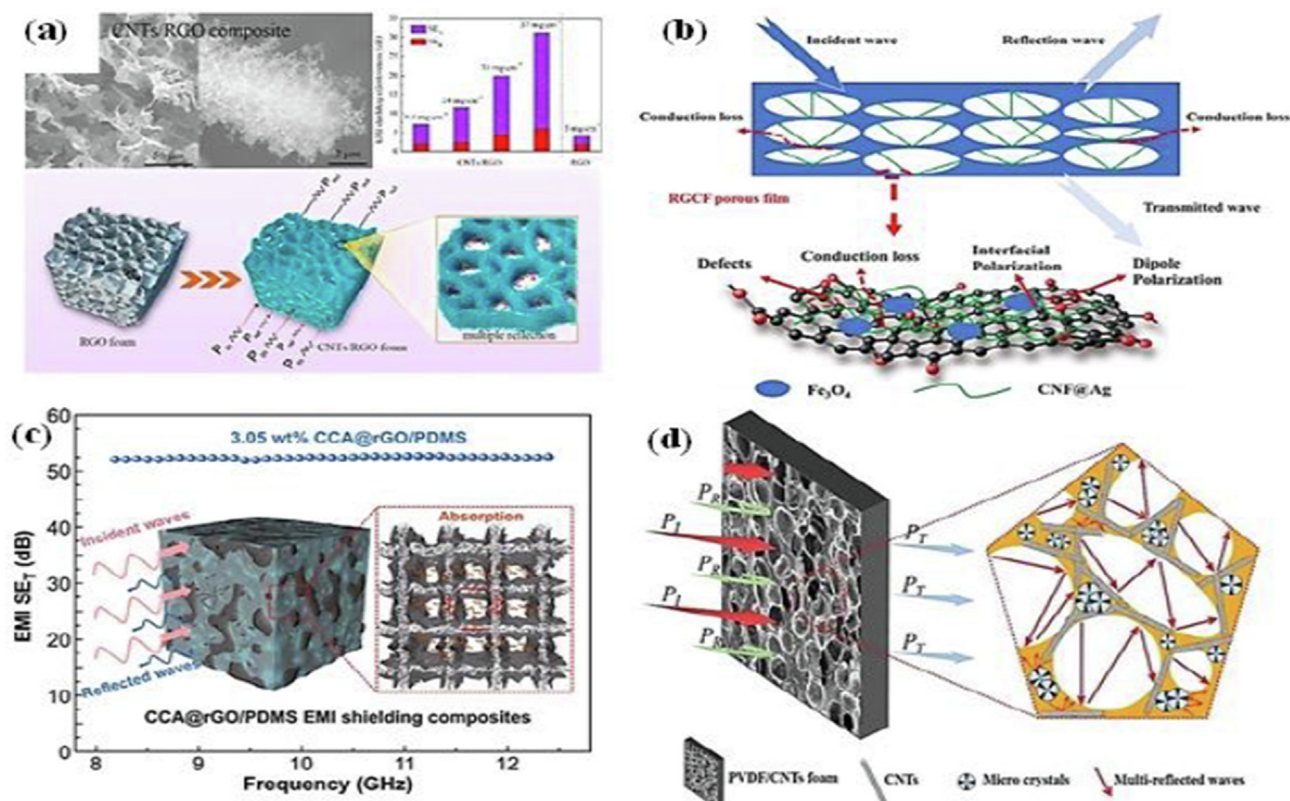


**Fig. 20** Preparation of graphene & carbon nanotubes (CNTs-rGO) and rGO/CNF@Ag-Fe<sub>3</sub>O<sub>4</sub>(rG-CF) porous film for EMI shielding application mechanism. Images were reproduced with the copyright materials by (a-Elsevier 2019 & b-Springer Nature 2020) (Guo et al., 2020; Kong, 2019), lightweight reduced graphene oxide, PDMS and flexible cellulose derived Carbon aerogel (c). This figure has been reproduced with the copyright permission by Springer Nature (2021) (Song et al., 2021), and Carbon nanotube-PVF nanocomposites for EMI. (d). The Figure has been reproduced with the copyright permission by John Wiley and Sons 2021 (Dun et al., 2021).

2 mm; which reaches up to EMI-SE of 547.0 dB cm<sup>3</sup>/g having an ultra-light density of 55–57 mg/Cm<sup>-3</sup>. Additionally, the shielding efficiency (SE) was reached around 49.6 dB with variable size and thickness of 3.1 mm. The developed 3D porous structure as shown in Fig. 20 (a) shows a unique hierarchical structure and a light density with outstanding SE performance; it showed a auspicious and desirable approach for the design and development of CNTs/rGO composite foam for micro-waves absorption and EMI shielding materials (Zhang et al., 2018). In addition to the optimizing the of flexible and wearable CF-based materials has excessive prospective in the applied solicitation of EMI shielding. The presented work be responsible for comprehensions interpretation on the design and production of EMI shielding with broader application.

Furthermore, to elaborate the structural design of such microstructural materials is suitable and critical to obtain a cutting-edge EMI shielding effectiveness, which is obtained to make lightweight, highly flexible, durable, and processable. In brief, the genetic dielectric genes from rGO, including defects and functional groups, are identified, and the interfaces generated from Fe<sub>3</sub>O<sub>4</sub> nanoparticles are dissected based on previous works. Through the tailoring of Fe<sub>3</sub>O<sub>4</sub> content, temperature, and spatial distribution, the microwave absorption is flexibly adjusted, with a R<sub>L</sub> of - 59 dB and a - 10 dB BW of ≈4 GHz. Significantly, benefiting from the synergy between the dielectric genes and the magnetic medium, the matching thick-

ness is as low as 1.17 mm. These important results are a powerful supplement to basic knowledge of high-temperature electromagnetism, laying a foundation for the construction of electromagnetic functional materials and devices that adapts to the environment at elevated temperature (Zhou, et al., 2020; Zhao, 2018).

However, on the other hand, the relationship between the mechanical attributes as well as shielding effectiveness for EMI material are related; especially based structural orientation and hierarchal composition of an ultrathin and porous assemblies based composites for suitable end uses. The work presented on light weight and highly flexible rGO base composites of rGO/CNF@Ag-Fe<sub>3</sub>O<sub>4</sub> (RGCF) as porous media for efficient EMI shielding application as shown in Fig. 20 (b). The assembly was designed using most widely used technique; vacuum filtration approach after chemical and thermal reduction. The graphene carbon fiber based porous structure exhibited an outstanding mechanical performance with tensile strength of 175.5 MPa, and composite showed a light weight RGCF as porous films with 20–21.0 dB; which much better than the compact films having 10.5 dB and an efficient wave attenuation properties on single cell level. Therefore, the highly flexible and light weight RG-CF as porous film with applicable EMI range of SE performance over a superior mechanical tensile strength as a promising candidate for smart and flexible wearable electronics (Zhao, 2018; Ryu, 2022).

Similarly cellulose based cotton composite fabric showing higher chemical bonding to develop a self-assembly of cellulose acetate (CA) self-assembly loaded with (NaOH) solution, subsequently developed via gelation and free drying method. Later on, the cellulose coated carbon fiber based aerogels covered the surface by rGO to develop CA/rGO aerogels are prepared via vacuum filtration followed by freeze drying and thermal reduction respectively. Finally, the CA-rGO covered with PDMS polymer towards an improved EMI shielding effectiveness of the composite are prepared through back filling of PDMS in polymer matrix. The designed structure owing to skin-core structure made up of CA@rGO, as porous (3D) structure coated with double-layer of graphene as conductive network was successfully constructed as shown in Fig. 20 (c) (Lan, 2022; Zhao, 2018). The study revealed that, the loading of rGO content percent of 3.5 % with CA over rGO and PDMS showed an exceptional EMI shielding performance (SE) 50–52 dB, which around four times greater as compared with the co-mixed CA-rGO and PDMS for microwave and EMI shielding of 13 dB loaded with same filler content percent. Similarly, the CA@rGO/PDMS composites showed an excellent thermal stability and thermal conductivity having coefficient ( $\lambda$ ) of  $0.65 \text{ W m}^{-1} \text{ K}^{-1}$  (Lan, 2022). The resultant assembly showed an excellent performance for CA@rGO/PDMS with EMI shielding of 12.5 dB for designed composites; which showed a great outlook for potential end use applications as highly efficient and lightweight EMI shielding composite material. A porous foam composite was made from poly(vinylidene fluoride) (PVDF) loaded with carbon nanotubes (CNTs) was developed for EMI shielding by using a solid-state supercritical  $\text{CO}_2$  foaming approach has been made so far. The PVDF was selected as a matrix due to its extra ordinary features and an

excellent chemical resistance, thermal stability, and flame retardancy. The incorporation of CNT enabled the composite viscosity and high modulus which at most twice greater than the pure and barely used PVDF as shown in Fig. 20 (d) (Lan, 2022). The EMI precise defensive efficiency of an acquired foams could reached the optimal significance of  $0.024 \text{ S m}^{-1}$  and  $29.1 \text{ dB cm}^3 \text{ g}^{-1}$ , individually, whereas, the instigating from the ongoing expansion of consistent CNTs and conductive network on the cellular assembly as porous media of the PVDF matrix. Stimulatingly, the orientation of CNTs triggered by frothing development marks in percolation threshold of PVDF/CNTs decreased with comparison to the un-foam based samples (Luo, 2022). The carbon fiber with  $\text{MoS}_2$ -carbon fiber ( $\text{MoS}_2$ -CNF) aggregates were produced for the first time by embedding  $\text{WS}_2$ . The designed heterogeneous assembly demonstrated the several imperfections on the exterior of carbon fiber (CF) by by means of a simple one-step hydrothermal method. The nanocomposite assembly was used to protect electronic equipment from electromagnetic waves on broader level. The (SE) performance of  $\text{MoS}_2$ -CNF was expressively enriched, exclusively for the S and C bands and was found to be highly stable against the propagation of thermal and electromagnetic waves up-to a broader range of 2–18 GHz. The typically several parameters including size, thickness of 3.00 mm showed an EMI shielding efficiency of 36.0 dB, which higher than the barely used pristine CF (25.5 dB) as shown in the Fig. 21 (a-e). The shielding performance of different organic compounds with different polymeric substances are presented in Table 5 (Shi et al., 2017; Xu, 2021).

Similarly, the tree-dimensional (3D) hierarchical composition of 2D materials as porous scaffolds may also be integrated

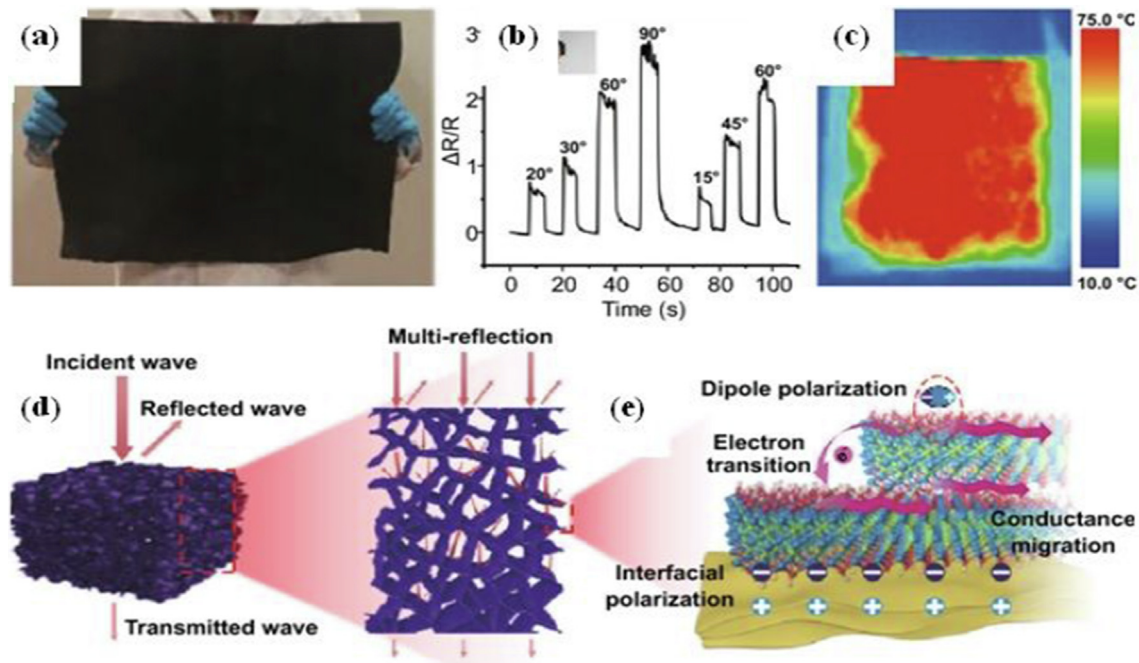


**Fig. 21** Large Scaleable fabrication of MXene based Fabrics(a), sheet resistance response (b), thermo-response (c), shielding mechanism (d), and multiple layered reflection and polarization of developed composite assembly (e). Reproduced with copyright materials, Springer 2022 (Zeng et al., 2022).

**Table 5** Shielding performance of polymer based composites loaded with a different filler loading with 3D conductive networks (Wang et al., 2021).

Nanocomposites	Filler content	Thickness	Conductivity	EMI SE	Frequency
	wt%	mm	S/m	dB	GHz
Ag NWs/PI	4.5	0.029	–	35	8–12
Graphene/PDMS		0.3	3600	83	2–18
MXene@NR	6.71	0.246	1400	54	8.2–12.4
CNTs/Ni@CNTs/	22	0.5	257	51	18–27
rGO/Fe <sub>3</sub> O <sub>4</sub> / cellulose	8	0.16	< 0.1	20.4	8.2–12.4
rGO/PU	10	60	–	40	8–12
CNTs/PDMS	1.74	2	66	43	8.2–12.4
CNTs/PI	67	2	17.1	41	8.2–12.4
MXene/PDMS	6.1	2	2211	71	8.2–12.4
MWCNTs/WPU	76.2	4.5	45	51	8.2–12.4
MXene/PVA	0.15	5	$8.3 \times 10^{-6}$	28	8.2–12.4
rGO/PI		2	1000	83	8–12
Graphene@Fe <sub>3</sub> O <sub>4</sub> /PEI	10	2.5	–	18	8–12
Ag@HGMS/Fe <sub>3</sub> O <sub>4</sub>	0.51	2	279	59	8.2–12.4
NCB/AgNS/epoxy foam	20	2	89	51	8.2–12.4
CNT sponge/epoxy	1.34	2	516	40	8–12
rGO foam/epoxy	1.2	3	40	38	8.2–12.4
MXene/C foam/epoxy	4.25	2	184	46	8.2–12.4
MXene/rGO aerogel/epoxy	0.74	2	696	50	8.2–12.4
Fe <sub>3</sub> O <sub>4</sub> /rGO aerogel/epoxy	2.7	3	27.5	35	8.2–12.4
Fe <sub>3</sub> O <sub>4</sub> -CNTs/rGO foam/epoxy	3	3	15.3	36	8.2–12.4
MXene aerogel/epoxy	0.40	2	416.6	34.5	8.2–12.4
MXene@PS	6.2	2	1081	62	8.2–12.4
rGO@PS	3.47	2.5	43.5	41	8.2–12.4

with silver nanowires (AgNWs) and polyurethane (PU) by mimicking natural leather by using a simple dip coating method over an ambient temperature (Zhao et al., 2017). The consistent micron-scale cavities and distinctive covered construction of such nanocomposites facilitate the homogeneously attached AgNWs and greater protective presentation by considerably aggregate the absorption loss of (98.5 %). remarkably, the leather-like combination demonstrates the paramount EMI shielding effect ranging (~110 dB) from 8.2 to 12.4 GHz) as compared to the natural leather-based materials reported in previous works. In addition, three dimensional (3D) and polyurethane-PU PDMS and CA with CNT and graphene with variable filler loading and thickness towards improved EMI Shielding (SE) are demonstrated (Liang, 2021). Making these composite stable and durable EMI shielding goods; that could withstand and restrict the ultrasonic, alkali, tape peeling, bending and abrasion resistance (Zhao, 2018). Graphene and polymer based composites have the advantages of light weight, informal handling, and outstanding electrical conductivity, and are encouraging entrants as well-designed EMI shielding materials. The conductive polymer are related to a type of materials which are majorly based on reflection loss ( $R_L$ ) and comprising of several advantages for example enhanced electrical conductivity and obviously improved shielding effect and absorption performance. The functionalization and surface modifications are considered as critical factor and important factor during the synthesis and designing an effective shielding (SE). There are several studies has been made to improve shielding performances with addition of different fillers in conductive polymers (Shayesteh Zeraati et al., 2021). So, rather a low fillers content percent is required in the nanocomposites not exceeding 10.0–20 by

wt% of the composite assembly and a very high level of thickness of 2.0–2.5 mm, can be achieved to work better and optimize the nanocomposites M@GAMS with a reflection loss ( $R_L$ ) of – 49.1 dB with a variable frequency range of 14.2–18.0 GHz. Therefore, the scalable technology is needed to reduce electromagnetic pollution from low-density and low-carbon footprint materials. Unfortunately, in most electromagnetic shielding materials, environmental adaptability, economic feasibility and light weight are far from these optimal factors (Li, 2017).

### 3.1.4. Graphene ICPs Polymer-based composites

The incorporation of dielectric and magnetic mechanism is an auspicious approach for the fabricating of EMI shielding materials with exceptional attributes. In order to further improve the shielding ability; while preserving extraordinary fascination presentation and its practical submission with an advanced shielding material (EMI) are instantly involves sensible and comprehensive organizational design (Cao, 2018). In this work, exceedingly permeable and porous nickel based foam (NF) with a macro to micro level builds to develop conductive framework. Then, the polyaniline (PANI) was successfully loaded on the surface of fibrous assembly NF by using a simple in situ fabrication approach. In another study made on addition of small fraction of polyvinyl alcohol (PVA) was used an adhesive, on the graphene (rGO/MXene). When the rGO loaded polymer was produced by using a spun lace non-woven fabric (SNF) technique, in which initially soaked and then dried soaking-drying consequently thermal and chemical reduction technique has been reported so far, the design of the sandwich structure wherein, the SNF sheet was covered with

rGO/MXene asupper and lower deposited with polymer Nano woven sheet as interlayer (Han et al., 2021). The outperformace related toward the EMI shielding effectiveness (SE), having good electrical, thermal and mechanical stability were perceive. On the other hand, the performance is attributed as highly efficient with multifunctional attributes for example the flame retardancy of the fabricated sandwich structure has been investigated. It is revealed from, the results that, when the mass fraction of rGO to MXene was 6:4 the reached to an average  $SE_T$  of 55.8 dB for X-band and also increased the absorption shielding when applied to a voltage of 4.0 V volts to rGO/MXene composite films. The temperature on the surface was exceeded to 110 °C within 10 s, which shows that the fabricated composite film can be functional application including enhanced electromagnetic shielding device with outstanding performance as demonstrated in Fig. 22 (a-c) (He, 2021; Xu, 2019). Similarly, the nanofibers NF/PANF with distinctive (3D) porous heterostructures were created. Even though the thickness is only increased by 2.7 % as compared to original NF, the shielding efficiency of the NPF assembly was greatly influenced and significantly enhanced and reached up to 93.8 dB which can shield  $\sim 99.96$  % of released incident waves as radiation. In precise, among the previously reported shielding materials, NPF has excellent absorption loss per unit thickness characteristics (147.64 dB/mm) (Zhang, 2022). This extraordinary performance can be attributed to 3DPorous heterostructures, existence of plentiful boundaries, and

dielectric-magnetic incorporation in NPFs (Liang, 2021). These properties greatly expand interfacial polarization, dielectric, dipole relaxation, decay constant, and multiple reflections as shown in Fig. 22 (d-f). In brief, the power balance and differentiation among the absorption and reflection attributes of the assembly shows that the waves absorption leads the shielding mechanism. The outstanding widespread shielding ability makes this heterostructure promising for electronic devices. In addition, prototypes for highly efficient and an effective shielding 3D porous heterostructures are studies for last several decades (Zhou, 2020).

### 3.1.5. Graphene/MXene-conductive polymer-based composites

The synthesis techniques used to modify and etching of the MXene structural and functional properties from MX-phase to MXene and their nanocomposites are widely achieved by a combination of different polymers and intrinsic conductive polymers to meet the requirements. The developed nanocomposite showed robust mechanical, hydrophobic and heat insulation towards durable and stable PMMA use without any deformation of the developed aerogel in variable temperature, humid environments. Presently, selection of various metal and non-metal based fillers has been put into practice with conductive polymers. Similarly, the use of intrinsic conducting polymer (ICPs) materials is more reliable and can be used to form highly conductive composites by converting conjugated

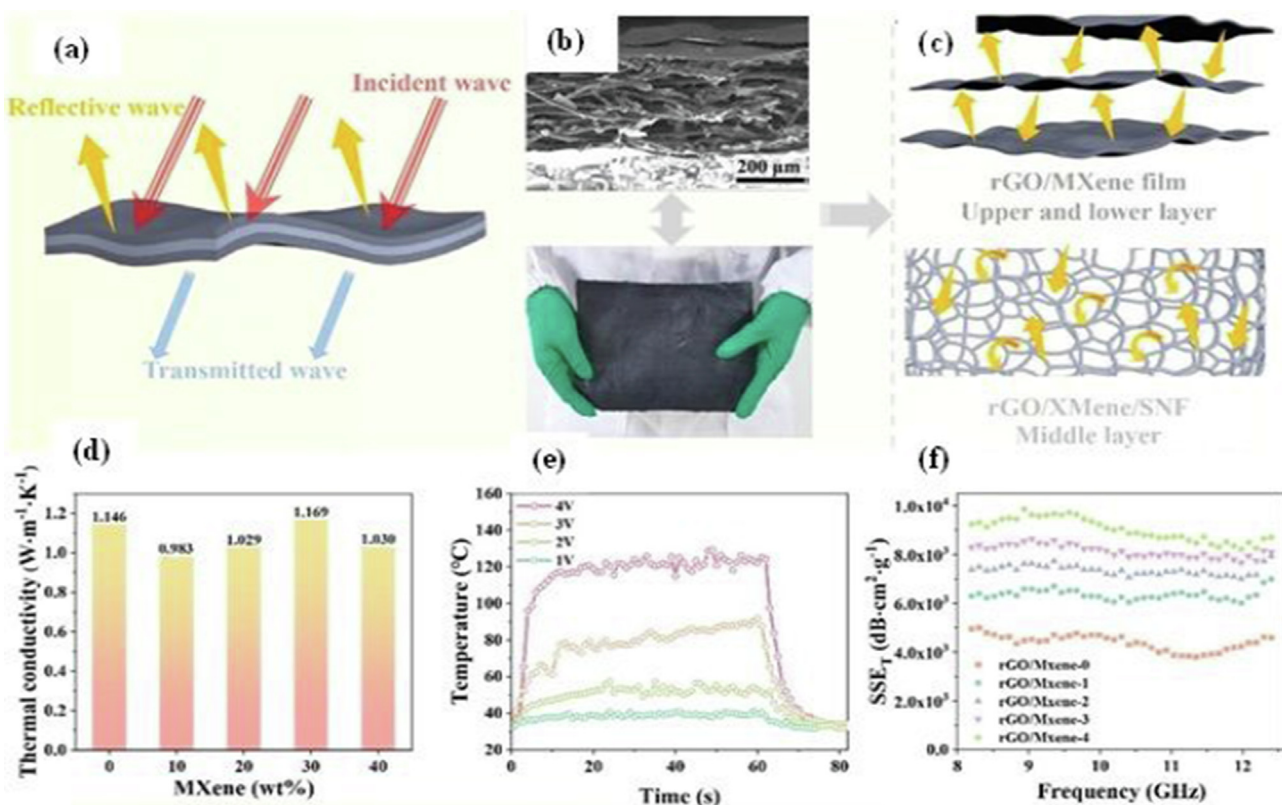


**Fig. 22** Graphene porous films coated MXene coated CNF fibrous assembly design model I for microwave mechanism (a), SEM and digital image of graphene porous films coated MXene coated fibrous films (b), porous MXene and Graphene films with SNF fibers as middle layer covered surface (c), thermal conductivity of MXene with variable wt% (d), effect of temperature on electrical performance of developed fibrous films (e), and SE efficiency of develop fibrous fabric with different rGO and MXene content percent (f). Reproduced with permission of copy right material Elsevier 2022 (Zhang et al., 2022).

$\pi$ -bond polymers into conductors via chemical doping as shown in Fig. 23 (a-e). The results indicate that the total shielding ( $SE_T$ ),  $SE_A$  and  $SE_R$  of the doped PPy and composites have a  $SE_T$  value of 79.9 dB. Further more significantly, the subsequent EMI shielding constituents are primarily recognized from an absorption loss ( $SE_A$ ). The different kind of filler showed great influence on the SE of the developed PPy-rGO based composites. Similar works related to EMI shielding with some other polymeric compounds polyimide(PI) has been reported in another study, without using any binder or thickness used with GO and MXene nanocomposites.

The newly developed robust composite showed better performance as compared to pristine GO-PES and MXene films with maximum EMI shielding response of 12.5–1.0 dB. Whereas, the higher stability and exceptional thermal conductivity as well as electrical conductivity reported with the developed rGO/MXene/PI composite aerogels. The exclusive and distinctive chemical, physical and thermal properties were obtained, when the polymer showed an enhanced bonding and better interactions between GO, MXene nanosheets with PI polymer based precursors (Huang et al., 2019). The resultant 3D structural assembly elaborated improved EMI shielding efficiency over a wide range of microwaves. Therefore, the designed 3D porous assembly showed better feature and considered as a distinguishing material. Similarly, in other work, the graphene and polymer composites (GMP) aerogels were

prepared using a with layered structure followed by a directional freeze drying method. The developed hetero structure have a low power density (8.97–12.71 mg/cm<sup>3</sup>), higher electrical conductivity (3.08 S/m), and incredible adjustable compression and fatigue resistance of (90 %) against 5000–10,000 loading and unloading of the composites (Elmobarak et al., 2017; Kim et al., 2019). Several studies have been reported on the designing of mesoporous, nano-porous and macroporous nano-hybrids with different conductive polymers for the synthesis of hydrogels and aerogels. Such microspheres are designed with the addition of Nanoparticulates in the polymeric substances with greater emphasis on graphene, graphene oxide (GO), reduced graphene oxide (rGO) and Ti<sub>3</sub>C<sub>2</sub>T<sub>x</sub> MXene by rapid ice-freezing technique. Collectively; the core-sheath nano-porous assemblies are attained by incorporation of different metallic particles, with the disparities to develop pores in the conductive polymer/rGO and Ti<sub>3</sub>C<sub>2</sub>T<sub>x</sub> MXene as separated apart from the nanostructures using phase separation techniques (Cao, 2021). A very fine and Lightweight, highly flexible, and conductive porous films were designed from graphene nanosheets, with wider opening of the GO films after chemical and thermal annealing. Therefore, the researchers practiced in several studies mechanically strong, highly flexible and electrically conductive porous films of the reduced graphene oxide (rGO)-Ti<sub>3</sub>C<sub>2</sub>T<sub>x</sub> MXene (rG-M) in the form a regular morphological shape of the films by a chemical treat-

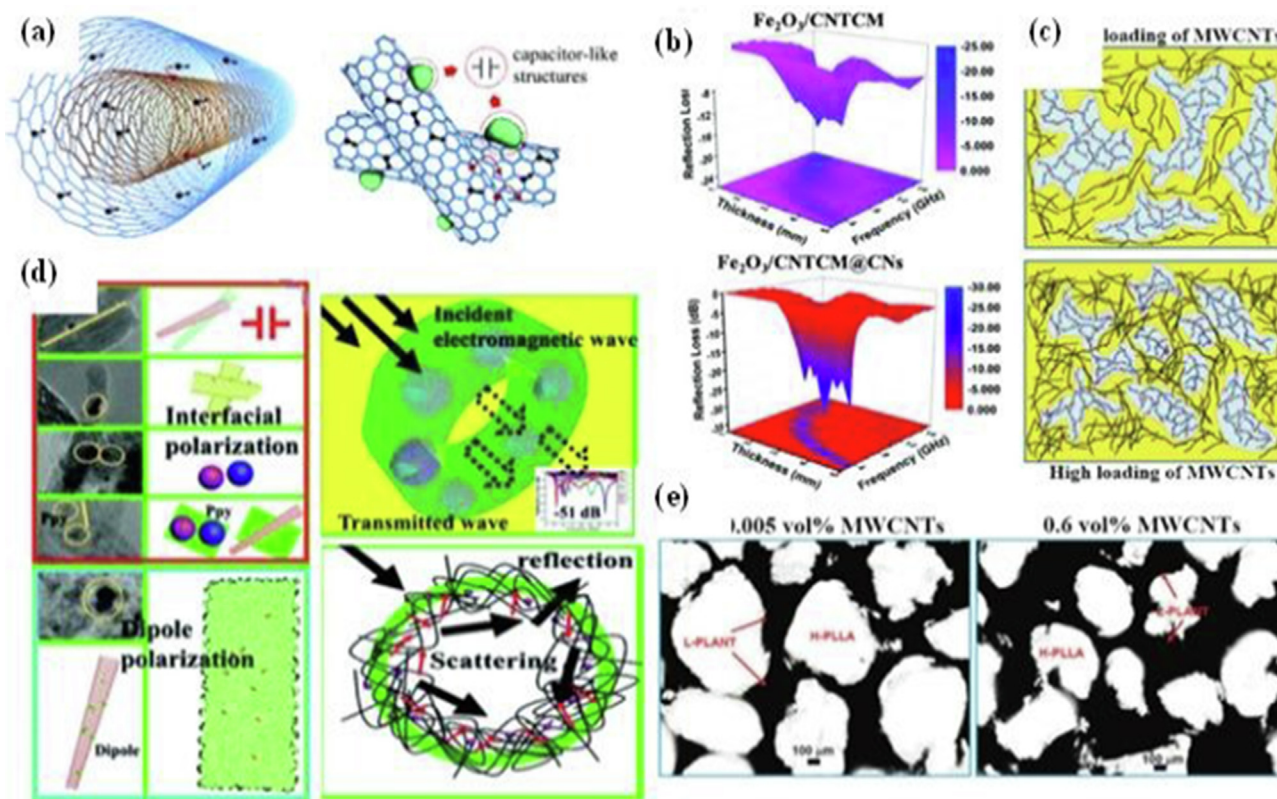


**Fig. 23** MWCNT cross-sectional view of carbon nanotubes as capacitance mode interconnected with each other, schematic of the microwave performance of composites(a), microwave absorption performance of a multi-dimensional assembly achieved by enhanced dielectric relaxation (b), ultralow percolation threshold and EMI shielding multi-walled carbon nanotube nanocomposites (c), with electrically conductive segregated networks (d), PLA-CNT porous films with variable content percent of CNT by Wt% (e). The image was reproduced with MDPI's copyright permission, 2021 (Huang et al., 2021).

ment with hydrazine as reducing agent being used in the synthesis and reduction process. The presence of MXene in the developed composite assisted in prevention of an extreme enlargement of the rGO- with MXene films as demonstrated in Fig. 24 (a-e) (Xu, 2021).

The resultant composites also enhanced the electronic properties, which is due to the availability of conduction channels among the rGO and MXene films, and resulted with an enhanced thermo-mechanical attributes (Xu, 2021). The resultant rGO-MXene films presented highly greater EMI-SE properties as well as mechanical stability of highest tensile strengths (24.5 MPa) among the porous films. These out performances are compared to pristine films of rGO counterpart, and MXene counterparts exhibited an electrical conductivity of  $74.4 \text{ S}\cdot\text{cm}^{-1}$ , and exceptional broadband EMI defensive ranging from 8 to 26.5 GHz (Saghlatoon et al., 2014). At most higher performance towards EMI-SE of 52.5 dB was accomplished by regulating its wideness and handling technique, as long as a practicable production course for inconsequential and highly suitable EMI-performance materials. Similarly, the carbon aerogels with ultra-low density and high mechanical properties were successfully prepared by the GO in the liquid form and crystal formation after reduction with stabile reinforced composites with cellulose nanofibers (CNFs) (Simorangkir et al., 2017). Combination of CNFs into GO and as reduced into rGO nanosheets enrich the interface between rGO nanosheets and CNT without and with using binder, thickeners which could work as soldering effect, thereby limiting the sliding of rGO nanosheets and the separation between microspheres, thereby significantly improving the mechanical properties performance (Rizwan et al., 2017; Razaq et al., 2018).

### 3.2. Metal-carbides (MXene)

During the last one decade, from earlier findings of MXene; metal carbides (Transition metals) carbides and nitrides received great significance and attention by the researchers due to their exceptional properties and variety of use in different uses in various fields (Xu, 2020). MXene films referred as 2D with transition metal oxide and carbides, which containing most effective features due to its diverse electrical, electronic and surface termination attributes, which makes her dominated in comparison to other metal oxides, and two dimensional materials. However, the barely used MXene are rarely used; as individual used of 2D material is very difficult to predict their potential use in EMI shielding and MA, and can only be attained through incorporation of different MOF, and metal oxide. The MXene and graphene are metallically conductive due to its, low band gaps, and high Fermi energy located at the d-bands as compared to other transition metals. Whereas, the most of the conductive 2D materials can be easily transformed and can work as metallic, semi-metallic and even though insulating material, in which these behavior of the such 2D materials can be finely tuned via surface functional groups and chemical modifications. For instance, the bandgaps of  $\text{Sc}_2\text{CF}_2$ ,  $\text{Ti}_2\text{CO}_2$ , and  $\text{Hf}_2\text{CO}_2$  are 1.03, 0.2, and 1.0 eV respectively (Li et al., 2021). However, among 2D materials, the MXene demonstrated favorable properties and potential candidate for EM shielding due to its high electrical conductivity, which is require for better EMI, and MA properties. These attributes of MXene are quite similar and highly attractive for the functional uses of graphene and MXene based nanocomposites on broader spectrum. Last but not least, the use of MXene ( $\text{Ti}_3\text{C}_2\text{T}_x$ ) films could be successful

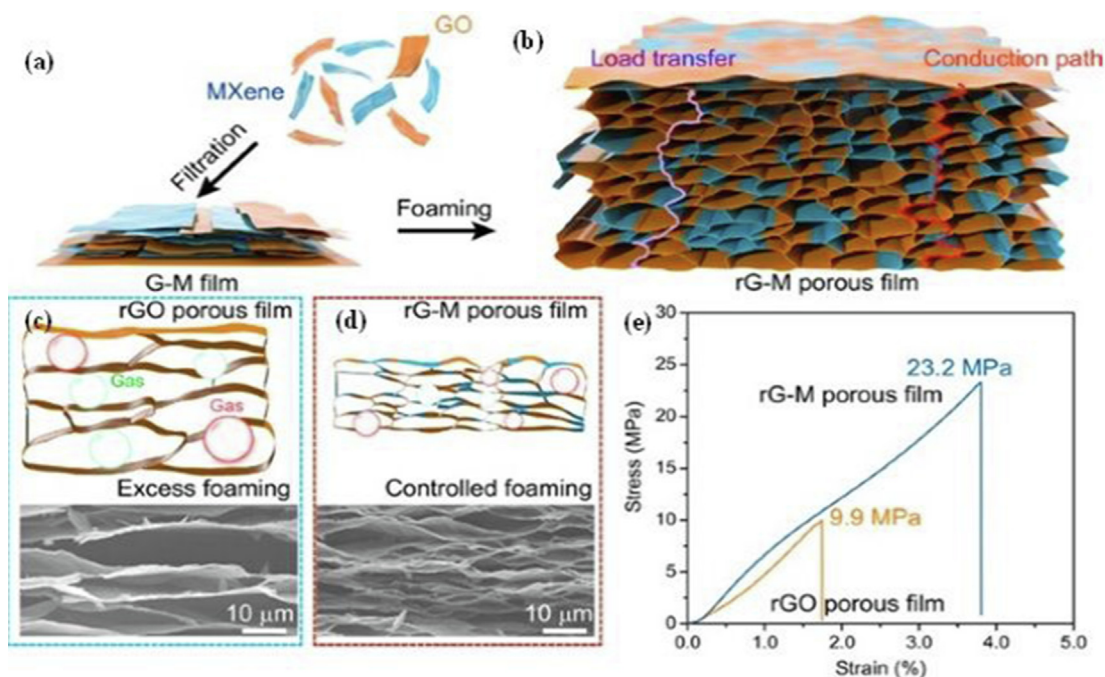


**Fig. 24** Development of MXene-rGO films via filtration and foaming developed composite (a & b), SEM images and model design for porous rGO-MXene films with excess foaming (c), controlled foaming (d), and mechanical performance of composites films (e). Reproduced with copyright materials by Springer Nature. 2022 (Zhang et al., 2022).

for potential end uses and application in the field of EMI shielding and MA purpose. The higher out performance values are reached nearly around to 92.0 dB with a very small thickness of 2.5  $\mu\text{m}$ . The resultant figures are more or less better than, that of reported for graphene, CNT, and copper foil. For instance, the EM wave absorption mechanics is based on two distinctive arrangements of pristine  $\text{Ti}_3\text{C}_2\text{T}_x$ , i.e., multilayer (ML) and few-layer (FL) structures, must be studied and analyzed individually (Nepal et al., 2021). This is indispensable since the distinction in the construction of an anisotropy and the variance amongst in-plane and out-plane conductivity values.

The most common and widely used synthesis methods of MX-phased materials require chemical etching and  $\text{Ti}_3\text{C}_2\text{T}_x$  based suspension is developed by chemicals routes for the development of nanomaterials. The chemical etching inevitably influences the performance and yield of the developed MX-phases with lower stability of colloidal dispersion of  $\text{Ti}_3\text{C}_2\text{T}_x$  nanosheets due to the electrostatic repulsion. The recent growth and interest of  $\text{Ti}_3\text{C}_2\text{T}_x$  and related MXenes continues to growth through incorporation and addition of surface termination groups (Tx: -F, -OH, and = O) (Shu, 2020). These groups could help out to manipulate their potential stability and interfacial reactivity due to the available functional groups, which could assists and provide better processing ability in different solid-liquid states in solution process required for the fabrication and coating on different polymeric films, fibers and surfaces. It is believed that the setting up of valences onto MXene via short ion-conducting PEG ligands further enhances the tunability and surface chemistry of MXene without compromising their properties for example solution processing ability, structural organization, thermal stability, and enhanced electrical conductivity (Wang et al., 2017). The recent progression and the state-of-the-art for EMI shielding and MA of MXene-based materials is still remained as major concern and big challenge with several problems and bottlenecks. Several research studies has been made so far, the better understanding these relationships for 2D, to 3D porous aerogels and different assemblies has been designed and fabricated on micro to nanoscale (Cao et al., 2010). The performance and characterization for potential applications are expanding for future applications in energy storage, harvesting, thermal, electrical and electronic applications for example electromagnetic, and microwave applications. The metal carbides (titanium carbide) as MXene comprising ( $\text{Ti}_3\text{C}_2\text{T}_x$ ), different elements, in which Tx refers to -Cl, -F, -OH and = O). These fine and ultrahigh surface properties need to be altered due to lower fixation and binding properties on fiber assemblies such as glass fiber, polymeric fibers, and their nanocomposites (Wen, 2013; He, 2019). The MXene sheets with poor processing and low surface area reduced their potential applications. The restacking behavior also restricted the uses of MXene but, new approaches and methods are introduced on micro to nanoscale. These limitations can only be overcome and reducing by some physio-chemical interaction and bonding with other metal complexes and organics materials.

However, it is still remains a large challenge to construct a multifunctional application framework to quickly adapt to the complex practical environment, making it to be efficiently applied in a variety of complex situation. Therefore, introducing the new approaches for the synthesis and production of such highly porous and flexible structures; could results in an

enhanced variable attributes MXene and graphene based materials. Furthermore, these films are fabricated on various materials, fibrous 2D, 3D porous heterostructures by addition of various polymeric fibers, for example CNF, CNC, PP, PU via in-situ chemical coating and layer by layer (LbL) assemblies (Wang et al., 2021). The fabrications has been reported so far including spray, dip, drop, casting, hydrothermal, microwave assisted chemical, thermal annealing, polymerization, and screen printing, for the design of such wearable MXene based electrodes, circuits, and mechanically, thermally stable fibrous films, foams and sheets (Cao, 2012). Nevertheless, several properties of 2D materials for example graphene and MXene are under investigation further more to improve, their mechanical and electrical possessions in the form of porous, aerogels, foams and films are far from optimal. Various studies has been made so far on MXene, graphene and their nanocomposites enabled wearable e-devices are focused and highlighted by depiction the attention towards current developments of nonstructural characteristics, counting 3D constituted strategies for example the textiles and other nature inspired assemblies as an alternative and effective shielding material (Cao et al., 2015; Cao et al., 2018).

The previous studies shows that, the existing exploration advancements on the dielectric attributes of MXene and graphene films are expansively concise and need to be further analyzed on broader level. The effective shielding of 2D materials is attributed to their high-performance mechanical stability, strength and electrical conductivity. In brief, the future perspective and newer opportunities are need to be well addressed towards more growth and process development for MXene, graphene and their nanocomposites for better use in MA and EMI shielding response (Cao et al., 2015; Sarycheva et al., 2018).

The unique three-dimensional conductive network of MX-CNT would greatly widen the applications of MXene/polymer and CNT based nanocomposites in the field of EMI shielding. MXene based composites displayed an excellent and comprehensive MA & EMI performance compared with other organic and inorganic materials as demonstrated in Fig. 25 (a-h). This indicates that MXene and graphene-based composites At 19.6 vol% of MXene, the EMI shielding effect obtained from a 1 mm thick nanocomposite film is 49 dB; the density of this film is 1.25 g/cm.

The recent progress on the developments of MXene and graphene based films also empowered the highly stable and flexible microchip technology for the designing of wearable electronics. The electromagnetic waves dissipated by multiple reflections and reabsorption in the highly conductive network and converted into thermal energy; which is being used for electrostatic energy (Wang et al., 2021; Bhuvanesh Kumar and Sathiya, 2021). For instance, the developed heat energy from the electromegnetic waves can be converted into electrical energy for potential applications for the reduction of electromegnetic and microwaves. Therefore, is the study based on graphene based layered films has been developed as thermo-electric device, which could work in the absence of light, in which the dual mode graphene and polymer films are coated as p-type and n-type material. The designed device is highly capable to converted the direct electromengantic waves generated heat into an electrical energy under applied voltage as demonstrated in Fig. 26 (a-e). The researchers studied, that how to utilize and convert EM energy into electrical energy

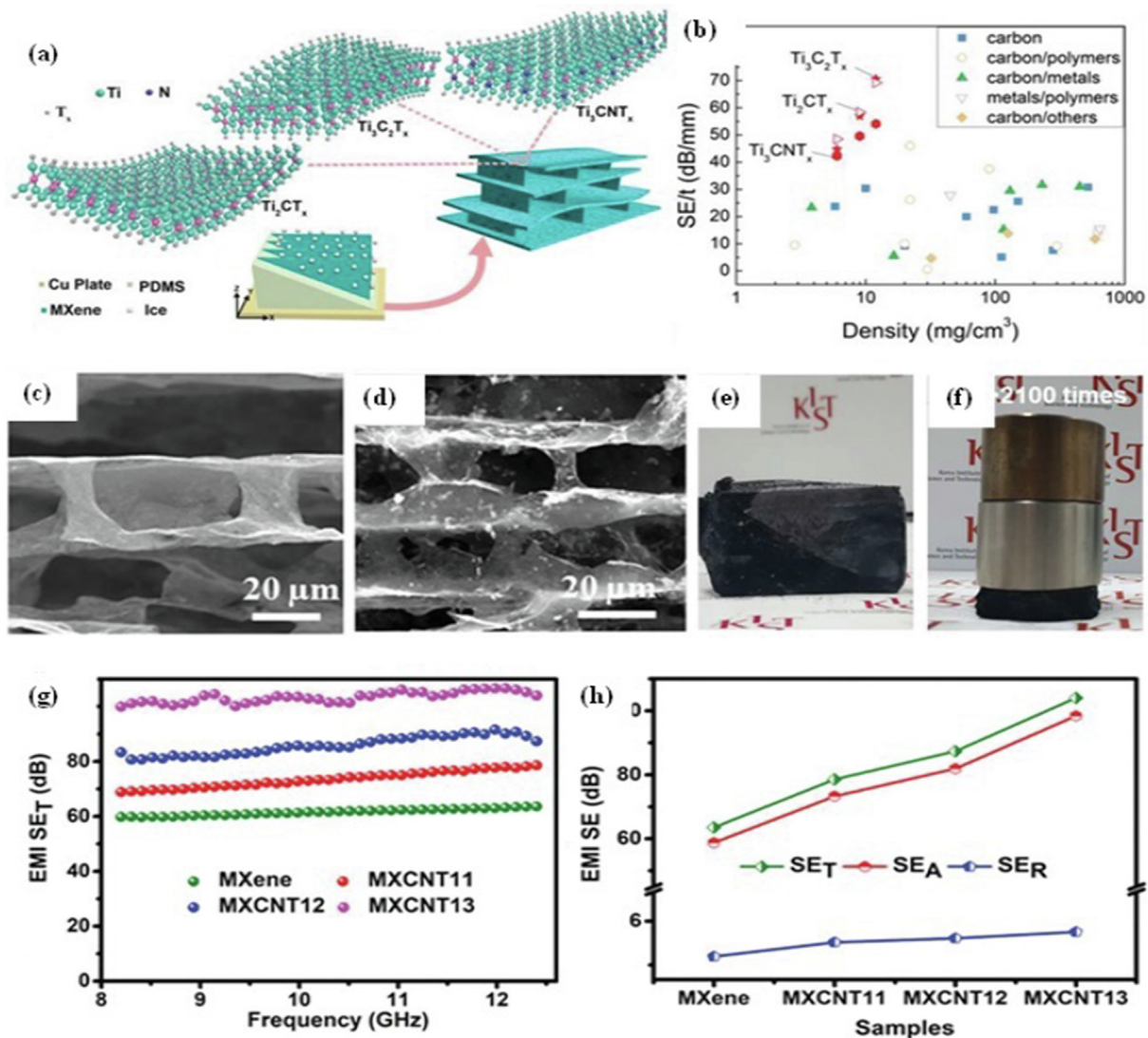


**Fig. 25** Chemical etching of MXene using Hydrazine (a), EMI SE performance of different polymer (PDMS) based films (b), SEM images of developed porous structure (c & d), development of composite structure under loading (e & f), and developed via freeze-drying approach EMI SE performance of resultant porous MXene sheets and MXene-CNT loading for Microwave and EMI shielding (SE) response over variable frequency and loading percent (g & h). Reproduced with copyright material, John Wiley and Sons 2020 (Iqbal et al., 2020).

as a great concern and challenge. Herein, they used the exfoliated/delaminated MXene ( $D-Ti_3C_2Tx$ ) sheets and successfully fabricated by the modified Gogotsi's method. The exfoliated MXene sheets showed a great choice of atomic level layers of the MXene which are tailored or fine tuned with controlled morphology having equal space between the each layer of  $Ti_3C_2Tx$ . These inner layer spacing could result as an improve interfacial polarization. The study shows that, the resultant films has higher performance EM wave absorption capability of  $D-Ti_3C_2Tx$  MXene sheets composites.

It is supposed that, the comprehensive performance towards EMI shielding and MA is superior as compared to pure  $Ti_3C_2Tx$ -based other composites. The attributes are dedicated due to the great competition between conduction loss and polarization loss (Liu et al., 2022; Balci et al., 2015). However, the higher the concentration of  $D-Ti_3C_2Tx$  in the polymer composites, resulted as more conversion of EM heat energy to

thermal energy which is then converted by the designed TE device into electrical energy without sunshine. Based on this mechanism, a simple prototype thermoelectric (TE) generator is designed, which is capable to directly convert the EM energy into power energy. This device thermoelectric generator would be the alternative energy source for low power electric devices as shown in Fig. 27 (a-g) (Liu et al., 2022; Li, 2020). Fig. 27 shows the schematic presentation of the graphene based device that works as an adaptive microwave surface in functions. The working principle of the device is based on the electrostatic fine tuning of high mobility carriers on graphene electrodes without using metallic structures. The device consists of two large-area graphene electrodes on flexible polymer support and electrolyte medium between them. Application of a bias voltage between the graphene electrodes polarizes the electrolyte and forms ionic double layers on the graphene-electrolyte interface with opposite polarizations. These ionic

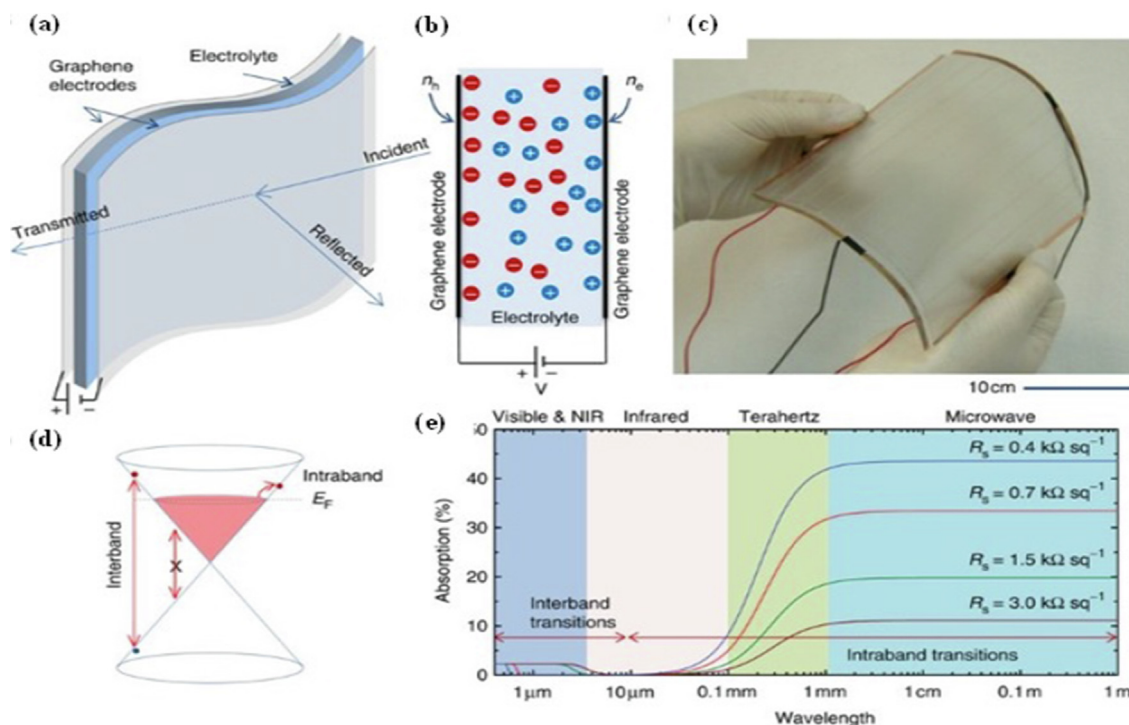


**Fig. 26** Illustration of graphene-based adaptive surface for microwave absorption (a), large-area graphene based electrodes cross-sectional view (b), developed via transfer printed polymeric substrate showing microwave-transparent on PVC films (c), optical response of the graphene direct cone model (d), and microwave broadband absorption of a single-layer graphene (e). Reproduced with copyright materials, Springer, 2015 (Balci et al., 2015).

double layers generate tunable high-mobility free carriers (electrons and holes) on the graphene electrodes that can respond to microwaves. Reflection due to the electrolyte is negligible, because the ions of the electrolyte have very low mobility; therefore they cannot respond to the electric field of microwaves (Han, 2021; Liu et al., 2017).

In another study, a highly ordered multiple-layered structure was constructed with cellulose nanofibers (CNF) and MXene composite using the LbL technique and vacuum filtration method as shown in Fig. 28 (a-e). There were four transition layers composed of low content and one reflection layer composed of higher content of MXene in the nanocomposite film. These layers not only reduced reflection loss from the surface of nanomaterials but also significantly increased multiple reflection loss at the interface between layers towards an incident wave. Furthermore, the developed nanocomposite films demonstrated excellent EMI-SE of 39 dB and absorption effectiveness (SE) of 28 dB by coordinating the polarization loss at the interface. The practical implication of such cellulose and MXene based nanocomposite proves that the developed assembly could greatly retain the mobile phone signals. However, the incident EM waves could reflect due to the variable surface orientation of the number of layers with more reflection and mismatching of impedance, resulting as an excellent EMI SE. Keeping in view these, consequence introduced by the developed assembly in its construction as a gradient structure, by which the waves (EM) are reflected and absorbed by maximum reflection loss between the layers at the interface. Moreover, the dielectric properties of the gradient structure and MXene could contribute to well-planned structures having

better adapting impedance. Therefore, composites reduce reflection efficiency and EMI SE. The present study shows that EMI shielding of gradient composites made with CNF/MXene can be enhanced by vacuum filtration as promising material for new generation electronic devices (Ma et al., 2022).

Here a microwave transmitter has been designed with a applied voltage of 2.5–10 mV. The device showed an outperformance of 15 mW of power over a microwave frequency range of 10.5 GHz, having real time microwave absorption and converting it into electrical voltage as an alternative approach for self powered devices. Whereas, the device work function is based on absorption, reflection and transmission mechanism with graphene based capacitor over a charging and discharging cycles. The design RC response time was recorded by the capacitor was examined by variation of resistance induced by the graphene films as an electrode and the difference of the total capacitance of the designed device as a model and systematic approach.

The design structure of the device demonstrated higher ability to optimize and control the density of the large area graphene films as an electrode, and capable to tune the metal like properties for potential application of next generation electronic devices, using electromagnetive and microwaves for energy harvesting. The potential ability of the device because of its electrostatic and electrochemical mechanisms may also result as energy storage device, made from graphene based electrode and capacitor. Herein, the electrostatic storage is used to prevent unfavorable properties of a single-layer graphene with Redox reactions which could resist, the electrical continuity in a single-layer graphene films. Whereas, the electro-

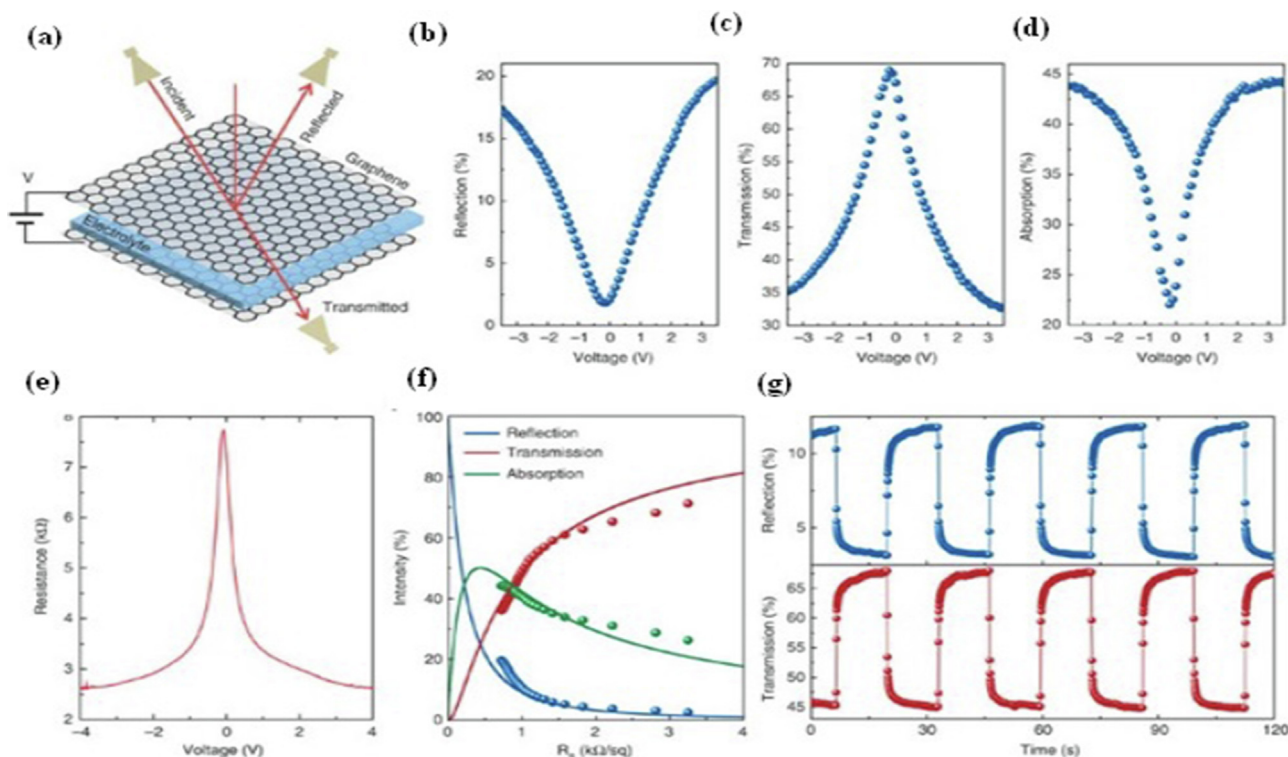


**Fig. 27** Experimental design model for microwave performance measurements from graphene surface with biased applied voltage (a), Measured intensity of the reflected and transmitted microwaves plotted against the bias voltage (b-d) respectively. Microwave absorption by the graphene based capacitor as a function of bias voltage (e), measured resistance of graphene electrodes (including contact resistance) as a function of bias voltage (f), Scattered plots with loops for microwave reflection transmission against resistance(g). Reproduced with copyright materials, Springer Nature, 2015 (Balci et al., 2015).

chemical storage potential of multi layered graphene films could work as apacitor for energy storage, instead of energy conversion capability. Therefore, the pristine graphene is not suitable for such uses, due to the lack of its electrical conductivity and thermal response with few layered to multi layered structures (Ma, 2022; Hu et al., 2019; He, et al., 2019).

The excellent electrical conductivity of MXene –  $4350 \pm 125 \text{ S cm}^{-1}$  provides free carriers in the matrix to absorb electromagnetic signals, leading to an absorption mechanism that is superior to a reflection mechanism. Due to the modification steps of the nanofiller, the nanocomposite films not only displayed excellent EMI shielding properties, but also possessed an appropriate SE efficiency. Meanwhile, this dramatic upsurge in the number of electronic devices has introduced EMI pollution; a kind of disturbance causing the malfunctioning of highly integrated circuits (Li et al., 2019). The two-dimensional materials with minimal thickness ease of processing and most importantly absorption dominant EMI shielding capability are strongly needed. 2D transition metal carbides and/or nitrides (MXene) have shown great potential for EMI shielding application as demonstrated in Fig. 29 (a-c). Consequently, the synthesis of  $\text{Ti}_3\text{C}_2$  MXene/polystyrene composite films with different shapes and sizes has achieved d the desired EMI shielding efficiency (Li et al., 2019; Sun, 2017).

The studies have been made to explore the features and potential applications of 2D materials. The aramid nanofibers (CNFs) with high mechanical strength and thermal stability

towards multi-purpose functions will bring huge applications. In another work, reported for an improved interfacial interaction through covalent bonds between two different components i.e graphene and conductive polymer (Sun, 2017; Zeng, 2020). The developed process was used to obtain a homogeneous CNF/rHGO nanocomposites for wide range of end uses. The developed porous CNF/rHGO media with high mechanical performance; developed via solvent exchange gelation process. However, the CNF/rGO/PANI hydrogel were produced towards an improved EMI shielding and MA properties as demonstrated in Fig. 29 (d-h) (Rajavel, 2020; Han, 2016).

The development of a lightweight aerogels towards high-performance EMI shielding is critical element and remained as challenging for several decades. Therefore, the use of an ultrathin cellulose nanofibril (CNFs) has been put into practice to assign in the construction or building with maximum packing capacity and very ultralow-density. The vigorous and extremely bendable conversion of MXene (metal carbides) and nitrides (MXene) based aerogels with significantly improved EMI-SE due to the highly oriented bio-mimetic cell walls as demonstrated in Fig. 30 (a-c). The study reveals, that there is substantial impact of the size, shape and angles amongst the concerned with cell walls assemblies with greater incident EM wave, under the electric field and the directional reflection of incident waves on EMI shielding performance by providing an fascinating micro scale design assembly and strategy. The orientation and formulation of MXene “bricks” and Mortyr has been attached with CNF as brick and mor-

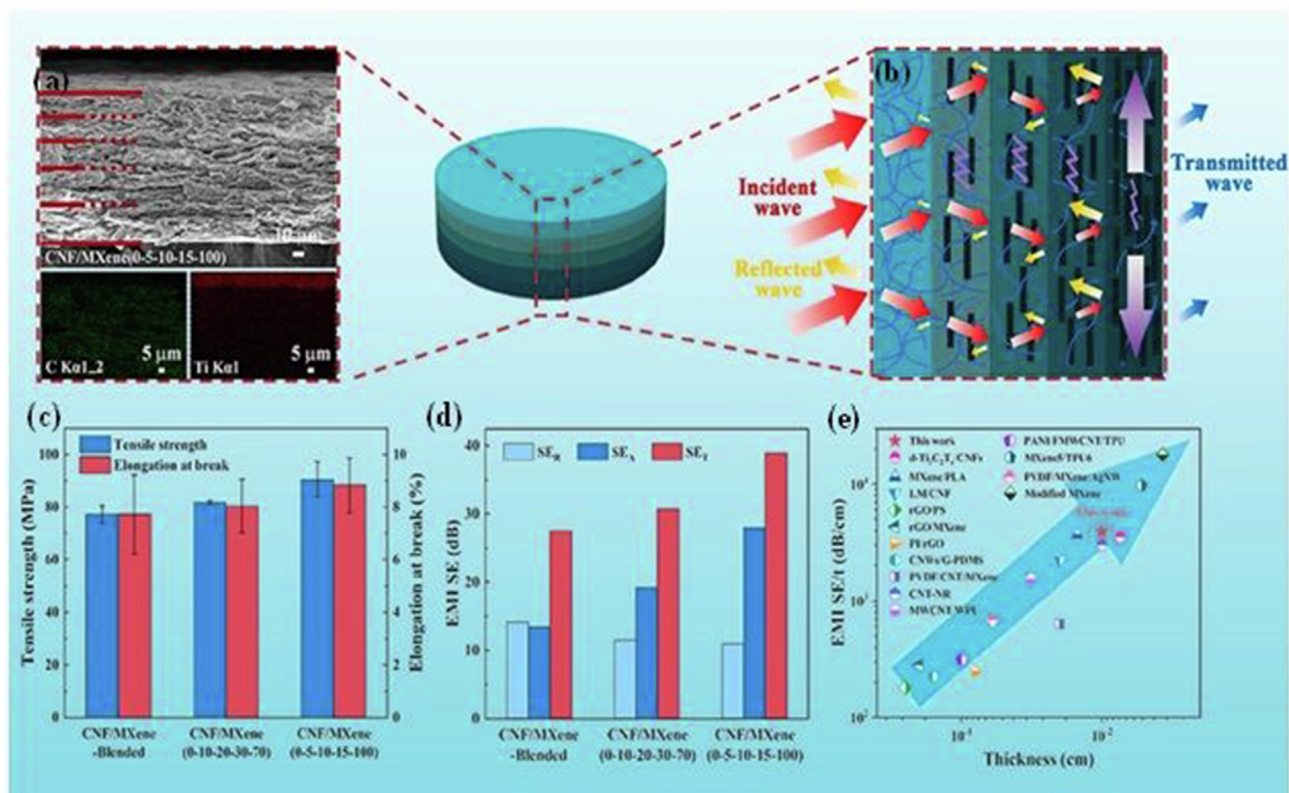


**Fig. 28** SEM images of developed MXene nanosheets with cellulose aerogels via solution processing (a), EMI shielding model for multiple layered films (b), tensile strength of developed CNF-MXene composites (c), EMI shielding performance of composites (d), Reflection loss (RL) response comparison of developed composite films with other materials for microwave absorption (e). Reproduced with permission to copyright material from Elsevier, 2022 (Ma et al., 2022).

tars” or nacre-like unit cell structure induced with a very high electrical conductivity, and interfacial polarization and deflection or absorption loss, which produced from the resultant MXene/CNF aerogels with an ultrahigh EMI shielding presentation. The results demonstrated that, SE was reached to 75.5 or 35.8 dB at a density of merely 8.0 or 1.5 mg cm<sup>-3</sup>, respectively (Wang, 2019). However, an ultrafine and multifunctional (ANF) fibrous based reinforced composite of graphene (rGO@ANF) was developed through in-situ synthesis followed by freeze casting method and thermal annealing. Wherein, the rGO is introduced into graphene to develop aerogel assemblies, showing higher stacking as well leading to strong mechanical performance towards compression and MA, performance. The study reveals that, the maximum stress retention of the designed nanocomposite was attained nearly 78.8 kPa (Song, 2020). Furthermore, the developed aerogel exhibited at least a reflection loss ( $R_{Lmin}$ ) of -56.5 dB and higher effective absorption bandwidth (EAB) of 7.0 GHz with a thickness 2.8 mm X and Ku bands. Additionally, the newly developed hybrid aerogel displayed an exceptional and outstanding microwave absorption with an average absorption coefficient greater than 0.56 at 2–6 kHz a thermal conductivity of about 49.18 mW m<sup>-1</sup> K<sup>-1</sup>. The incorporated graphene based aerogels worked as multifunctional purposes, and embraces an extraordinary potential MA, comprehensive sound absorption, and heat protection as revealed in Fig. 30 (a & b). In this work, the SE performance was improved

freeze-drying method based on polymerization-induced aramid nanofibers (PANF) for the effective groundwork of all *para*-aramid nanofibers (PANF) aramid aerogels. During the preparation process, the PANF hydrogels were first frozen at -18 °C and then dried at 20–150 °C to form PANF aerogels. The PANF structure fashioned in the course of freeze drying is critical to establish the PANF aerogels (Ji, 2020; Liang, 2019; Rajavel et al., 2020).

In addition, the occupancy effect of ice crystals also contributes to the development of macroscopic pore structures in aerogels. Large size or shape-controlled aerogels can be magnificently acquired by this method. It is perceived from the findings that, by varying the PANF concentration and drying temperature significantly improved mechanical performance and cyclic stability of the hydrogels. The overall performance over different densities (20–185 mg/cm<sup>3</sup>), and the lowest density was reached at 150 °C with concentration of 0.7 %. The resultant PANF aerogels exhibit higher compressive strength and low thermal conductivity, as compare with the freeze-drying and microwave drying methods. Furthermore, the elongation and shrinkage was observed during microwave drying with more compact assembly of the nanocomposites. whereas, the freeze drying approach was used to fabricate PANF aerogels with more wider and opened layers of PANF aerogels; which can potentially be used for thermal/heat insulation, shock absorbing, shielding and microwave absorption properties of aramid fibers based mate-

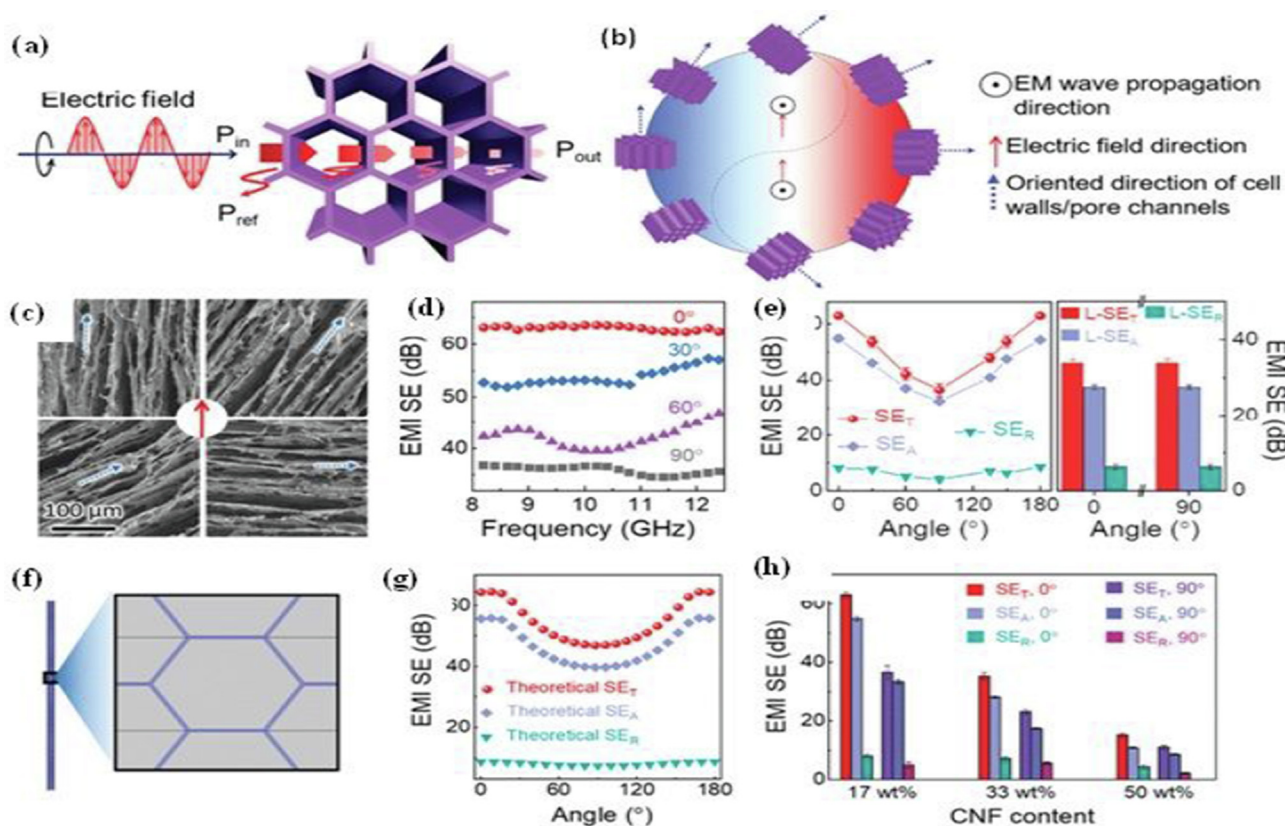


**Fig. 29** Development of MXene and CNF based porous films design model (a & b), SEM images of developed lightweight unidirectional 3D porous foam structure (c), EMI shielding response over variable frequency range (d), EMI SE at variable angle (e), design model of unit cell structure (f), EMI shielding performance for absorption and reflection loss (g), variable CNF content percent and its effect on microwave and EMI Shielding(h). Reproduced with permission @copy right material of Wiley Online, 2020 (Zeng et al., 2020).

rial in various conditions including solid, gases states as presented in Fig. 30 (c & d) (Rajavel et al., 2020).

A honeycomb permeable graphene HPG/AgNWs composite films was reached up to 292 754 dB cm/g. Moreover, the HPG nanocomposites showed an tremendous presentation steadiness and robustness against cyclic loading and unloading; Therefore, the designing of such light weight and flexible HPG not only used for such wearable smart device, but can also work as highly efficient and potential material for EMI shielding is anticipated. The synthesis and production of such HPG nanocomposites could be potential candidate due to their inexpensive and mass scale fabrication; which is auspicious for EMI shielding (Cao et al., 2021). The results demonstrate that  $Ti_3C_2T_x$ -PVA possesses the best MA performance with the robust absorption of  $-50$  dB. The qualified absorption bandwidth ( $R_L \leq 10$  dB) is up to 4.3 at the matching thickness of 1.5 mm as presented in Fig. 31 (a & b). The use of carbon materials and inorganic metals has been increased due to the increasing demand of protective wearable shielding materials. The current research and development of MXene and graphene would provide new opportunities and open a new window for a widespread variety of presentations (Liu, 2022; Song, 2020; Raagulan, et al., 2020; Shahzad, 2016; Xu, Aug 2021).

The synthesis of MXene films with different polymeric materials demonstrate a bottom-up and top down approaches to design various polymers and  $Ti_3C_2T_x$  MXene nanocompos-

ites for MA and EMI shielding. Despite of their higher stability with  $Ti_3C_2T_x$  MXene; films and sheets highly oriented and staged multiple layered structures which are being used for high performance electrodes, energy harvesting, and storage devices as demonstrated in Fig. 31 (c & d) (He, et al., 2019; Jin, 2020). The synthesis of such nacre like nature inspired stretchable and flexible electronic device for potential shielding and efficient microwave absorption is still under progress and remained as challenge for future electronics. The syntactic films coated highly stretchable film exhibits a highly stable mechanical, thermal and electrical performance with various MOF for enhanced EMI shielding performance (Jin, 2020). The developed nanocomposites showed outperformance about 30 dB under 50 % tensile strength and their EMI-SE, which is further improved to 10–68 dB by developing a thick films assembly as compared to few layered graphene film structure. The resultant electrodes showed a very high sensitivity ( $66.3$  nF  $kPa^{-1}$ ) under repeating variable 1000 at different frequencies. The composite assemblies also exhibited an excellent dynamic cycling steadiness over 500 cycles, with greater mechanical strength at 50 % strain (Yun, 2020).

### 3.2.1. MXene-CNT polymer-based composites

Similarly in stuy researcher team established a mild hydrothermal technique to assemble 2D MXene into 3D architecture which can act as the conducting pathway for polymer nanocomposite. They synthesized  $Ti_3C_2T_x$  MXene through

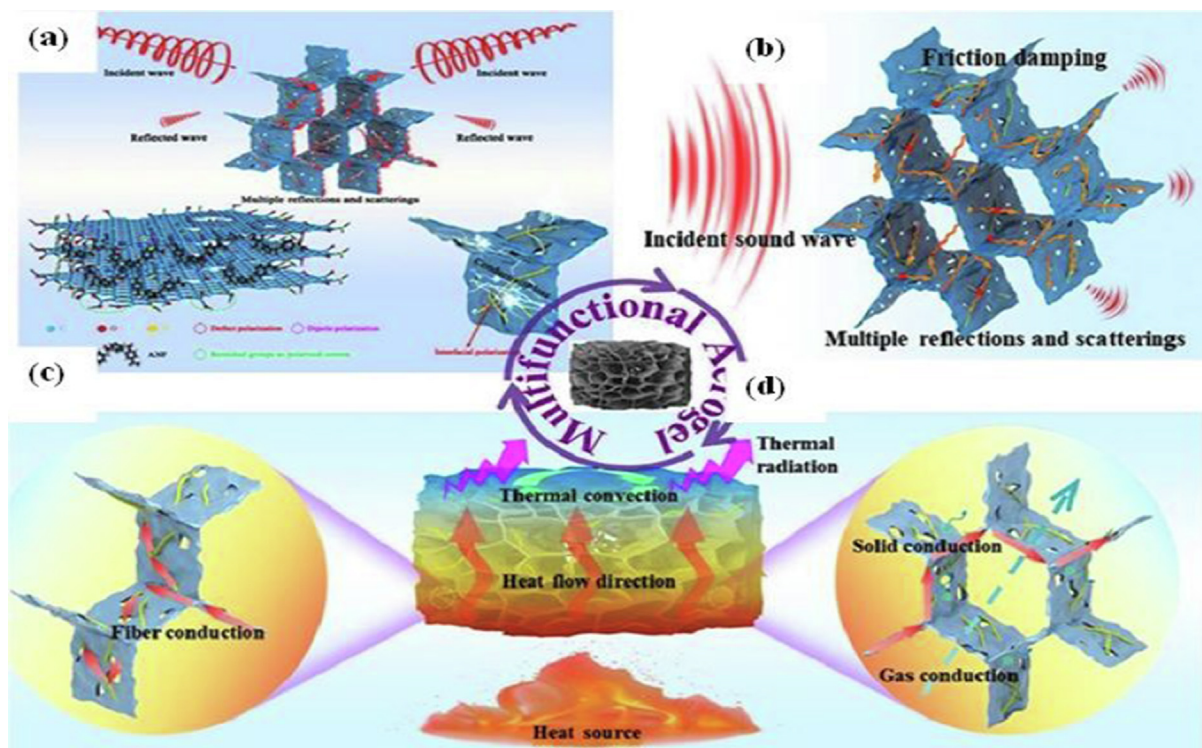


**Fig. 30** Multiphase reflection of electromagnetic waves and EMI shielding of incident waves (a & b), thermal conduction and heat flow of aramid fiber based assembly in solids and gases states for EMI and Microwave shielding (c & d). Reproduced with permission to copyright materials, Elsevier, 2022, (Liu et al., 2022).

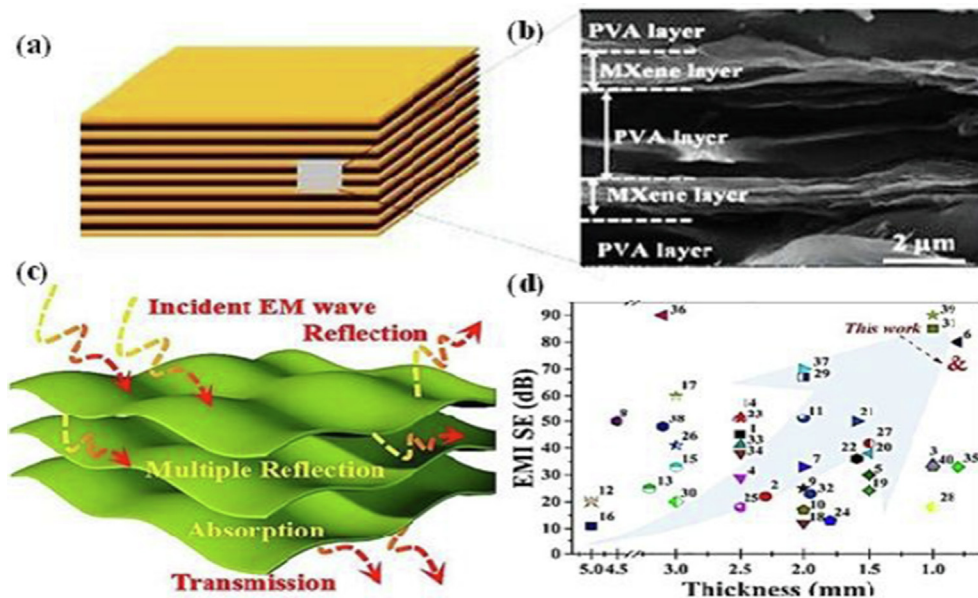


**Fig. 31** MXene & PVA based multiple layered staged films (a), SEM images of MXene and PVA layered films (b), this Figure has been reproduced with the copyright permission by Elsevier, 2020 (Jin et al., 2020), Model of shielding mechanism of layered MXene sheets (c), and shielding response of MXene films with different thickness (mm) compared with other reported materials (d). Figure has been reproduced by copyright permission by Elsevier, 2019 (Li et al., 2019).

HF etching method and systematically investigated how filler loading, coating thickness influence the dielectric properties and microwave absorption ability from 2 to 18 GHz. The resultant MXene-rGO based aerogel collective with the well

reserved essential structure of MXene and aligned core-shell structure, shows promising electrical conductivity as high as  $1085 \text{ S m}^{-1}$ . When used as conductive networks in shielding materials, the aerogel endows epoxy nanocomposite with

remarkable electrical conductivity ( $695.9 \text{ S m}^{-1}$ ), and EMI-SE of the nanocomposite exceeds 50 dB; with a determined rate of 56.4 dB over X-band (Iqbal, 2020; Han, 2020).

The electrochemical property was significantly enhanced due to the CNT supporting the original multilayer structure of MXene, bridged the pathways for electron transport between each particle, and providing extra-ordinary performance toward shielding effectiveness as shown in Fig. 32 (a-c). The design and development of a highly efficient MA material for electromagnetic fortification have established extensive consideration. The recent progress and dielectric microwave absorption materials become a research direction for development of new material and the complementary use as a function to study the mechanisms of synergistic loss. In addition, the compact structures of MXene films are wide-open to surface area from reduced complex compositions. Several unique composites are consistently grown-up with MWCNTs and carbon cloth (CC)-reinforced with MXene sheets (CC-MX). The results of rGO-MXene@BC discloses the synergistic amalgamation of chemically exfoliated large surface area having an excellent electrical conductivity and SE over a variable w% of rGO in MXene as shown in Fig. 32 (d-f) (Han, 2020; Xie, et al., 2019).

Modern microelectronic devices urgently need functional composite films with great EMI shielding and light-to-heat conversion properties, especially for use in extreme environments. Here, by incorporating 1-D AgNWs and 2-D MXene into a nanocomposite heterostructure, with (PVP) polymer based assembly. The light weight and flexible Poly urethane

with MXene and silver nanowires (MX-AgNWs/PU) foam and films were developed for EMI and light to heat conversion solar cells. The developed 3D porous assembly of AgNWs and MXene showed improved multiple interphase with SE of 45–50 dB at minimum density of  $0.15 \text{ g/cm}^3$  for X-band as demonstrated in Fig. 33 (a-d) respectively (Weng, 2020; Zhao et al., 2017).

### 3.2.2. MXene and polymer based aerogels/hydrogels/Foams

The synthesis and fabrication of ultra-fine, highly flexible and mechanically robust MXene films is still under growth and requires certain developments. The use of MXene films with different natural polymers for example bacterial cellulose has been made to develop flexible and very fine films produced via mass scale production using in-situ bio-processing technique. The sheets are well oriented and fine-tuned during the synthesis stage, to formulate the MXene-BC nanocomposite network with highly entangled nano-cellulose (Wan et al., 2021). However, several biomass driven carbonous compounds (BC) has been developed as porous structural arrays. Here, a novel biomass carbon was developed from soyabean bregs, followed by chemical (KOH) treatment and sequential hydrothermal treatment. The developed biomass-carbon foam structure showed a significant enriched precise surface area which assists in charge transmission channels, and more conductive paths. As a result, the sponge structures showed an increased multi-direction reflections and scattering As a multiple loss and due to a better-quality impedance matching, leading to an enhancement of EMW absorption performances. The

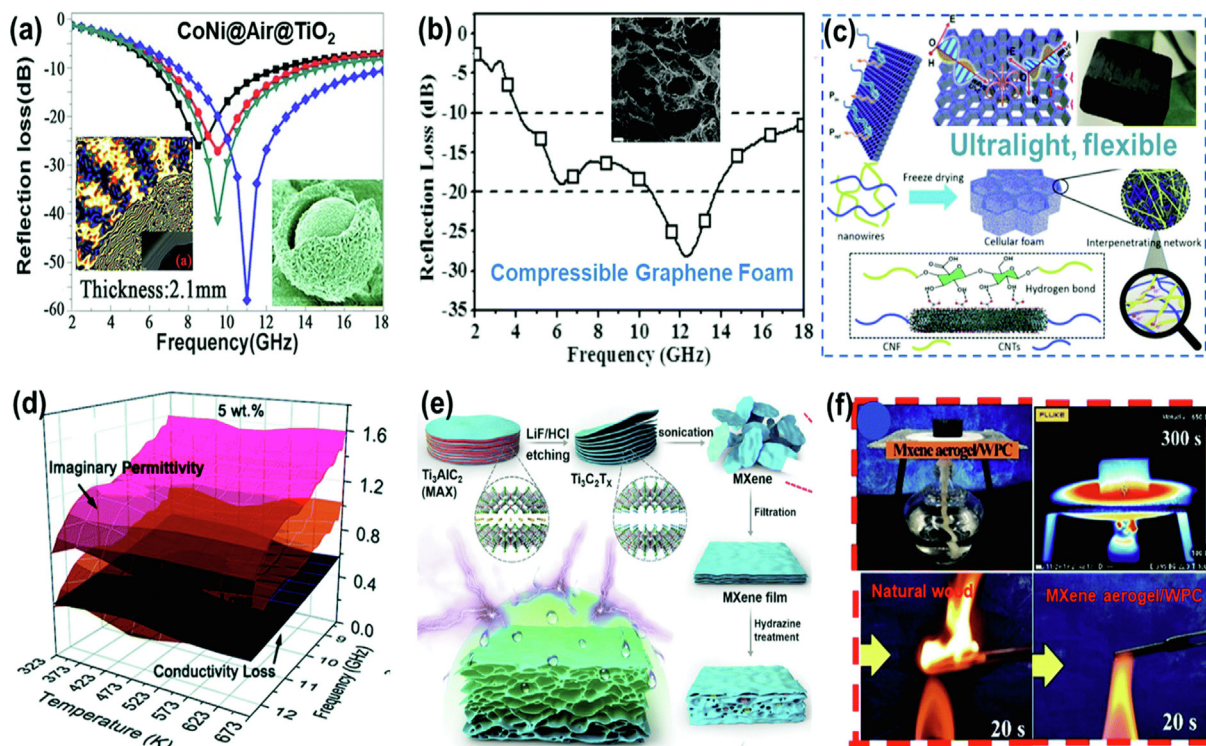


**Fig. 32** EMI shielding performance of CoNi@AirTiO<sub>2</sub> based segregated nanocomposites (a) & EMI response under compressible graphene foam (b), Ultralight and flexible developed assembly (c), EMI response (d), chemical etching of MX-Phase into MXene (e), and flame retardancy/hydrophobic property of the developed MXene based composite assembly (f). Reproduced with permission of the Royal Society of Chemistry, copyright 2021 (Wang et al., 2021).

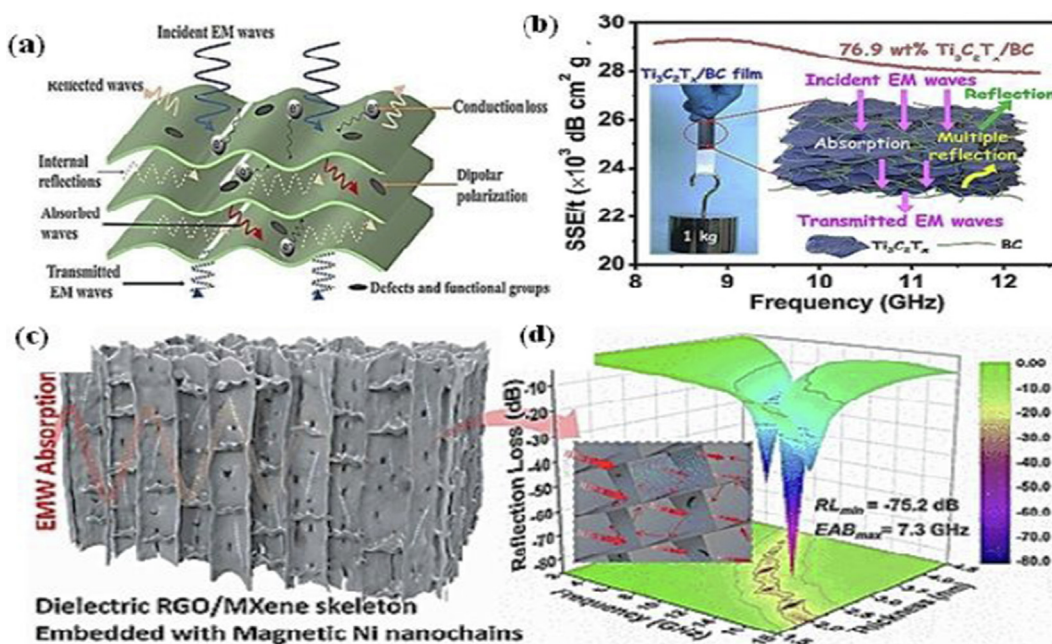


**Fig. 33** Simulated model for EMI shielding mechanism of graphene films (a), reproduced with permission to copyright materials by Elsevier 2021, (Zhang et al., 2021); chemically modified MXene-BC films with total (SE) (b), reproduced with permission; Copyright 2021, ACS (Wan et al., 2021); EMW absorption with dielectric loss and reflection loss in rGO-MXene skeleton loaded with Ni-nanochains (c), and reflection loss of developed composite assembly via freeze drying (d) for electromagnetic shielding (EMI) SE mechanism. Reproduced with permission; Copyright 2021, ACS (Liang et al., 2021).

acquired single-component based carbonous foams having without any practical filler demonstrating an operative EMW absorption proficiency over a wide range absorption band width of 4.8 GHz with a thickness of 3.5 mm. The developed resultant 3D assembly exhibits long lasting performance towards EMI shielding as well as mechanical stability with tensile strength of 295–297 MPa; when loaded with 20–25 % of MXene by weight. More importantly, a composite film with 4  $\mu\text{m}$  thickness of BC with 74.9 wt% reveals a specific shielding efficiency (SE of  $29141 \text{ dB cm}^2 \text{ g}^{-1}$ , which is greater than, the previously reported MXene and polymer based composites. The variable filler content of MXene and other carbon-based polymeric compounds composites showed that the facile fabrication could benefit an enhanced SE and mechanical performance (Lei et al., 2020). The designed composite assembly is environmentally friendly and can be fabricated using several scalable fabrication methods to produce ultrathin, very strong, and highly flexible material for example, the freestanding  $\text{Ti}_3\text{C}_2\text{T}_x/\text{BC}$  for efficient EMI shielding as presented in Fig. 34 (a & b) (Wei et al., 2020).

Similarly, a 3D nanostructure made of MXene/reduced graphene oxide (rGO) aerogels attached with nickel Ni nanoparticles and wires were produced by using directional-freezing, soft template, Simple dip coating, and thermal annealing methods (Li, 2017). The as prepared composites films contains GO, were subsequently reduced with hydrazine hydrate and other reducing agents under inert environment as well vapor reduction process. The designed composite contains the highly oriented cell structure as heterogeneous nature, which results in dielectric/magnetic loss and interfaces (Ma, 2020). The metallic and reduced graphene (M-rGO) based nanocomposite could benefit the higher MA and EMI shielding performance with perfect impedance matching, multiple polarizations, and

electric/magnetic-coupling (Zhou, 2020). Remarkably, the equipped under ultralight Ni/MXene/rGO (NiMR-H) aerogels with density of ( $6.45 \text{ mg cm}^{-3}$ ) and delivered with the best EMI presentation in previously informed MXene-based fascinating constituents with a insignificant replication loss ( $R_{L_{\min}}$ ) of  $-75.2 \text{ dB}$  (99.9 %) MA and larger EAB of 7.3 GHz respectively (Zhou, 2020). The designed heterostructure showed an improved SE of 85.8 %. The synergistic effect of the MXene and WPU based foam exhibited an improved shielding effectiveness of 60 dB with addition of AgNWs and absorption performance was reached to 95 %, The foam structure showed better stability against heat, compression, under variable cycles. In addition, the syntactic foam structure also capable to convert the heat into electrical energy harvesting and other related fields for multiple purposes (Cui, 2019; Zhou et al., 2020; Xin et al., 2019). The developed flexible and light weight MX-AgNWs/PU films and foam could provide better solution and facile approach for EMI and MA, photothermal and heat energy conversion in military, aerospace and wearable electronics (Cao et al., 2019). The study is based on revealing electrical conductivity ( $\sigma$ ) and shielding efficiency (SE) values of rGMH/epoxy nanocomposites by increasing the filler, shape & size of honeycomb unit cell as shown in Fig. 34 (c & d) (Wei et al., 2020).

The shielding effective performance was attained; by variable wt% of fillers rGO and AgNWs covered with MXene sheets, in epoxy nanocomposites by directly blend ding as filler. Similar to these studies on different conductive polymer are also loaded with variable content percent of (GO), MXene, and silver nanowires (AgNPs) for the development of light weight and porous graphene based hydrogels towards the microwave shielding over a high frequency of 2–18 GHz (Cao et al., 2019). In the meantime, the obtained MXene/

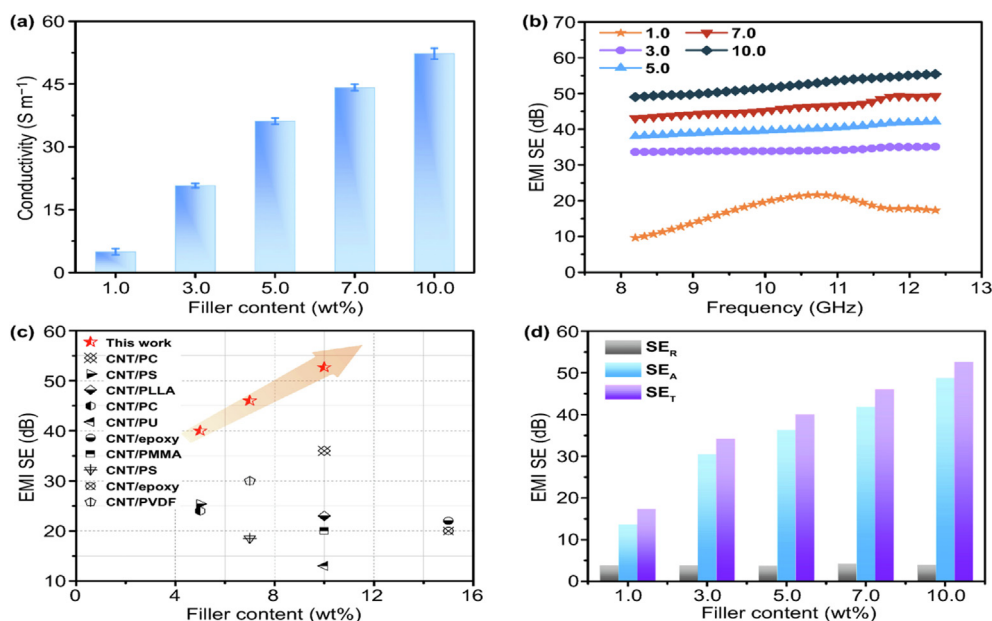


**Fig. 34** Electrical conductivity (a), EMI-SE of CG@CFA composites with various CNT/GO contents (b), comparison of EMI SE of CG@CPA composites and other reported composites (c), comparison on SET, SEA and SER of CG@CPA composites. Copied with permission Copyright 2021, Springer (Wang, 2021).

rGO based porous nanocomposite structures including foams, films and fibrous structures are more hydrophobic than Ti<sub>3</sub>C<sub>2</sub>-T<sub>x</sub> film, which is favorable during the reduction process as during reduction the oxidation caused by water agglomeration on the surface (He et al., 2020). Whereas, the prepared MXene/rGO porous composite structure showed superior thermal stability, electrical conductivity & EMI shielding performance. The EMI shielding materials are demonstrated in Table 6.

In general, the as generated heterostructures covers the greater area and interacted due to the surface functional moieties present on the films or edges of the rGO and MXene sheets as reactive groups. Heterogeneous silicone silver-coated glass fibers (Ag@GF)/MWCNT/ferrous oxide (Fe<sub>3</sub>O<sub>4</sub>) syntactic foam. SC-CO<sub>2</sub>) bubbling. Due to a reasonable dissipation mechanism, the average EMI -SE) efficiency and MA measurements of 78.6 dB and 0.82 respectively as demonstrated in Fig. 35 (a & b). The significance in confirmation fashioned and come across by instance for both of the replicated electromagnetic and incident waves. The performance is further improved to 94 % absorption at 7.68 GHz (Vural, 2018). In another work presented on EM and MA based on MXene and nickel composite; with 1D nanowires of nickel (Ni) and 2D material MXene nanofilms has been developed. The developed composite assembly showed an exceptional attributes for the MA and EMI shielding effectiveness (SE) with a minimum reflection (R<sub>L</sub>) of 49.5 dB was attained with a mild thickness of 1.75 mm over a frequency range of 11.9–18 GHz. As the filler content percent of Ni was improved in the MXene composite, showed significant raise in the SE of 59.9 dB which further enhanced to 66.9 dB by using at least 50 % by wt. The resultant assembly showed a absorption effectiveness of (SE) of around 60.0 dB as demonstrated in Fig. 35 (c) (Shi et al., 2021; Liu et al., 2018). It is also revealed from furthermore studies, that the better microwave and EM shielding performance is related with the synergistic

effect of conductive paths of MXene; and hetero junction through soldering of nickel nanowires. The magnetic properties are attributed to nickel Ni which greatly imparted effect on dielectric loss and electromagnetic losses. These attributes can be fine-tuned and altered by using appropriate dosing of filler in the MXene assembly as well as processing operational parameters to tune the depiction or absorption of electromagnetic waves (Sang, 2022; Luo et al., 2019).

The synthetic foam reveals an admirable EMI shielding stability under multiple bending of the incident waves. This syntactic foam has wide-ranging solicitation predictions of electromagnetic fortification for wearable portable gadgets and can be used for fifth-generation communication appliances. In this case, the method is equipped with a simple method. EMI-SE with a thickness of 1 mm and thin film EMI-SE with 36 dB of X-wave stage, special cause of electromagnetic wave absorption from the other manifestation (SE) for 32 min (Sang, 2022). Processing of PVA thin film had great expression for crack healing characteristics, with higher tear extension rate of 160 %. The MXene inks has significant progress towards EMI and MA materials loaded with Fe<sub>3</sub>O<sub>4</sub> particles having several advantages in electromagnetic SE performance by addition to ternary MXene/graphene@Fe<sub>3</sub>O<sub>4</sub> composition. The developed MXene and GO based carbonous porous 3D composites as shown in Fig. 35 (a–c) (Wang et al., 2019). The use of traditional materials for example single-phase Ni, silver (Ag) and copper materials exhibits extraordinary ferromagnetic compartment, and dielectric and magnetic loss, which are key considerations for an efficient EMW absorbing materials. Though, underneath the accomplishment of EMWs, particularly in the GHz frequency range of X-band, Nickel nano-materials lean towards to produce a eddy current loss this effect, confines their potential end uses and application. Still there is great demand and higher interest for modification of these composite materials through their hierarchal

**Table 6** Typical MXene-based materials and their EMI shielding properties (He et al., 2021).

Type	Materials	Ratio (wt%)	d (mm)	$\sigma$ (S m <sup>-1</sup> )	SE (dB)	SEE <sub>t</sub> (dB cm <sup>2</sup> g <sup>-1</sup> )
Pure MXene	Ti <sub>3</sub> C <sub>2</sub> T <sub>x</sub>	60	2.0	–	39.1	–
	Ti <sub>3</sub> C <sub>2</sub> T <sub>x</sub>	60	1.0	0.42	26.7	–
	Ti <sub>2</sub> CT <sub>x</sub>	40	0.8	1.63 × 10 <sup>-16</sup>	6	–
	Ti <sub>3</sub> C <sub>2</sub> T <sub>x</sub>	1.9	2.0	1081	62	–
MXene hybrid	Ti <sub>3</sub> C <sub>2</sub> T <sub>x</sub> -Ni	50	2.8	4	66.4	–
	Ti <sub>3</sub> C <sub>2</sub> T <sub>x</sub> -Ag	60	1.0	3.813	62.7	–
	Nb <sub>2</sub> CT <sub>x</sub> -Ag	60	1.0	3.123	72.04	–
	r GO-Ti <sub>3</sub> C <sub>2</sub> T <sub>x</sub>	4.5	0.5	387.1	55	–
MXene film	Ti <sub>3</sub> C <sub>2</sub> T <sub>x</sub>	100	0.045	4.665 × 10 <sup>5</sup>	92	25,863
	Ti <sub>3</sub> C <sub>2</sub> T <sub>x</sub>	100	5.5 × 10 <sup>-5</sup>	5 × 10 <sup>5</sup>	20	3.89 × 10 <sup>6</sup>
	Ti <sub>3</sub> C <sub>2</sub> T <sub>x</sub> -SA	90	0.008	2.9 × 10 <sup>5</sup>	57	30,830
	Ti <sub>3</sub> C <sub>2</sub> T <sub>x</sub> /ANF	80	0.017	1.733 × 10 <sup>4</sup>	28	1317.64
	ANF/Ti <sub>3</sub> C <sub>2</sub> T <sub>x</sub> /Ag	20	0.045	9.22 × 10 <sup>4</sup>	48.1	8907.4
	Ti <sub>3</sub> C <sub>2</sub> T <sub>x</sub> /CNF	90	0.047	739.4	24	2647
	Ti <sub>3</sub> C <sub>2</sub> T <sub>x</sub> /PEDOT:PSS	87.5	0.0111	3.405 × 10 <sup>4</sup>	42.10	19,497.8
	Ti <sub>3</sub> C <sub>2</sub> T <sub>x</sub> /PVA	19.5	0.027	716	44.4	9343
MXene foam	Ti <sub>3</sub> C <sub>2</sub> T <sub>x</sub> /GO	90	0.007	2.64 × 10 <sup>5</sup>	50.2	–
	Ti <sub>3</sub> C <sub>2</sub> T <sub>x</sub>	100	0.006	58,820	32	136,752
	Ti <sub>2</sub> CT <sub>x</sub> /PVA	0.15	5	8.3 × 10 <sup>-6</sup>	28	5136
MXene aerogel	Ti <sub>3</sub> C <sub>2</sub> T <sub>x</sub> /rGO	33	1.5	1000	28.6	6217
	Ti <sub>3</sub> C <sub>2</sub> T <sub>x</sub>	100	1	–	70.5	64,182
	Ti <sub>2</sub> CT <sub>x</sub>	100	1	–	69.2	62,909
MXene fabric	Ti <sub>3</sub> CNT <sub>x</sub>	100	1	–	54.1	49,182
	Ti <sub>3</sub> C <sub>2</sub> T <sub>x</sub> /rGO	0.99	2	695.9	56.4	–
	Ti <sub>3</sub> C <sub>2</sub> T <sub>x</sub> /CNT	25	3	943	103	8253.17
	Ti <sub>3</sub> C <sub>2</sub> T <sub>x</sub>	6	0.33	5 Ω sq <sup>-1</sup>	36	–
	Ti <sub>3</sub> C <sub>2</sub> T <sub>x</sub>	5.2 mg/cm <sup>2</sup>	–	670.3	31.04	–
Ti <sub>3</sub> C <sub>2</sub> T <sub>x</sub>	1.89	0.2	2756	42.7	–	

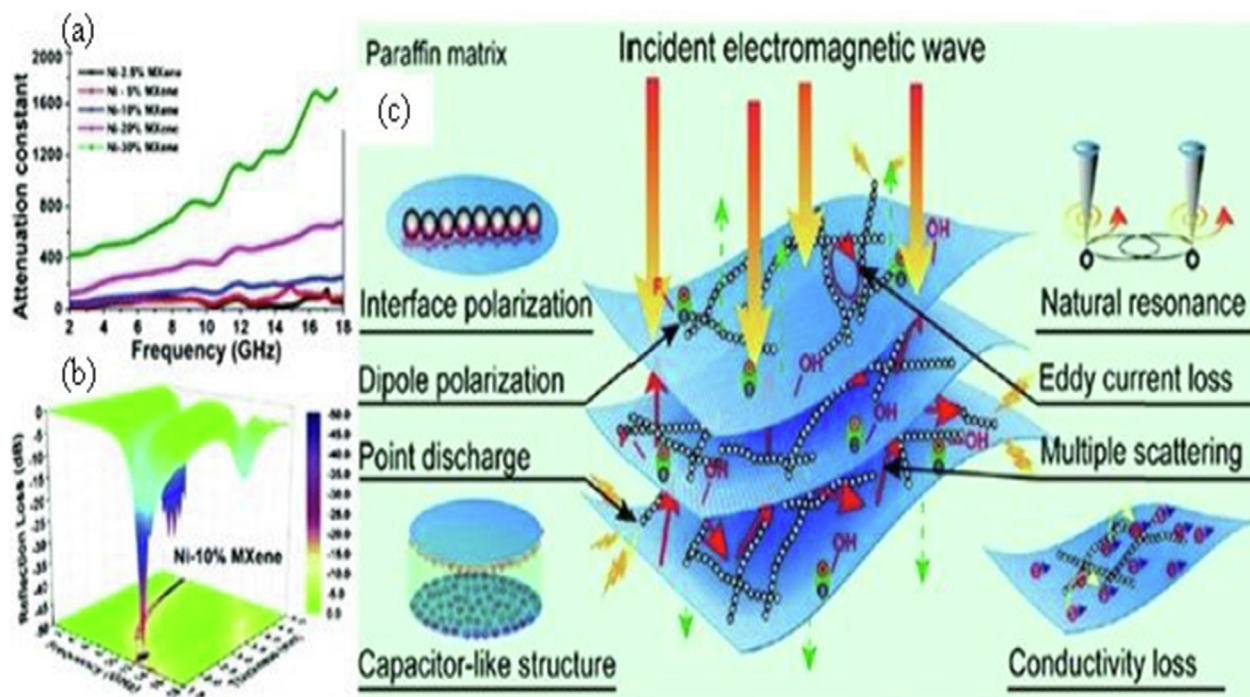


**Fig. 35** EMI shielding reflection loss of Nickel over MXene self-assembly via thermal decomposition (a), EMI-s SE total over variable frequency range with different Ni content%, and thickness (b), and design model showing EMI shielding mechanism of MXene sheets (c). Reproduced with permission; Copyright 2021, RSC (Deng et al., 2021).

structures during preparation and synthesis, as traditional single phase and multiphase carbon materials which are considered as an efficient materials and are widely used in various fields due to their light weight and superior conductivity (Zhou et al., 2019).

Therefore, the evaluation and design principles of the such matrix material to fabricate composites towards MW absorbing properties of the EMW-shielding is key consideration in which the shape and size are fine-tuned from 0D to 3D structures with carbonous compounds for example (carbon black, carbon nanotubes, carbon fiber, graphite oxide, reduced graphene oxide, and biomedical carbon) (Ameri et al., 2022; Zhou et al., 2019). Therefore, the designs of the composite as a matrix material are considered in various studies; to fabricate composites with metals, metal oxides, or polymer materials to obtain carbon-containing absorbing materials. However, the main purpose and ultimate goal of developing such light weight microwave absorbing and shielding materials composed of Ni-MXene and Ni-Graphene and carbon materials are the key target for design with high efficiency (EMW) absorption (Cao et al., 2021). The results showed an increased mechanical stability and elastic-plastic recovery material; and were found to be suitable for electromagnetic waves in multi-order reflection. The study reveals that, with the increase and decrease of filler content percent of rGO and MXene in polymer PVA thin film, as flexible electronic sheets, the EMI shielding of the developed materials was greatly influenced (Liu, et al., 2020).

Another work study focused on restacking issue was addressed and resolved by opening up the restacked layers of MXene and graphene films loaded with silver nanowires and epoxy-based nanocomposites. In this concern, the most and widely used technique is the freeze-drying approach for creat-

ing porous and impermeable membranes of rGO films decorated with silver nanowires and MXene sheets in the conductive polymer for the proposed application (Liu, 2020). Some other techniques have also been reported in previous studies through instantaneous photo thermal gasification in water, to develop hydrogels filled with water in the interlayers and introduced reactive functional surface groups as shown in Fig. 36 (a & b).

The two-dimensional nanomaterials have fascinated wide-range of contemplations in the present investigation due to their distinctive properties among various two-dimensional materials. MXene is a new type of material which is been widely used for the water, air filtration, energy storage and other electronic applications, due to its excellent surface enhancement properties, it has shown great potential in microwave performance (Zhang, 2020). Very fine and an effective EMI shielding material has been designed with waterborne polyurethane (WPU) composite films MXene and rGO for low microwave reflection loss. As pure MXene and graphene are considered by fabricating with ferric carboxide (FeCo) metal alloys for the embellishment of graphene (FeCo@rGO) and Ag nanoparticles as a layered structure (Weng, 2018). The composite assembly was molded by simple sedimentation technique with polymer(WPU). The produced film acted as a MA layer, and the ultra-fine particles of Ag layer covered the entire surface of the polymer which served as a highly efficient shielding layer as presented in Fig. 36 (c & d).

This distinctive layered structure comprises the microwave-reflecting attributes of nano Ag and the MA behavior of rGO@FeCo to accomplish robust MA and EMI-SE performance with low reflection loss. The composite assembly has acquired significant improvements over a filler content of (10 wt% rGO@FeCo) with silver nanoparticles as a layer of

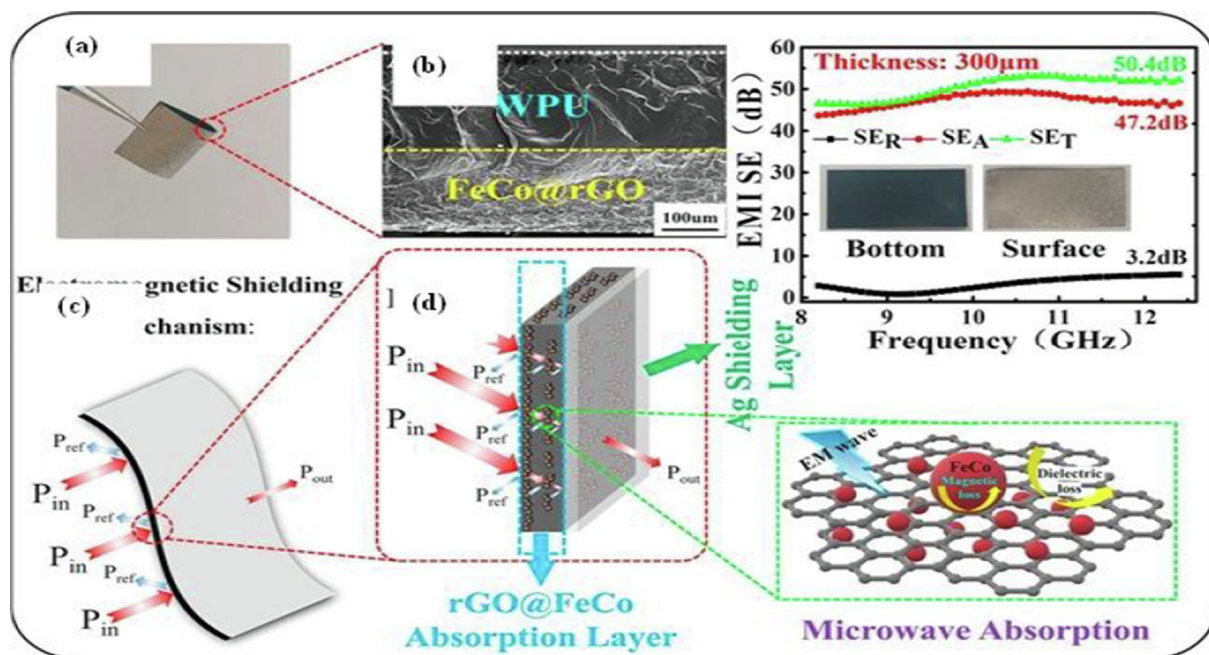


**Fig. 36** FeCO-rGO/WPU waterborne polyurethanes based nanocomposites Film and its SEM image toward EMI shielding properties of films (a), shielding design model and Microwaves absorption properties of rGO@FeCO layered assembly with atomic level microwave absorption behavior of graphene film (b), WPU-rGO/FeCo assembly in crosssectional view (c), shielding mechanism for layered assembly covered in two layers (d). Reproduced with permission; Copyright 2019, Elsevier (Zhu et al., 2019).

500  $\mu\text{m}$ , to 300  $\mu\text{m}$  in its thickness. The developed composite assembly of (Ag/rGO@FeCo/WPU) possesses an outstanding EMI-SE of 50.5 dB and the microwave reflection coefficient of 0.49 with an average  $\text{SE}_R$  of 3.2 dB (Xiang, 2019; Liu, 2020). The results reveal that, the structure is potentially strategy and new method for flexible EMI materials with low reflection characteristics.

In general, the as generated hetero-structures covers the greater area and interacted with each other due to the surface functional moieties present on the films or edges of the rGO and MXene sheets. Whereas as the reactive groups are attributed to develop such mesoporous assemblies made from graphene foams. The MXene@GO based hybrid aerogels are converted into porous aerogels; in which the microspheres (M@PDMS) exhibit higher level of impedance with an improved MA and shielding performance (Wan et al., 2018; Liu, 2020). On contrary, the attributes of such developed mesoporous assemblies from graphene foams, MXene@GO based hybrid aerogels are converted into porous aerogels; in which the microspheres (M@GAMS) exhibits higher level of impedance matching with an improved MA and shielding performance as presented in Fig. 37 (a & b).

Beside, this the developed hydrogels, aerogels, and sol-gels not only offers the porosity but are also assists in less reflection, dissipation or delocalization of incident waves; which is only possible through attenuating of the conductive paths for the enhanced MA and SE performance. The electrically con-

ductive 2D fibre-based porous assemblies with excellent mechanical flexibility and electrochemical properties are considered as promising candidates for flexible electrode materials, but the key challenge is to improve the MA performance by the addition of filler and geometrical alignment of 2D sheets for potential applications of MXene coated fabrics as shown in Fig. 37 (c & d) (Wan et al., 2018; Fan, 2020). So, rather than the structural arrangements, the low fillers content percent is required during the loading of nanoparticles in the nanocomposites; which should not exceeding 10.0–20% by weight % of the composite assembly and a very higher level of thickness of 2.0–2.5 mm, can be achieved to work better and optimize reflection loss ( $R_L$ ) of  $-49.1$  dB at a variable range of frequencies 14.2–18.0 GHz for M@GAMS. However the scalable fabrication technology is needed to reduce electromagnetic pollution from low-density and low-carbon footprint materials. Unfortunately, in most of the EMI shielding materials, environmental adaptability, economic feasibility and light-weight are far from these optimal factors (Liu, et al., 2020).

### 3.2.3. MXene and ICPs polymer-based nanocomposites

The MXene nanosheets were intended under a least level temperature by using an in-situ synthesis with a conductive polymer to develop nanocomposites. The micro scale assemblies of electrochemical properties. The metal carbides ( $\text{Ti}_3\text{C}_2$ /PPy) nanocomposites with variable mass fractions of PPy and  $\text{Ti}_3\text{C}_2$  were considered for suitable shielding materials as

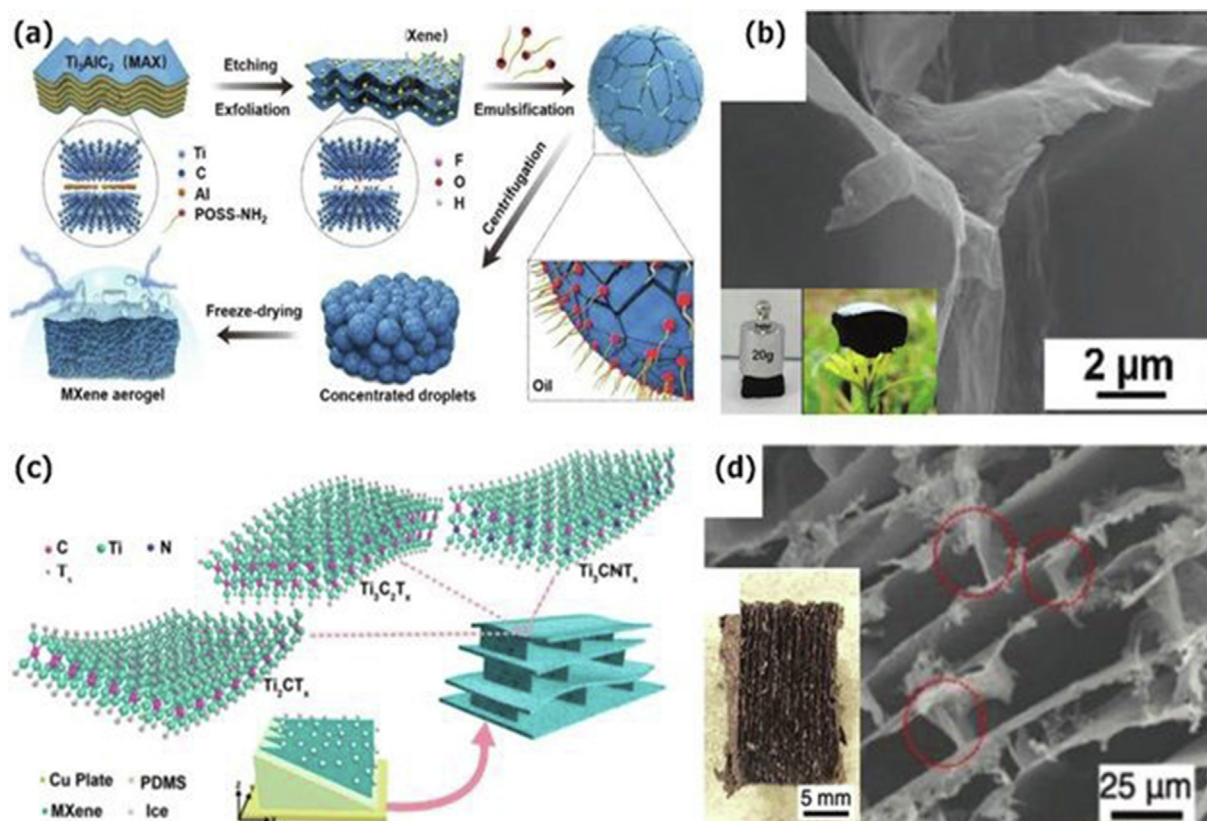


**Fig. 37** Development of MXene aerogels via surfactants (a), SEM images of MXene aerogels (b), MXene aerogels and bidirectional freeze-casting of MXene aerogels (c), and SEM image of a free-standing MX-phase exfoliated into MXene on Cu plate with PDMS and SEM image of the developed MXene aerogels (d) development Microwave shielding. Reproduced with permission; Copyright 2022, Wiley Online reproduced with copyright materials, Wiley online (Wu et al., 2020).

nanocomposites. Remarkably, the higher specific capacitance and unresolved cycling permanence are principally recognized to the arrangement of organ-like MXene nanosheets; in the form of double-layered capacitance (EDLCs) and PPy showed higher pseudo capacitance performance, which proceeds the upgradation of the synergistic consequence amongst dissimilar electrode made of two different ingredients and diverse features of the instruments to improve the electrochemical routine (Feng, 2020). The designing of MXene-based materials for particular use of EMI shielding is reported in several studies in the literature. As the MXene are formulated with different compounds and having an excellent mechanical, thermal and electrical properties. Therefore, here a highly robust, flexible and durable MXene/carbon fiber(CF) based fabric has been introduced which is blended with thermoplastic polyurethanes (MXene/CFf/TPU) composite. The developed composites were fabricated through simple electro hydrodynamic atomization deposition, layer-by-layer and hot pressing methods as demonstrated in Fig. 38 (a-d) (Miao, et al., 2020). However, in these compounds, the synergistic effect is attributes to van-der Waals forces and covalent bonds. These attributes resulted as increased tensile strength and out performance of the newly formed composite up to 170.5 MPa, which is better performance as compared to pristine MXene and its composites as previously reported in literature. Additional, to this the EMI shielding performance of the designed assembly of MXene on carbon fibers loaded with thermoplastic polyurethane (MXene/CFf/TPU) composite was also enhanced with MXene and its mass fraction (Li et al., 2020; Liu, 2017). The overall stability and SE performance were reached to

40.5 dB, which is attribute to the dielectric loss. This synergistic effect may be introduced due to the presence of the conductive channels and the improved MA in the sandwich structure of the composites. More remarkably, the composite engaged an excellent resistance stability; EMI-SE stability and flexibility, even after multiple bending and releasing cycles as shown in Fig. 38 (e & f).

The study shows that, facile fabrication method for the preparation of the composites had an excellent EMI shielding material, which may easily reached with greater number of possibilities in intelligent wear and electronic systems. The MXene based as a framework limits the growth of PPy, precludes the re-stacking of PPy, and endorses the operational steadiness of  $Ti_3C_2T_x$ /PPy nanocomposite (Liao, 2022; Wang, 2019). Furthermore, the intersegment of reliable PPy particles increases the interlayer space MXene sheets itself, and the exceedingly accompanying with polymeric restriction, which can deliver supplementary trails for electrolyte ions dispersal and charge distribution. Therefore by aggregation of developed assemblies explicate EMI-SE and may reduce the charge transmission confrontation is managed. Most of all it has exposed as a low-cost and a suitable way to construct such structures on large-scale made up of MXene/PPy nanocomposites films and requires excessive impedance matching and auspicious forecasts as conductor constituents for super capacitors (Xu, 2019).

The development of different material assemblies for restriction of EMI is great concern of the developing society in recent years, which requires more attention of the scientific community to reduce such pollution; with the recent develop-

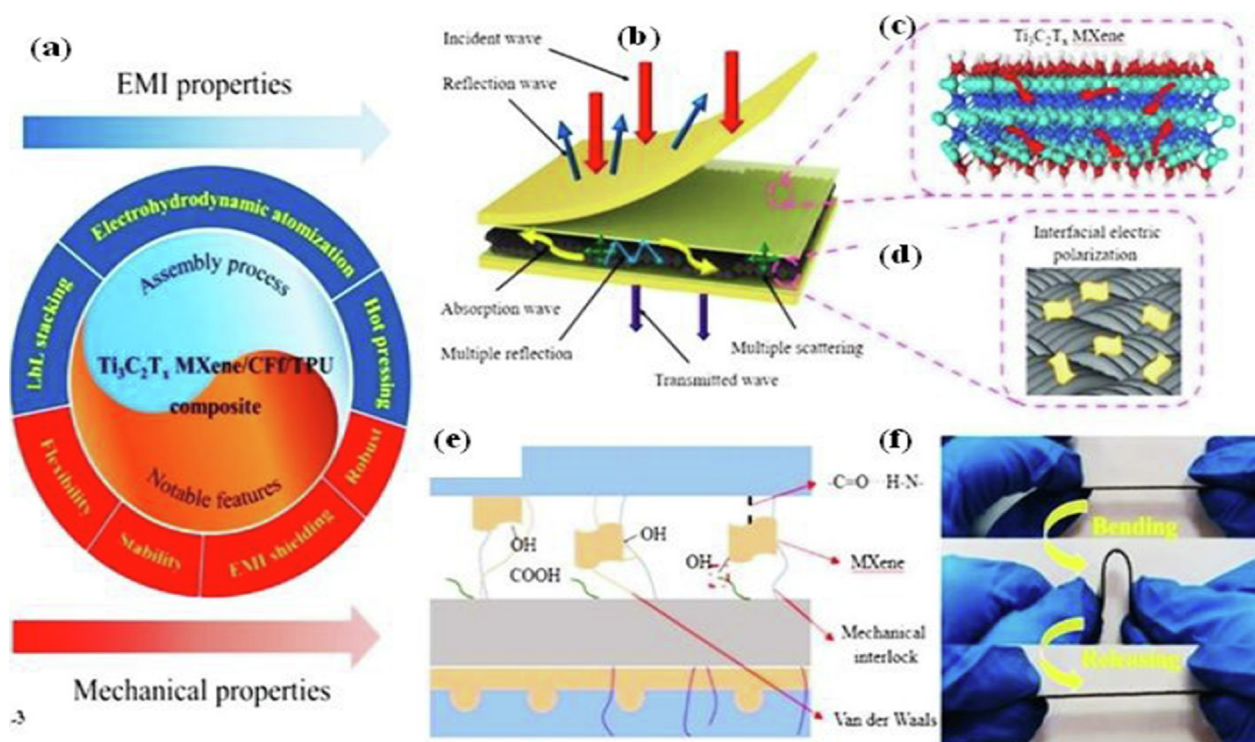


**Fig. 38** MXene coated fibers and thermoplastic polyurethane composites (a), EMI shielding model for multiple layered composite assembly (b), reflection of electromagnetic waves from MXene sheets (c), reactive functional groups present on MXene sheets on fiber surface (d), foldable and stretchable highly flexible fabric coated with MXene for EMI and Microwave shielding via thermal treatment(e & f). Reproduced with copyright materials. Elsevier, 2022 (Duan et al., 2022).

ments of research in the field of science and technology. In order, to resolve these complex problems of EMW absorbing over a variable bandwidth and environmental protection with oxidation and reduction which is resistant other than traditional single phase nickel spheres and MXene based composites exhibited the remarkable ferromagnetic attributes as presented in Fig. 39 (a-e); showing double-loss including dielectric and magnetic loss and is considered as an efficient EM absorbing materials (Shi et al., 2021; Fan, 2020). The resultant MXene-based aerogel pooled with the well retained essential construction of MXene and aligned core-shell structure shows promising electrical conductivity of  $1085 \text{ S cm}^{-1}$ . When used as conductive networks in shielding materials, the aerogel made by mixing the epoxy nanocomposite; also demonstrated with remarkable electrical conductivity of  $695.9 \text{ S m}^{-1}$ . Whereas, the EMI shielding effectiveness of the nanocomposite exceeded to 50 dB with a determined value of 56.4 dB over X-band. The development of 3-D MXene-based architecture releases a innovative path for the use of MXene in various arenas. Though, the re-stacking problem still exists in these materials, which can significantly decrease their EMI-SE performance; and can be optimized with increasing thickness and mass loading (Yin, 2020).

### 3.2.4. MXene-rGO/polymer-based nanocomposites

The MXene modified with poly dopamine ( $\text{Ti}_3\text{C}_2\text{T}_x/\text{PDA}$ ) composite film electrode was reasonably intended and effectively produced by one-step in situ polymerization. The as modified films with dopamine developed an opposite charge

on the surface of films coated nano fibers, films and sheets (Wu, 2020). Similarly another work is proposed to investigate the conductive polymer (PEDOT) as a spacer between the MXene sheets and graphene sheets to avoid the agglomerations. In which the 2-D materials are incorporated and employed as 3D architecture of a aerogel to restrict the restacking of 2-D MX nanosheets without the use of additives; which exhibited an improved performance as compared to untreated ones MX-rGO films for EMI shielding and MA absorption in operational manner (Han, 2019). The MXene modified with poly dopamine ( $\text{Ti}_3\text{C}_2\text{T}_x/\text{PDA}$ ) compound electrodes were effectively produced by in-situ polymerization reasonably used for MA and EMI shielding. The PDA modified films developed opposite charge on the surface of the  $\text{Ti}_3\text{C}_2\text{T}_x$  films coated nano fibers, films and sheets as preceded in Fig. 40 (a-f) (Huan, 2022; Rajavel, 2020; Bian et al., 2019).

The 3-D MX-CNTs aerogel films were developed by using a vacuum filtration and freeze-drying process. The results show that the carbon nanotubes into the MXene-based aerogel can prevent the restaging of MXene nanosheets with each other due to the Van-der Waals forces, and lead to three-dimensional interconnected porous structure with large specific surface area and excellent compressive recovery (Ryu, 2022). However, it is anticipated to consistently anchor a hydrous ruthenium oxide ( $\text{RuO}_2 \cdot x\text{H}_2\text{O}$ ) nanoparticles on MXene nanosheets. The resulting  $\text{RuO}_2@\text{MXene}$  composites loaded with silver nanowires (AgNWs) to ultimately assist as a printed textile electrode on micro-scale for the high-performance shielding effectiveness. Furthermore, the performance of the

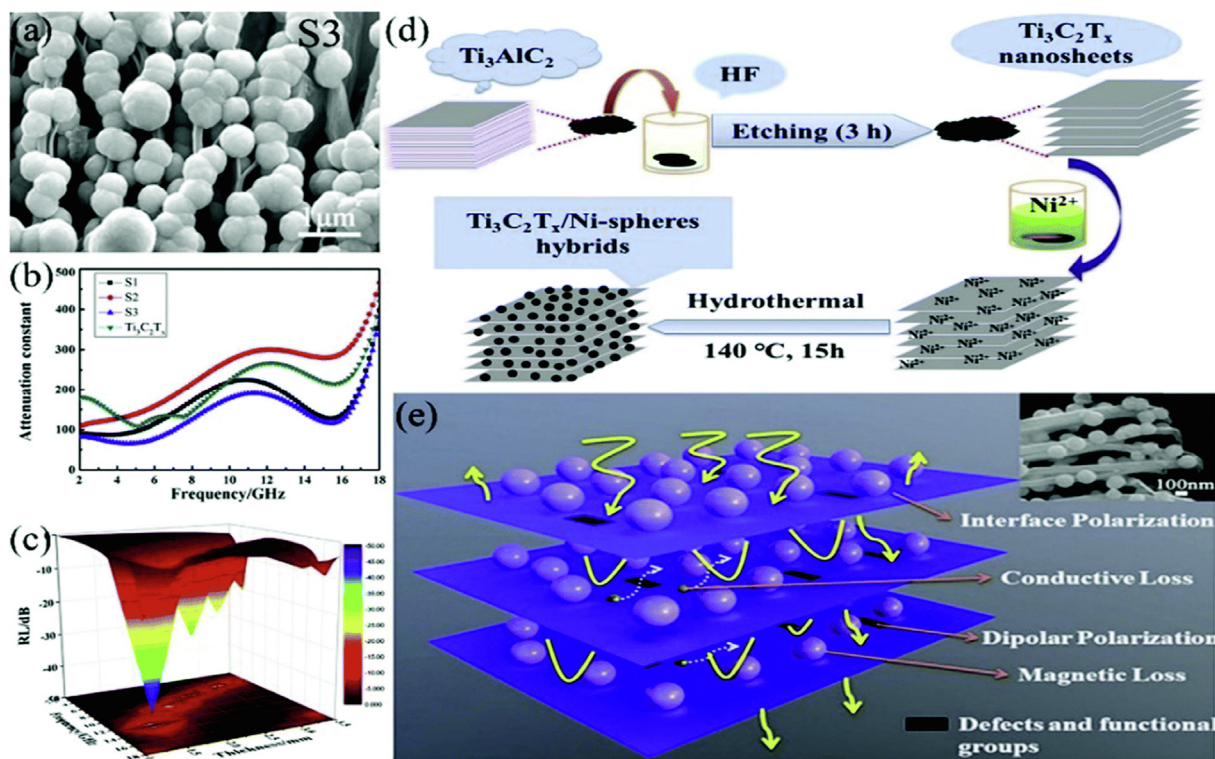


**Fig. 39** SEM image of MXene loaded Nickel micro-spheres (a), EMI response of developed MXene@Ni-based composite (b), reflection loss ( $R_L$ ) response of composite (c), chemical exfoliation of MXene and in-situ loading of Ni-Particles via hydrothermal (d), and layered MXene sheets loaded with Ni-Spheres in between design model for Microwave and EMI shielding (e), reproduced with copy right material @ Royal Society of Chemistry, 2021 (Deng et al., 2021).

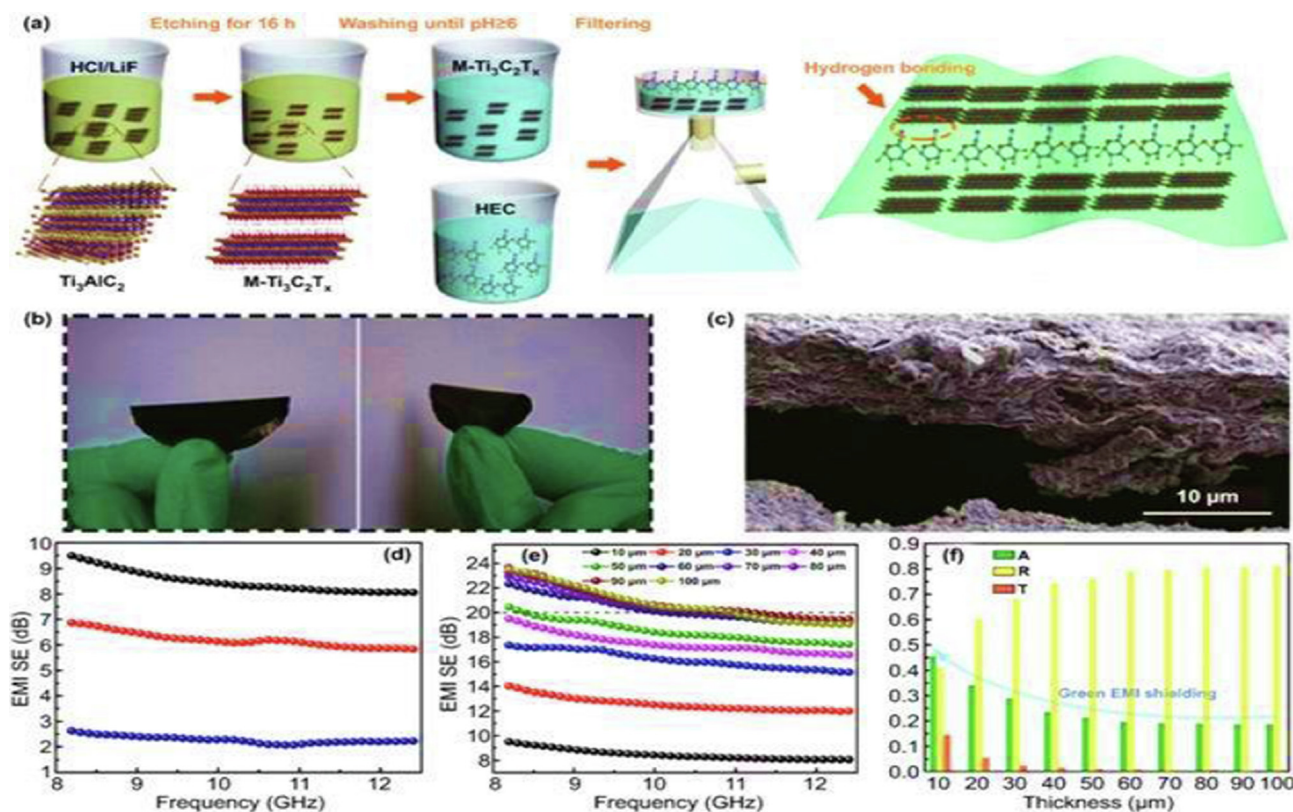


**Fig. 40** Digital image for the chemical etching and Fabrication of MXene-HEC films (a), MXene-HEC composites films foldeable (b), SEM images showing crosssectional view of composite films (c), EMI Shielding response of developed composite films with different thickness (d), EMI SE of  $\text{M-Ti}_3\text{C}_2\text{T}_x/\text{HEC}$  composite film at different stacking thicknesses (e), and an average A, R and T of  $\text{M-Ti}_3\text{C}_2\text{T}_x/\text{HEC}$  composite film at different stacking thicknesses (f), reproduced with copyright materials, Springer an open access 2021 (He et al., 2021).

nanocomposite was dependent on thickness and diffusion mechanism with different types of hydrated ions by combining the experimental and DFT results. Owing to higher electrical conductivity, MXene@PS heterogeneous structure of micrometer thickness shows an excellent EMI-SE with foremost absorption contribution in the microwave frequency range of (X-band) (Zhang et al., 2021). The total shielding efficiency along with EM waves' absorption capability of the composite films were optimized by different beads sizes of polymers(PS). Composite films with smaller beads size possessing a higher dielectric domain density due to the larger surface area and revealed better EMI shielding performance (Zhan, 2021).

Even though electrically conductive polymer compounds (ECPCs) are considered as an auspicious material in the solicitation of EMI shielding, however to endow the ECPCs for multifunctional use is a great challenge. Here an innovative polyurethane/polydopamine/silver nanoparticle (PU/PDA/Ag) sponges were developed with outstanding protection against EMI shielding. The complex assembly was magnificently conceived by a facile technique and acquired by two fold processing:

- (i) Polydopamine (PDA) was decorated on the surface of PU exfoliators with dopamine coated self-polymerization as demonstrated in Fig. 41 (a & b).
- (ii) Ag nanoparticles were in-situ grown on the surface of PU sponges by electroless plating.

The developed sponge like structure showed a maximum EMI-SE of 84.6 dB with the consistent SE response with an unconditional SE value of  $2625 \text{ dB cm}^3 \text{ g}^{-1}$  and  $5250 \text{ dB cm}^2 \text{ g}^{-1}$ . These results are much higher as compared to the other shielding foams and sponges. Meanwhile, the developed sponge retained as little thermal conductivity of (52.72 mW/mK) but exceptional compression resilience and piezoresistive properties as demonstrated in Fig. 41 (c & d) (Zhan, 2021; Zhang et al., 2021). In addition, the chemical and electrochemical stability of MXene electrodes was achieved through unconventional assembly methods. These highly conductive polymers are also extensively used for EMI and MA purposes with improved electrical, thermal, mechanical and electronic properties of the MXene-rGO nanocomposites for effective EMI, shielding, and supercapacitors applications (Sambyal, 2019). Whereas, the fabrication of a free-standing porous substrate as a 3D network of graphene and MXene, may have weak inter-sheet interfaces due to more gapes or vacuoles; which can trap and entangle the electromagnetic waves. Nevertheless, the higher interfacial polarization may be increased for the constructed assembly from the lightweight 3D porous structure through bridging the MXene films with polyamide (PDA) structure on macro-molecules (Liang et al., 2020). These outstanding performance and higher flexibility with improved electrical conductivity makes these aerogels; as a new class of materials and favorable applicant for restraining the EMS. More interestingly, more improvements in MA

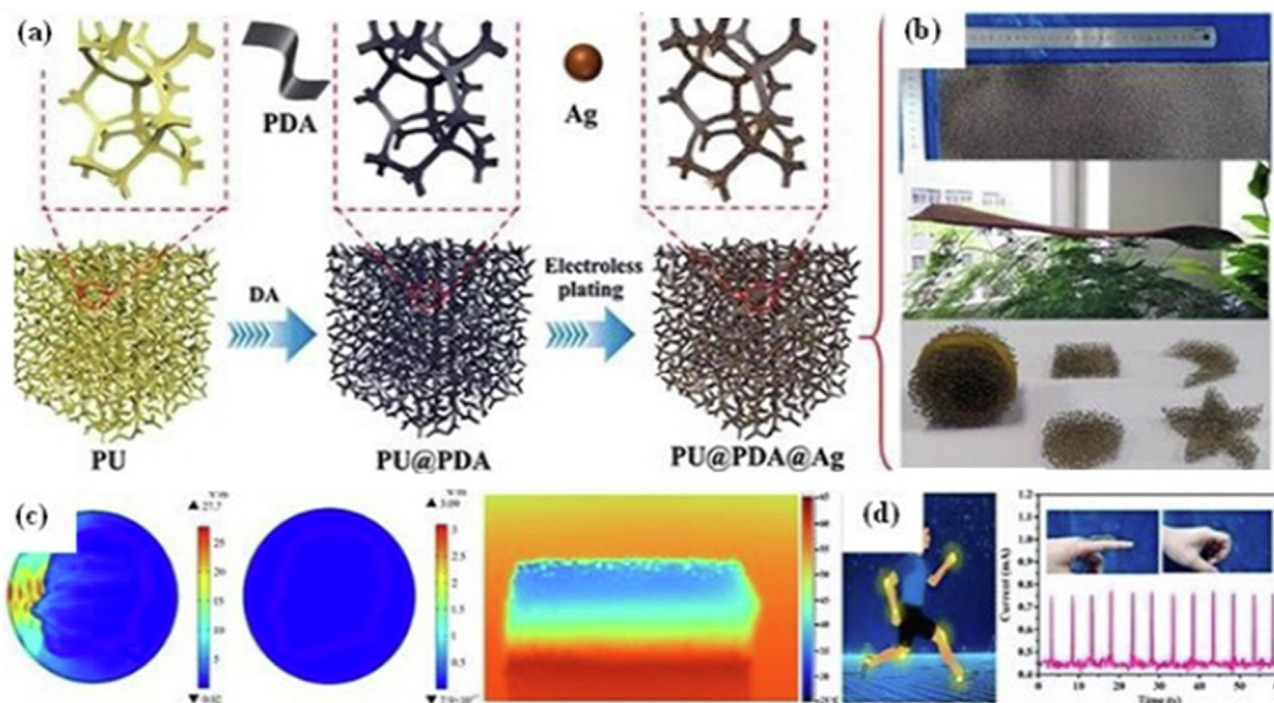


**Fig. 41** Development of PU-modified with Polydopamine PDA via hydrothermal reduction foams extended image size of pure PU after loading with Ag (a & b), simulation of microwave absorption under IR rendering of developed foam (c), and sensory and body movement response (d). The Figure has been reproduced with copyright permission from Elsevier, 2020 (Liang et al., 2020).

performance and EMI shielding can be attained with a maximum reflection loss ( $R_L$ ) value of  $-45.4$  dB at 9.59 GHz and an operational (MA) fascination bandwidth ( $< -10$  dB) of 5.1 GHz were attained with greater sensitivity and long-term stability under variable working conditions.

In addition, the thermal insulation and SE performances stability against the heat of the porous MXene/PI aerogel were also explored. Thus, the novel techniques may also provide a new dimensions are concerns for the design and development of new 3D highly porous MXene based assemblies and would expand significantly the potential applications of MXene materials. Furthermore,  $Ti_3C_2Tx/CNF$  composite paper is a highly flexible, which can withstand variable loading, and even under folded into complex shapes; which exhibits a negligible loss of electrical conductivity after repeated folding/unfolding process. The  $Ti_3C_2Tx/CNF$  nanocomposite shows better performance towards microwave and EMI shielding effectiveness. The results also demonstrate that the  $Ti_3C_2Tx/CNF$  composite paper is a promising candidate for the presentations of bendable, portable and e-textile devices (Liang et al., 2020; Geng, 2019). Similarly in another work, an anisotropic composite of a sponge like structure containing of (CNFs) and chemically reduced silver nanowires over ferric oxide ( $AgNW$ )@ $Fe_3O_4$  were in-situ synthesized. The developed composites showed an improved (SE) performance due to the addition of anisotropic materials in the composites, which resulted as synergistic effect among CNFs,  $AgNW$ s, and  $Fe_3O_4$ . The sponge showed a low density ( $16.76$  mg/cm<sup>3</sup>), better saturation magnetization of ( $4.21$  emu/g) with an conductivity ( $0.02$  S/cm), and anisotropic EMI shielding capability by varying the ratios of (1:0.3) among  $AgNW$ s and  $Fe_3O_4$  with a loading of ( $0.15$  vol%) in the sponge. The reflection loss ( $R_L$ ) of the sponge with the

an improved interface polarization and impedance mismatch reached around 2.3 dB, and resulting 7.2 % improvement of the total reflection loss (Zhang, 2020). In another work; researcher investigated the properties of hybrid materials consisting of MXene and PEDOT: PSS nanocomposites with graphene and silver nanowires for microwave and EMI shielding effectiveness. However several (ICPs) polymers are generally applied on wearable fibrous assemblies for mass-scale production of such fabrics and films coating to enhance the EMI and MA shielding performances. The shielding performance and electrical properties of the developed nanocomposites were improved made of the conducting polymer; after coating on the textile fabric and are greatly influenced by various parameters; including the weight, deposition level and fabric or composite; thickness of the polymer coating layer, the thickness of the fabric, nature and type of the substrate, its surface functionality, and chemical or physical binding strength on the surface of the textile substrate (Chen, et al., 2022). The study showed an improved performance as compared to the pure MXene and graphene. The shielding effectiveness and MA performance were greatly influenced by the addition of conductive polymers i.e PEDOT: PSS, MXene/PPy and PANi nanohybrids, which exhibited an enhanced shielding performance as compared to pristine ones. The hybrid structures of conductive polymers with graphene and MXene showed the highest response towards MA and EMI shielding with a maximum efficiency of 99.9 % absorption at temperature and the highest EMI shielding effectiveness was attained. Similarly MXene and rGO with PANi and PPy  $AgNW$ s; showing a synergistic effect of conductive polymers with rGO and  $Ti_3C_2Tx$  MXene sheets with higher electrical conductivity due to the conductive paths (Cheng, 2020). However, the highest selective shielding

range of the developed nanocomposites was attained by the MXene, PEDOT: PSS, rGO-PANi, and MXene-rGO/AgNWS ternary structures respectively with conductive polymer a shielding layer. Previous studies made on MA over a variable bandwidth of 2–20 GHz for paraffin-MXene and ferric oxide ( $\text{Ti}_3\text{C}_2\text{T}_x$ )/ $\text{Fe}_3\text{O}_4$  coated MXene composites. The electromagnetic characterization of such developed composites was carried out in the broad frequency range (2–18 GHz) using a CST-microwave. The simulated result indicates that the solitary coating of MXene complexes exhibits an outstanding reflection loss ( $R_L$ ),  $-30$  dB, however, bandwidth is very narrow even if increasing the thickness to 8 mm, which was well matched with experimental data (Hu et al., 2020).

The results demonstrate that the conductive polymers would open new opportunities for exploring more MXene and graphene-based nanocomposites with controlled composition and morphologies towards higher MA and EMI shielding performance. The designed a macro-scopical pyramidal configuration succeeding in an excellent  $R_L$  bandwidth at a certain configuration, which is due to the higher interfacial impedance matching. This shows that the importance of the structural design of MXene containing polymer nanocomposites for real-time applications such as military communication. Generally, the graphene and 2D materials are widely used to develop solgel and hydrogels using freeze-drying techniques. As other chemical reduction and thermal reduction techniques also be used to reduce the interaction of the sheets with each other and restacking of graphene sheets (Sambyal, 2019). Therefore, the most widely used and preferred technique is freeze-drying, in which water content is evaporated at the lowest temperature

of  $-48$ – $50$  °C to keep separate sheets with ice flakes to keep apart sheets from each other and avoid any re-binding of oxidized GO sheets, and can easily be dissolved in different solvents and even in water-based solution, as presented in Fig. 42 (a-c). The effect of cell size can be studied over a broader extent with variable loading of MXene on the electrical conductivity ( $\sigma$ ), EMI effectiveness, SE values, mechanical, and thermal properties. Similarly, the designed rGMH/epoxy nanocomposites were evaluated and converted (Sambyal, 2019; Wang, 2019). Herein, the work also validated and well-organized method for the fabrication exceedingly the conductive 3-D MXene films and porous constructions made up of GO. The structure was desiccated by vacuum assisted filtration and a hydrothermal reduction followed by freeze-drying method (Yin et al., 2020). The developed nanocomposites aerogel may comprise a highly aligned and more oriented micro-structure (wall-brick like) in which graphene work as core skeleton, whereas the tightly packed MXene ( $\text{Ti}_3\text{C}_2\text{T}_x$ ) sheets work as a shell of the walls of the structure as presented in Fig. 42 (d-f). The resultant nacre like structure could facilitate in higher attenuating of microwave and electromagnetic waves due to its highly porous and conductive infrastructures (up to  $1085$  S  $\text{cm}^{-1}$ ).

This highly efficient performance and conductivity are endowing to stable epoxy interference in the nanocomposite; with an electrical conductivity of  $695.9$  S  $\text{m}^{-1}$  and an EMI-SE values greater than  $50$  dB in the X-band by using very minimum content percent of rGO and MXene sheets with the content of  $0.74$  vol%. The presented work concludes; that the results are best for epoxy nanocomposites as compared to

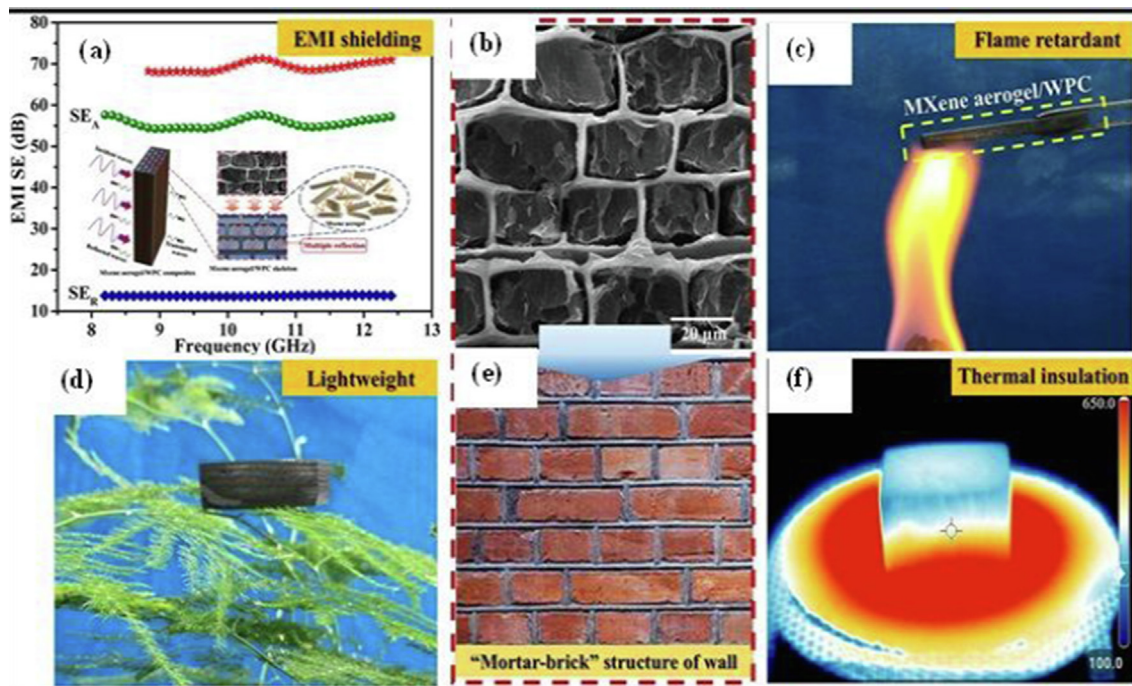


**Fig. 42** Chemical etching of MXene for the development of few layered sheets of MXene and MXene/WPC based composite's fabrics (a), composites hydrogel films like brick-wall mortar like SEM image of aerogels (b), MXene aerogel with WPC as flame retardant foam (c), light weight foam standing (d), model design mortar brick structure (e), thermal insulation performance of aerogel microwave assisted thermal reduction of nanocomposites films (f) for microwave and EMI shielding. Reproduced with the copyright permission by Elsevier 2020 (Liang et al., 2020).

other polymer type nanocomposites over the same loadings of MXene reported in previous works (Liu et al., 2019). The natural cotton fibers dispersed in the sucrose aqueous solution and was consolidated by means of pressure filtration, drying, and carbonization techniques, to prepare heat-insulating and fire-resistant carbon composite foam. When the sucrose concentration is higher than 200 g/L, the carbon syntactic foam undergoes a partial flexible to rigid transition. Tubular carbon fibers were formed from cotton and were welded by sucrose-generated amorphous carbon at their contact points, resulting in low sucrose concentrations. The lower part is pliable, and the advancement of the fiber-to-fiber bonding area was attained at high sucrose concentrations and resulted in formation of a rigid foam. The interfere spaces and porosity in the lumen of carbonized cotton fibers results in low thermal conductivity. The developed nanocomposite fiber assemblies may be considered as potential candidates for MA and EMI SE

due to their very thin structure, which can be used in multiple layered composites for effective shielding performance (Jia et al., 2020). The work as previously reported on the fabrication and coating of different intrinsic conductive polymers i.e Pyrrole, and PPy based aerogels, which does not significantly change the mechanical performance but allows the development of highly flexible, stretchable and bendable conductive textile substrates with enhanced EMI shielding performance as shown in Fig. 43 (a & b).

Whereas, the performance of textiles substrates coated with MXene can also be improved with the number of coating layers on the fiber structures such as woven, and non-woven fabrics as shown in Fig. 43 (c-f) (Qing et al., 2016). The commercially available fabrics and laminates are produced with different materials on textile fibers; which exhibits higher SE and satisfactory performance with isotropic behavior. Interestingly, previously reported materials were prepared by

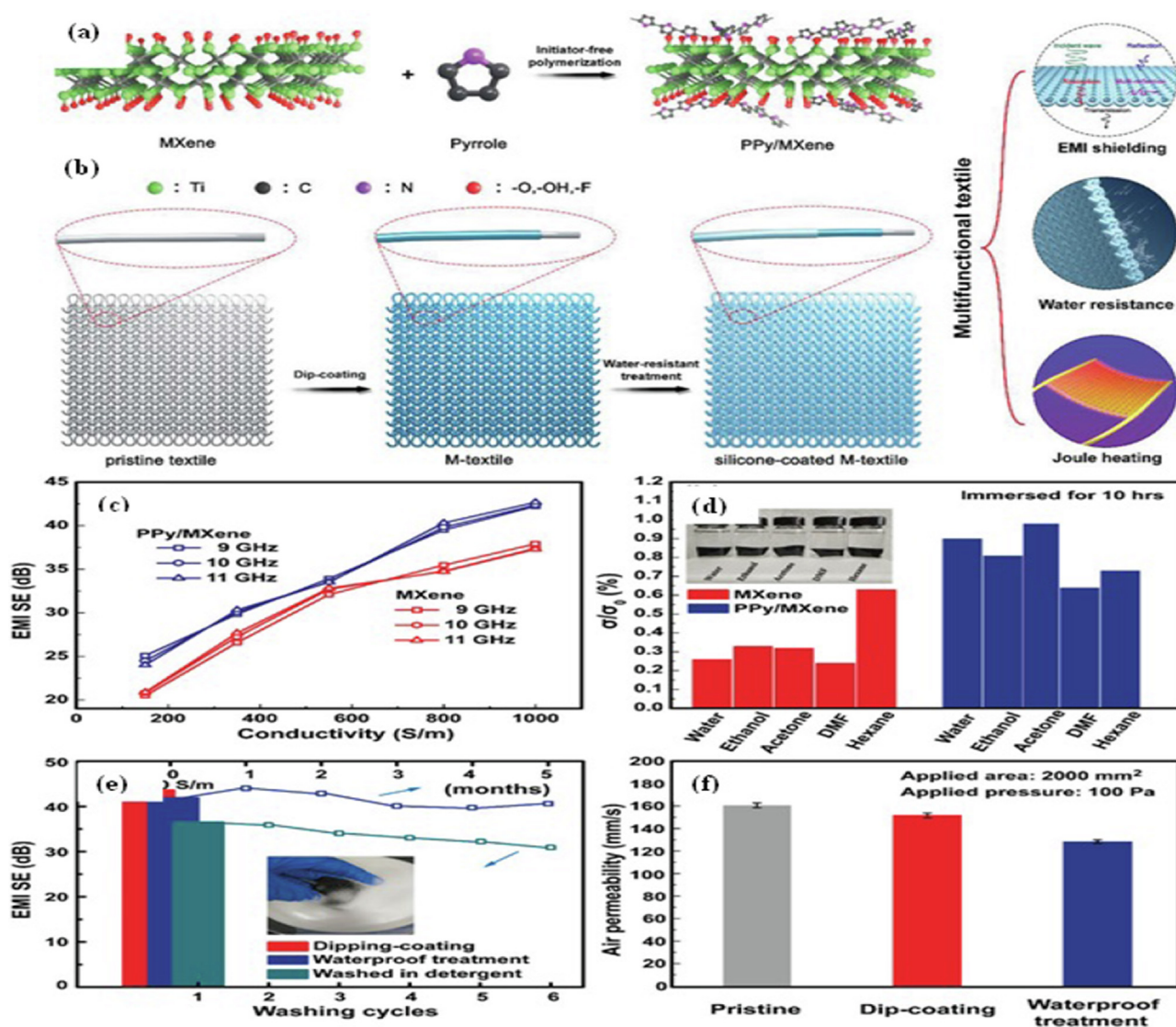


Fig. 43 Developed MXene and pyrrole coated fabrics with PPy/MXene composites and knitted fabric coated with MXene (a & b), Shielding response of fabric (c), Electrical conductivity of MXene based composites (d), Stability of EMI shielding by effects of water resistant, (e) Air permeability of synthesized materials. Reproduced with copyright material by John Wiley and Sons, 2021 (Wang et al., 2019).

using ultra-light Ni/MXene/rGO (NiMR-H) aerogels with EAB of  $6.45 \text{ mg cm}^{-3}$  and provides the highest MA performance for MXene-based absorbing materials with a minimum reflection loss of ( $R_{L\text{min}}$ ) value of  $-75.2 \text{ dB}$  and higher (ES) percentage of (99.9 %) for microwave over a broadest EAB range of 5.0–7.3 GHz (Feng et al., 2018).

#### 4. Perspective and outlook

There is a great demand for MXene into flexible devices and functionally reinforced composites due to metallic behavior and surface enriched with reactive functional groups. Furthermore, the graphene-like 2D constituents with a multilayer feature of MXene has extraordinary dielectric loss as persistent in the polymer matrix at low grade levels. The limit ensuing as a capable assembly with ultra-light weight towards microwave absorption. Yet, the prospective of MXene needs to be more studied and elaborated with its coordination, construction with different polymer composites need to be discovered. The main purpose of this review would provide better understanding and recent work being made on different materials using various scientific approaches towards the development of new two dimensional materials including polymers, conductive polymers, organic and inorganic metals for significant improvements in the EMI shielding and microwave absorption. This review work provides the better understanding of MXene and graphene based nanocomposites for potential end uses particularly their binding or fixation attributes and behavior with metal complex to address their limitation and recent challenges. However, the current review article is mainly focused on 2D Materials  $\text{Ti}_3\text{C}_2\text{T}_x$  MXene and reduced graphene oxide. It is very important to understand their uses in wireless communication for effective and efficient shielding efficiency of microwave and EM mechanism. Furthermore, the recently used methods to construct the graphene and MXene significantly influenced the overall EM and MA through a modification of conductivity of MXene sheets. The use of different methods for constructing of MXene, graphene, metal complexes, and conductive polymers regulates the conduction as a future direction of research activities in recent years. However, during synthesis process the oxidation of MXene is not preventable issue especially in case of few-layered to multilayered graphene and MXene.

#### 5. Conclusions

In conclusion, the two-dimensional materials are highly efficient and suitable candidate for EMI shielding and MA properties in the form of different nanocomposite films, 2D, 3D porous assemblies, and composite foams are demonstrated. The broader use and potential application prospective in terms of novel EMI and MA materials are expatiated and reviewed in this article. The design and development of these nanocomposites in combination with organic and inorganic fillers are discussed to address well current state of the art and different challenges for the development of effective SE materials. Whereas, several techniques has been practices and proposed in several studies till today for 2D materials using using polymers and conductive polymers to work as binders and binder free approach towards an improved EMI shielding and microwave absorption. Nevertheless, the limitation and challenges are well addressed and focused on alternative solution. However, the research work and studies are facing several challenges concerned to 2D materials using some new techniques for synthesis and fabrication on mass scale production. Whereas, the effective and

efficient performance are also remained challenging and are under investigation; these concerns are well addressed. The intention for the design and development of new vigorous, eco-friendly and cost-effective nano-materials is remained as major concern and global challenge. The future growth and uses may require certain improvements in terms of cost effective and efficient methods for synthesis and fabrication keeping in view prolonged exposure and long-lasting use in various working environments. Secondly, the foremost and challenging concern of these materials is environment friendliness and user friendly, without significantly influencing the environment and personal health due to their toxic behavior. The future perspective and growth of novel 2D materials require more attention related to synthesis and fabrication with certain improvements in microwave and electromagnetic shielding effectiveness.

#### Declaration of Competing Interest

The authors declare that they have no known competing financial interests or personal relationships that could have appeared to influence the work reported in this paper.

#### Acknowledgement

This work was supported by National Natural Science Foundation of China (Grant No. 51972077) and Harbin Engineering University, China.

#### References

- Abdolhosseinzadeh, S., Jiang, X., Zhang, H., Qiu, J., Zhang, C., 2021. Perspectives on solution processing of two-dimensional MXenes. *Mater. Today* 48, 214–240. <https://doi.org/10.1016/j.mattod.2021.02.010>.
- Ameri, Z., Soleimani, E., Shafyei, A., 2022. Preparation and identification of a biocompatible polymer composite: shielding against the interference of electromagnetic waves. *Synth. Met.* 283, <https://doi.org/10.1016/j.synthmet.2021.116983> 116983.
- Amini, M., Kamkar, M., Rahmani, F., Ghaffarkhah, A., Ahmadi-jokani, F., Arjmand, M., 2021. Multilayer structures of a  $\text{Zn}_0.5\text{Ni}_0.5\text{Fe}_2\text{O}_4$ -reduced graphene oxide/PVDF nanocomposite for tunable and highly efficient microwave absorbers. *ACS Appl. Electron. Mater.* 3 (12), 5514–5527. <https://doi.org/10.1021/acsaem.1c00940>.
- Bai, W. et al, 2022. Graphene oxide nanosheets and Ni nanoparticles coated on glass fabrics modified with bovine serum albumin for electromagnetic shielding. *ACS Appl. Nano Mater.* 5 (6), 8491–8501. <https://doi.org/10.1021/acsnm.2c01760>.
- Bai, Y., Qin, F., Lu, Y., 2020. Multifunctional electromagnetic interference shielding ternary alloy (Ni–W–P) decorated fabric with wide-operating-range joule heating performances. *ACS Appl. Mater. Interfaces* 12 (42), 48016–48026. <https://doi.org/10.1021/acsaem.0c15134>.
- Balci, O., Polat, E.O., Kakenov, N., Kocabas, C., 2015. “Graphene-enabled electrically switchable radar-absorbing surfaces”. *Nat. Commun.* 6 (1), 6628. <https://doi.org/10.1038/ncomms7628>.
- Bhuvanesh Kumar, M., Sathiya, P., 2021. *Methods and materials for additive manufacturing: a critical review on advancements and challenges. Thin-Walled Struct.*
- Bian, R., He, G., Zhi, W., Xiang, S., Wang, T., Cai, D., 2019. Ultralight MXene-based aerogels with high electromagnetic interference shielding performance. *J. Mater. Chem. C* 7(3), 474–478. 10.1039/C8TC04795B. doi: 10.1039/C8TC04795B.
- Cai, C., Wei, Z., Deng, L., Fu, Y., 2021. Temperature-invariant superelastic multifunctional mxene aerogels for high-performance photoresponsive supercapacitors and wearable strain sensors. *ACS*

- Appl. Mater. Interfaces 13 (45), 54170–54184. <https://doi.org/10.1021/acsami.1c16318>.
- Cao, M.-S. et al, 2012. Ferroferric oxide/multiwalled carbon nanotube vs polyaniline/ferroferric oxide/multiwalled carbon nanotube multiheterostructures for highly effective microwave absorption. *ACS Appl. Mater. Interfaces* 4 (12), 6949–6956. <https://doi.org/10.1021/am3021069>.
- Cao, W.-T. et al, 2018. Binary strengthening and toughening of MXene/cellulose nanofiber composite paper with nacre-inspired structure and superior electromagnetic interference shielding properties. *ACS Nano* 12 (5), 4583–4593. <https://doi.org/10.1021/acsnano.8b00997>.
- Cao, M.-S. et al, 2019. Electronic structure and electromagnetic properties for 2D electromagnetic functional materials in gigahertz frequency. *Ann. Phys.* 531 (4), 1800390. <https://doi.org/10.1002/andp.201800390>.
- Cao, F. et al, 2021. Tailing size and impedance matching characteristic of nitrogen-doped carbon nanotubes for electromagnetic wave absorption. *Carbon* 174, 79–89. <https://doi.org/10.1016/j.carbon.2020.12.013>.
- Cao, F. et al, 2021. Hierarchically three-dimensional structure assembled with yolk-shelled spheres-supported nitrogen-doped carbon nanotubes for electromagnetic wave absorption. *Carbon* 185, 177–185. <https://doi.org/10.1016/j.carbon.2021.09.026>.
- Cao, F. et al, 2022. Regulation of impedance matching feature and electronic structure of nitrogen-doped carbon nanotubes for high-performance electromagnetic wave absorption. *J. Mater. Sci. Technol.* 108, 1–9. <https://doi.org/10.1016/j.jmst.2021.08.048>.
- W.-Q. Cao, X.-X. Wang, J. Yuan, W.-Z. Wang, and M.-S. Cao, “Temperature dependent microwave absorption of ultrathin graphene composites,” *Journal of Materials Chemistry C*, 10.1039/C5TC02185E vol. 3, no. 38, pp. 10017-10022, 2015, doi: 10.1039/C5TC02185E.
- M.-S. Cao, J.-C. Shu, B. Wen, X.-X. Wang, and W.-Q. Cao, “Genetic Dielectric Genes Inside 2D Carbon-Based Materials with Tunable Electromagnetic Function at Elevated Temperature,” *Small Structures*, vol. 2, no. 11, 2021, doi: 10.1002/sstr.202100104.
- Cao, W., Ma, C., Tan, S., Ma, M., Wan, P., Chen, F., 2019. Ultrathin and flexible CNTs/MXene/cellulose nanofibrils composite paper for electromagnetic interference shielding. *Nano-Micro Lett.* 11 (1), 72. <https://doi.org/10.1007/s40820-019-0304-y>.
- Cao, M.-S., Song, W.-L., Hou, Z.-L., Wen, B., Yuan, J., 2010. The effects of temperature and frequency on the dielectric properties, electromagnetic interference shielding and microwave-absorption of short carbon fiber/silica composites. *Carbon* 48 (3), 788–796. <https://doi.org/10.1016/j.carbon.2009.10.028>.
- Cao, M., Wang, X., Cao, W., Fang, X., Wen, B., Yuan, J., 2018. Thermally driven transport and relaxation switching self-powered electromagnetic energy conversion. *Small* 14 (29), 1800987. <https://doi.org/10.1002/sml.201800987>.
- Chen, Y. et al, 2021. Recent progress on nanocellulose aerogels: preparation, modification, composite fabrication, applications. *Adv. Mater.* 33 (11), 2005569. <https://doi.org/10.1002/adma.202005569>.
- Chen, Y., Li, J., Li, T., Zhang, L., Meng, F., 2021. Recent advances in graphene-based films for electromagnetic interference shielding: review and future prospects. *Carbon* 180, 163–184. <https://doi.org/10.1016/j.carbon.2021.04.091>.
- Chen, J., Shen, B., Jia, X., Liu, Y., Zheng, W., 2022. “Lightweight and compressible anisotropic honeycomb-like graphene composites for highly tunable electromagnetic shielding with multiple functions”. *Mater. Today Phys.* 24,. <https://doi.org/10.1016/j.mtphys.2022.100695> 100695.
- T. Chen et al., “Hexagonal and cubic Ni nanocrystals grown on graphene: phase-controlled synthesis, characterization and their enhanced microwave absorption properties,” *Journal of Materials Chemistry*, 10.1039/C2JM31171B vol. 22, no. 30, pp. 15190-15197, 2012, doi: 10.1039/C2JM31171B.
- R. Chen et al., “Interface design of carbon filler/polymer composites for electromagnetic interference shielding,” *New Journal of Chemistry*, 10.1039/D1NJ00147G vol. 45, no. 19, pp. 8370-8385, 2021, doi: 10.1039/D1NJ00147G.
- Y. Chen et al., “Anisotropic cellulose nanofibril composite sponges for electromagnetic interference shielding with low reflection loss,” *Carbohydr Polym*, vol. 276, p. 118799, Jan 15 2022, doi: 10.1016/j.carbpol.2021.118799.
- Cheng, W. et al, 2020. Highly efficient MXene-coated flame retardant cotton fabric for electromagnetic interference shielding. *Ind. Eng. Chem. Res.* 59 (31), 14025–14036. <https://doi.org/10.1021/acs.iecr.0c02618>.
- Cheng, J. et al, 2022. Tailoring self-polarization of bimetallic organic frameworks with multiple polar units toward high-performance consecutive multi-band electromagnetic wave absorption at gigahertz. *Adv. Funct. Mater.* 32 (24), 2201129. <https://doi.org/10.1002/adfm.202201129>.
- Cui, C. et al, 2019. Flexible and ultrathin electrospun regenerate cellulose nanofibers and d-Ti3C2Tx (MXene) composite film for electromagnetic interference shielding. *J. Alloy. Compd.* 788, 1246–1255. <https://doi.org/10.1016/j.jallcom.2019.02.294>.
- Cui, C. et al, 2022. FeNi LDH/loofah sponge-derived magnetic FeNi alloy nanosheet array/porous carbon hybrids with efficient electromagnetic wave absorption. *Ind. Eng. Chem. Res.* <https://doi.org/10.1021/acs.iecr.2c01051>.
- J. Deng et al., “Opportunities and challenges in microwave absorption of nickel-carbon composites,” *Physical Chemistry Chemical Physics*, 10.1039/D1CP03522C vol. 23, no. 37, pp. 20795-20834, 2021, doi: 10.1039/D1CP03522C.
- Du, Z. et al, 2022. MXene/polylactic acid fabric-based resonant cavity for realizing simultaneous high-performance electromagnetic interference (EMI) shielding and efficient energy harvesting. *ACS Appl. Mater. Interfaces* 14 (12), 14607–14617. <https://doi.org/10.1021/acsami.2c01160>.
- Duan, N. et al, 2022. Mechanically robust Ti3C2Tx MXene/carbon fiber fabric/Thermoplastic polyurethane composite for efficient electromagnetic interference shielding applications. *Mater. Des.* 214,. <https://doi.org/10.1016/j.matdes.2022.110382> 110382.
- Dun, D. et al, 2021. Electromagnetic interference shielding foams based on poly(vinylidene fluoride)/carbon nanotubes composite. *Macromol. Mater. Eng.* 306 (12), 2100468. <https://doi.org/10.1002/mame.202100468>.
- Elmobarak, H.A., Rahim, S.K.A., Abedian, M., Soh, P.J., Vandembosch, G.A.E., Yew Chiong, L., 2017. Assessment of multilayered graphene technology for flexible antennas at microwave frequencies. *Microwave Opt. Technol. Lett.* 59 (10), 2604–2610. <https://doi.org/10.1002/mop.30783>.
- Fan, X. et al, 2020. Electromagnetic interference shielding Ti3C2Tx-bonded carbon black films with enhanced absorption performance. *Chin. Chem. Lett.* 31 (4), 1026–1029. <https://doi.org/10.1016/j.ccl.2020.01.030>.
- Fan, Z. et al, 2020. A lightweight and conductive MXene/graphene hybrid foam for superior electromagnetic interference shielding. *Chem. Eng. J.* 381,. <https://doi.org/10.1016/j.cej.2019.122696> 122696.
- Fan, X. et al, 2021. Microcellular epoxy/graphene nanocomposites with outstanding electromagnetic interference shielding and mechanical performance by overcoming nanofiller loading/dispersion dichotomy. *Compos. Sci. Technol.* 215,. <https://doi.org/10.1016/j.compscitech.2021.109000> 109000.
- Feng, X. et al, 2020. Functional integrated electromagnetic interference shielding in flexible micro-supercapacitors by cation-intercalation typed Ti3C2Tx MXene. *Nano Energy* 72,. <https://doi.org/10.1016/j.nanoen.2020.104741> 104741.
- W. Feng et al., “Ti3C2 MXene: a promising microwave absorbing material,” *RSC Advances*, 10.1039/C7RA12616F vol. 8, no. 5, pp. 2398-2403, 2018, doi: 10.1039/C7RA12616F.

- Fu, H. et al, 2020. SWCNT-modulated folding-resistant sandwich-structured graphene film for high-performance electromagnetic interference shielding. *Carbon* 162, 490–496. <https://doi.org/10.1016/j.carbon.2020.02.081>.
- Gao, L. et al, 2020. MXene/polymer membranes: synthesis, properties, and emerging applications. *Chem. Mater.* 32 (5), 1703–1747. <https://doi.org/10.1021/acs.chemmater.9b04408>.
- Gao, H., Wang, C., Yang, Z., Zhang, Y., 2021. 3D porous nickel metal foam/polyaniline heterostructure with excellent electromagnetic interference shielding capability and superior absorption based on pre-constructed macroscopic conductive framework. *Compos. Sci. Technol.* 213. <https://doi.org/10.1016/j.compscitech.2021.108896> 108896.
- Geng, L. et al, 2019. A facile approach for coating Ti<sub>3</sub>C<sub>2</sub>T<sub>x</sub> on cotton fabric for electromagnetic wave shielding. *Cellulose* 26 (4), 2833–2847. <https://doi.org/10.1007/s10570-019-02284-5>.
- Geng, D., Yang, H.Y., 2018. Recent advances in growth of novel 2D materials: beyond graphene and transition metal dichalcogenides. *Adv. Mater.* 30 (45), 1800865. <https://doi.org/10.1002/adma.201800865>.
- Gunda, H. et al, 2021. “Progress, challenges, and opportunities in the synthesis, characterization, and application of metal-boride-derived two-dimensional nanostructures”. *ACS Mater. Lett.* 3 (5), 535–556. <https://doi.org/10.1021/acsmaterialslett.1c00086>.
- Guo, T., Li, C., Wang, Y., Wang, Y., Yue, J., Tang, X.-Z., 2020. A highly flexible and porous graphene-based hybrid film with superior mechanical strength for effective electromagnetic interference shielding. *Appl. Phys. A* 126 (10), 776. <https://doi.org/10.1007/s00339-020-03965-w>.
- Guo, D., Yuan, H., Wang, X., Zhu, C., Chen, Y., 2020. Urchin-like amorphous nitrogen-doped carbon nanotubes encapsulated with transition-metal-alloy@graphene core@shell nanoparticles for microwave energy attenuation. *ACS Appl Mater Interfaces* 12 (8), 9628–9636. <https://doi.org/10.1021/acami.9b20412>.
- Han, M. et al, 2016. Ti<sub>3</sub>C<sub>2</sub> MXenes with modified surface for high-performance electromagnetic absorption and shielding in the X-band. *ACS Appl. Mater. Interfaces* 8 (32), 21011–21019. <https://doi.org/10.1021/acami.6b06455>.
- Han, M. et al, 2019. Anisotropic MXene aerogels with a mechanically tunable ratio of electromagnetic wave reflection to absorption. *Adv. Opt. Mater.* 7 (10), 1900267. <https://doi.org/10.1002/adom.201900267>.
- Han, M. et al, 2020. Beyond Ti<sub>3</sub>C<sub>2</sub>T<sub>x</sub>: MXenes for electromagnetic interference shielding. *ACS Nano* 14 (4), 5008–5016. <https://doi.org/10.1021/acsnano.0c01312>.
- H, Wang, Li, S., Liu, M., 2021. Review on Shielding Mechanism and Structural Design of Electromagnetic Interference Shielding Composites. *Macromolecular Materials and Engineering* 306. <https://doi.org/10.1002/mame.202100032>.
- Han, M. et al, 2021. Solution-processed Ti<sub>3</sub>C<sub>2</sub>T<sub>x</sub> MXene antennas for radio-frequency communication. *Adv. Mater.* 33 (1), 2003225. <https://doi.org/10.1002/adma.202003225>.
- Han, X., Huang, Y., Ding, L., Song, Y., Li, T., Liu, P., 2021. Ti<sub>3</sub>C<sub>2</sub>T<sub>x</sub> MXene nanosheet/metal–organic framework composites for microwave absorption. *ACS Appl. Nano Mater.* 4 (1), 691–701. <https://doi.org/10.1021/acsnm.0c02983>.
- Hao, H., Hui, D., Lau, D., 2020. Material advancement in technological development for the 5G wireless communications. *Nanotechnol. Rev.* 9 (1), 683–699. <https://doi.org/10.1515/ntrev-2020-0054>.
- He, P. et al, 2019. Atomic layer tailoring titanium carbide mxene to tune transport and polarization for utilization of electromagnetic energy beyond solar and chemical energy. *ACS Appl. Mater. Interfaces* 11 (13), 12535–12543. <https://doi.org/10.1021/acami.9b00593>.
- He, X. et al, 2021. High-performance multifunctional carbon-silicon carbide composites with strengthened reduced graphene oxide. *ACS Nano* 15 (2), 2880–2892. <https://doi.org/10.1021/acsnano.0c08924>.
- He, P., Cao, M.-S., Cai, Y.-Z., Shu, J.-C., Cao, W.-Q., Yuan, J., 2020. Self-assembling flexible 2D carbide MXene film with tunable integrated electron migration and group relaxation toward energy storage and green EMI shielding. *Carbon* 157, 80–89. <https://doi.org/10.1016/j.carbon.2019.10.009>.
- He, P., Cao, M.-S., Cao, W.-Q., Yuan, J., 2021. Developing MXenes from wireless communication to electromagnetic attenuation. *Nano-Micro Lett.* 13 (1), 115. <https://doi.org/10.1007/s40820-021-00645-z>.
- P. He et al., “Tailoring Ti<sub>3</sub>C<sub>2</sub>T<sub>x</sub> nanosheets to tune local conductive network as an environmentally friendly material for highly efficient electromagnetic interference shielding,” *Nanoscale*, 10.1039/C8NR10489A vol. 11, no. 13, pp. 6080–6088, 2019, doi: 10.1039/C8NR10489A.
- Hong, W., Wyatt, B.C., Nemani, S.K., Anasori, B., 2020. Double transition-metal MXenes: atomistic design of two-dimensional carbides and nitrides. *MRS Bull.* 45 (10), 850–861. <https://doi.org/10.1557/mrs.2020.251>.
- Hu, D., Huang, X., Li, S., Jiang, P., 2020. Flexible and durable cellulose/MXene nanocomposite paper for efficient electromagnetic interference shielding. *Compos. Sci. Technol.* 188. <https://doi.org/10.1016/j.compscitech.2020.107995> 107995.
- Hu, S., Li, S., Xu, W., Zhang, J., Zhou, Y., Cheng, Z., 2019. Rapid preparation, thermal stability and electromagnetic interference shielding properties of two-dimensional Ti<sub>3</sub>C<sub>2</sub> MXene. *Ceram. Int.* 45 (16), 19902–19909. <https://doi.org/10.1016/j.ceramint.2019.06.246>.
- Huan, X. et al, 2022. Integrating multi-heterointerfaces in a 1D@2D@1D hierarchical structure via autocatalytic pyrolysis for ultra-efficient microwave absorption performance. *Small* 18 (13), 2105411. <https://doi.org/10.1002/sml.202105411>.
- Y. Huang, M. Chen, A. Xie, Y. Wang, and X. Xu, “Recent Advances in Design and Fabrication of Nanocomposites for Electromagnetic Wave Shielding and Absorbing,” *Materials*, vol. 14, no. 15, p. 4148, 2021. [Online]. Available: <https://www.mdpi.com/1996-1944/14/15/4148>.
- Huang, G., Liang, J., Zhao, L., He, D., Sim, C., 2019. Package-indielectric liquid patch antenna based on liquid metal alloy. *IEEE Antennas Wirel. Propag. Lett.* 18 (11), 2360–2364. <https://doi.org/10.1109/LAWP.2019.2932048>.
- Iqbal, A. et al, 2020. Anomalous absorption of electromagnetic waves by 2D transition metal carbonitride Ti<sub>3</sub>C<sub>2</sub>N<sub>x</sub> (MXene). *Science* 369 (6502), 446–450. <https://doi.org/10.1126/science.aba7977>.
- Iqbal, A., Sambyal, P., Koo, C.M., 2020. 2D MXenes for electromagnetic shielding: a review. *Adv. Funct. Mater.* 30 (47), 2000883. <https://doi.org/10.1002/adfm.202000883>.
- Ji, B. et al, 2020. Electromagnetic shielding behavior of heat-treated Ti<sub>3</sub>C<sub>2</sub>T<sub>x</sub> MXene accompanied by structural and phase changes. *Carbon* 165, 150–162. <https://doi.org/10.1016/j.carbon.2020.04.041>.
- Ji, B. et al, 2021. Microwave absorption properties of multilayer impedance gradient absorber consisting of Ti<sub>3</sub>C<sub>2</sub>T<sub>x</sub> MXene/polymer films. *Carbon* 181, 130–142. <https://doi.org/10.1016/j.carbon.2021.05.018>.
- Jia, X., Shen, B., Zhang, L., Zheng, W., 2020. Waterproof MXene-decorated wood-pulp fabrics for high-efficiency electromagnetic interference shielding and Joule heating. *Compos. B Eng.* 198. <https://doi.org/10.1016/j.compositesb.2020.108250> 108250.
- Jiang, Y., Chen, Y., Liu, Y.-J., Sui, G.-X., 2018. Lightweight spongy bone-like graphene@SiC aerogel composites for high-performance microwave absorption. *Chem. Eng. J.* 337, 522–531. <https://doi.org/10.1016/j.cej.2017.12.131>.
- Jin, X. et al, 2020. Flame-retardant poly(vinyl alcohol)/MXene multilayered films with outstanding electromagnetic interference

- shielding and thermal conductive performances. *Chem. Eng. J.* 380, <https://doi.org/10.1016/j.cej.2019.122475> 122475.
- Jin, L., Cao, W., Wang, P., Song, N., Ding, P., 2022. Interconnected MXene/graphene network constructed by soft template for multi-performance improvement of polymer composites. *Nano-Micro Lett.* 14 (1), 133. <https://doi.org/10.1007/s40820-022-00877-7>.
- K. Khan et al., "Recent developments in emerging two-dimensional materials and their applications," *Journal of Materials Chemistry C*, 10.1039/C9TC04187G vol. 8, no. 2, pp. 387-440, 2020, doi: 10.1039/C9TC04187G.
- Kim, J. et al, 2021. Fabrication of highly flexible electromagnetic interference shielding polyimide carbon black composite using hot-pressing method. *Compos. B Eng.* 221, <https://doi.org/10.1016/j.compositesb.2021.109010> 109010.
- Y. K. Kim, Y. Lee, K.-Y. Shin, and J. Jang, "Highly omnidirectional and frequency tunable multilayer graphene-based monopole patch antennas," *Journal of Materials Chemistry C*, 10.1039/C9TC02454A vol. 7, no. 26, pp. 7915-7921, 2019, doi: 10.1039/C9TC02454A.
- Kong, L. et al, 2019. Powerful absorbing and lightweight electromagnetic shielding CNTs/RGO composite. *Carbon* 145, 61–66. <https://doi.org/10.1016/j.carbon.2019.01.009>.
- Kumar, P., Narayan Maiti, U., Sikdar, A., Kumar Das, T., Kumar, A., Sudarsan, V., 2019. Recent advances in polymer and polymer composites for electromagnetic interference shielding: review and future prospects. *Polym. Rev.* 59 (4), 687–738. <https://doi.org/10.1080/15583724.2019.1625058>.
- Lai, D., Chen, X., Wang, Y., 2020. Controllable fabrication of elastomeric and porous graphene films with superior foldable behavior and excellent electromagnetic interference shielding performance. *Carbon* 158, 728–737. <https://doi.org/10.1016/j.carbon.2019.11.047>.
- Lan, X. et al, 2022. All-ceramic SiC aerogel for wide temperature range electromagnetic wave attenuation. *ACS Appl. Mater. Interfaces* 14 (13), 15360–15369. <https://doi.org/10.1021/acsnano.1c23087>.
- Lei, C., Zhang, Y., Liu, D., Wu, K., Fu, Q., 2020. Metal-level robust, folding endurance, and highly temperature-stable MXene-based film with engineered aramid nanofiber for extreme-condition electromagnetic interference shielding applications. *ACS Appl. Mater. Interfaces* 12 (23), 26485–26495. <https://doi.org/10.1021/acsnano.1c23087>.
- Li, N. et al, 2017. Enhanced microwave absorption performance of coated carbon nanotubes by optimizing the Fe<sub>3</sub>O<sub>4</sub> nanocoating structure. *ACS Appl. Mater. Interfaces* 9 (3), 2973–2983. <https://doi.org/10.1021/acsnano.1c23087>.
- Li, Y. et al, 2019. Multifunctional organic-inorganic hybrid aerogel for self-cleaning, heat-insulating, and highly efficient microwave absorbing material. *Adv. Funct. Mater.* 29 (10), 1807624. <https://doi.org/10.1002/adfm.201807624>.
- Li, Y. et al, 2020. Reversible crumpling of 2D titanium carbide (MXene) nanocoatings for stretchable electromagnetic shielding and wearable wireless communication. *Adv. Funct. Mater.* 30 (5), 1907451. <https://doi.org/10.1002/adfm.201907451>.
- Li, B. et al, 2021. Partially contacted Ni<sub>x</sub>Sy@N, S-codoped carbon yolk-shelled structures for efficient microwave absorption. *Carbon* 182, 276–286. <https://doi.org/10.1016/j.carbon.2021.05.057>.
- Li, J. et al, 2021. Recent progress in two-dimensional materials for microwave absorption applications. *Chem. Eng. J.* 425, <https://doi.org/10.1016/j.cej.2021.131558> 131558.
- Li, C. et al, 2021. Robust superhydrophobic and porous melamine-formaldehyde based composites for high-performance electromagnetic interference shielding. *Colloids Surf., A: Physicochem. Eng. Asp.* 624, <https://doi.org/10.1016/j.colsurfa.2021.126742> 126742.
- Li, B. et al, 2022. Grafting thin N-doped carbon nanotubes on hollow N-doped carbon nanoplates encapsulated with ultras-small cobalt particles for microwave absorption. *Chem. Eng. J.* 435. <https://doi.org/10.1016/j.cej.2022.134846>.
- Li, J. et al, 2022. Coral-like polypyrrole/LiFe<sub>5</sub>O<sub>8</sub>/MoS<sub>2</sub> nanocomposites for high-efficiency microwave absorbers. *ACS Appl. Nano Mater.* 5 (6), 7944–7953. <https://doi.org/10.1021/acsnano.2c01022>.
- Li, L., Cao, Y., Liu, X., Wang, J., Yang, Y., Wang, W., 2020. Multifunctional MXene-based fireproof electromagnetic shielding films with exceptional anisotropic heat dissipation capability and Joule heating performance. *ACS Appl. Mater. Interfaces* 12 (24), 27350–27360. <https://doi.org/10.1021/acsnano.2c01022>.
- Li, X., Yin, X., Liang, S., Li, M., Cheng, L., Zhang, L., 2019. 2D carbide MXene Ti<sub>2</sub>CTx as a novel high-performance electromagnetic interference shielding material. *Carbon* 146, 210–217. <https://doi.org/10.1016/j.carbon.2019.02.003>.
- Li, L., Zhao, S., Luo, X.-J., Zhang, H.-B., Yu, Z.-Z., 2021. Smart MXene-based Janus films with multi-responsive actuation capability and high electromagnetic interference shielding performances. *Carbon* 175, 594–602. <https://doi.org/10.1016/j.carbon.2020.10.090>.
- Liang, C. et al, 2016. Nature of electromagnetic-transparent SiO<sub>2</sub> shell in hybrid nanostructure enhancing electromagnetic attenuation. *J. Phys. Chem. C* 120 (24), 12967–12973. <https://doi.org/10.1021/acs.jpcc.6b04721>.
- Liang, L. et al, 2019. Promising Ti<sub>3</sub>C<sub>2</sub>T<sub>x</sub> MXene/Ni chain hybrid with excellent electromagnetic wave absorption and shielding capacity. *ACS Appl. Mater. Interfaces* 11 (28), 25399–25409. <https://doi.org/10.1021/acsnano.0c09982>.
- Liang, C. et al, 2020. Multifunctional sponges with flexible motion sensing and outstanding thermal insulation for superior electromagnetic interference shielding. *Compos. A Appl. Sci. Manuf.* 139, <https://doi.org/10.1016/j.compositesa.2020.106143> 106143.
- Liang, L. et al, 2021. Multifunctional magnetic Ti<sub>3</sub>C<sub>2</sub>T<sub>x</sub> MXene/graphene aerogel with superior electromagnetic wave absorption performance. *ACS Nano* 15 (4), 6622–6632. <https://doi.org/10.1021/acsnano.0c09982>.
- Liang, C., Qiu, H., Song, P., Shi, X., Kong, J., Gu, J., 2020. Ultralight MXene aerogel/wood-derived porous carbon composites with wall-like "mortar/brick" structures for electromagnetic interference shielding. *Sci. Bull.* 65 (8), 616–622. <https://doi.org/10.1016/j.scib.2020.02.009>.
- Liang, C., Gu, Z., Zhang, Y., Ma, Z., Qiu, H., Gu, J., 2021. "Structural design strategies of polymer matrix composites for electromagnetic interference shielding: a review". *Nano-Micro Lett.* 13 (1), 181. <https://doi.org/10.1007/s40820-021-00707-2>.
- Liao, S.-Y. et al, 2022. Metallized skeleton of polymer foam based on metal-organic decomposition for high-performance EMI shielding. *ACS Appl. Mater. Interfaces* 14 (2), 3302–3314. <https://doi.org/10.1021/acsnano.1c21836>.
- Liu, X.G. et al, 2010. Influence of a graphite shell on the thermal and electromagnetic characteristics of FeNi nanoparticles. *Carbon* 48 (3), 891–897. <https://doi.org/10.1016/j.carbon.2009.11.011>.
- Liu, J. et al, et al. 2017. Hydrophobic, flexible, and lightweight mxene foams for high-performance electromagnetic-interference shielding. *Adv. Mater.* 29 (38), 1702367. <https://doi.org/10.1002/adma.201702367>.
- Liu, L. et al, 2018. Three-dimensional hierarchical MoS<sub>2</sub> nanosheets/ultralong N-doped carbon nanotubes as high-performance electromagnetic wave absorbing material. *ACS Appl Mater Interfaces* 10 (16), 14108–14115. <https://doi.org/10.1021/acsnano.1c21836>.
- Liu, T. et al, 2019. Tailor-made core/shell/shell-like Fe<sub>3</sub>O<sub>4</sub>@-SiO<sub>2</sub>@PPy composites with prominent microwave absorption performance. *J. Alloy. Compd.* 779, 831–843. <https://doi.org/10.1016/j.jallcom.2018.11.167>.
- Liu, J. et al, 2020. Ultrastrong and highly conductive mxene-based films for high-performance electromagnetic interference shielding. *Adv. Electron. Mater.* 6 (1), 1901094. <https://doi.org/10.1002/aelm.201901094>.
- Liu, F. et al, 2020. Well-aligned MXene/chitosan films with humidity response for high-performance electromagnetic interference shield-

- ing. *Carbohydr. Polym.* 243, [https://doi.org/10.1016/j-carbpol.2020.116467](https://doi.org/10.1016/j.carbpol.2020.116467) 116467.
- Liu, H. et al, 2021. MXene confined in shape-stabilized phase change material combining enhanced electromagnetic interference shielding and thermal management capability. *Compos. Sci. Technol.* 210, <https://doi.org/10.1016/j.compscitech.2021.108835> 108835.
- Liu, Q. et al, 2022. Multifunctional aramid nanofibers reinforced RGO aerogels integrated with high-efficiency microwave absorption, sound absorption and heat insulation performance. *J. Mater. Sci. Technol.* 130, 166–175. <https://doi.org/10.1016/j.jmst.2022.05.014>.
- Liu, J., Cao, M.-S., Luo, Q., Shi, H.-L., Wang, W.-Z., Yuan, J., 2016. Electromagnetic property and tunable microwave absorption of 3D nets from nickel chains at elevated temperature. *ACS Appl. Mater. Interfaces* 8 (34), 22615–22622. <https://doi.org/10.1021/acsami.6b05480>.
- Liu, T.-T., Cao, M.-Q., Fang, Y.-S., Zhu, Y.-H., Cao, M.-S., 2022. Green building materials lit up by electromagnetic absorption function: a review. *J. Mater. Sci. Technol.* 112, 329–344. <https://doi.org/10.1016/j.jmst.2021.10.022>.
- L.-X. Liu, W. Chen, H.-B. Zhang, Q.-W. Wang, F. Guan, and Z.-Z. Yu, “Flexible and Multifunctional Silk Textiles with Biomimetic Leaf-Like MXene/Silver Nanowire Nanostructures for Electromagnetic Interference Shielding, Humidity Monitoring, and Self-Derived Hydrophobicity,” *Advanced Functional Materials*, <https://doi.org/10.1002/adfm.201905197> vol. 29, no. 44, p. 1905197, 2019, doi: <https://doi.org/10.1002/adfm.201905197>.
- Liu, R., Miao, M., Li, Y., Zhang, J., Cao, S., Feng, X., 2018. Ultrathin biomimetic polymeric Ti3C2Tx MXene composite films for electromagnetic interference shielding. *ACS Appl. Mater. Interfaces* 10 (51), 44787–44795. <https://doi.org/10.1021/acsami.8b18347>.
- Liu, S., Qin, S., Jiang, Y., Song, P., Wang, H., 2021. Lightweight high-performance carbon-polymer nanocomposites for electromagnetic interference shielding. *Compos. A Appl. Sci. Manuf.* 145, <https://doi.org/10.1016/j.compositesa.2021.106376> 106376.
- Liu, X., Wu, J., He, J., Zhang, L., 2017. Electromagnetic interference shielding effectiveness of titanium carbide sheets. *Mater. Lett.* 205, 261–263. <https://doi.org/10.1016/j.matlet.2017.06.101>.
- Z. Liu et al., “Electrically conductive aluminum ion-reinforced MXene films for efficient electromagnetic interference shielding,” *Journal of Materials Chemistry C*, 10.1039/C9TC06304H vol. 8, no. 5, pp. 1673–1678, 2020, doi: 10.1039/C9TC06304H.
- Z. Liu et al., “Bioinspired ultra-thin polyurethane/MXene nacre-like nanocomposite films with synergistic mechanical properties for electromagnetic interference shielding,” *Journal of Materials Chemistry C*, 10.1039/D0TC01249A vol. 8, no. 21, pp. 7170–7180, 2020, doi: 10.1039/D0TC01249A.
- Lu, Z., Jia, F., Zhuo, L., Ning, D., Gao, K., Xie, F., 2021. “Microporous MXene/Aramid nanofibers hybrid aerogel with reversible compression and efficient EMI shielding performance”. *Compos. B Eng.* 217, <https://doi.org/10.1016/j.compositesb.2021.108853> 108853.
- Luo, H. et al, 2021. Bimetallic oxalate rod-derived NiFe/Fe3O4@C composites with tunable magneto-dielectric properties for high-performance microwave absorption. *J. Phys. Chem. C* 125 (44), 24540–24549. <https://doi.org/10.1021/acs.jpcc.1c04386>.
- Luo, Y. et al, 2021. Porous carbon foam based on coassembled graphene and adenine-polyimide for electromagnetic interference shielding. *Polymer* 236, <https://doi.org/10.1016/j.polymer.2021.124328> 124328.
- Luo, Y. et al, 2022. Fabrication of rigid polyimide foams with superior compressive properties. *Ind. Eng. Chem. Res.* 61 (2), 1089–1099. <https://doi.org/10.1021/acs.iecr.1c04059>.
- Luo, W. et al, 2022. Overview of MXene/conducting polymer composites for supercapacitors. *J. Storage Mater.* 52, <https://doi.org/10.1016/j.est.2022.105008> 105008.
- Luo, J.-Q., Zhao, S., Zhang, H.-B., Deng, Z., Li, L., Yu, Z.-Z., 2019. Flexible, stretchable and electrically conductive MXene/natural rubber nanocomposite films for efficient electromagnetic interference shielding. *Compos. Sci. Technol.* 182, <https://doi.org/10.1016/j.compscitech.2019.107754> 107754.
- Ma, Z. et al, 2020. Ultraflexible and mechanically strong double-layered aramid nanofiber–Ti3C2Tx MXene/silver nanowire nanocomposite papers for high-performance electromagnetic interference shielding. *ACS Nano* 14 (7), 8368–8382. <https://doi.org/10.1021/acsnano.0c02401>.
- Ma, M. et al, 2022. Construction of gradient conductivity cellulose nanofiber/MXene composites with efficient electromagnetic interference shielding and excellent mechanical properties. *Compos. Sci. Technol.* 226, <https://doi.org/10.1016/j.compscitech.2022.109540> 109540.
- Ma, W., Cai, W., Chen, W., Liu, P., Wang, J., Liu, Z., 2021. Microwave-induced segregated composite network with MXene as interfacial solder for ultra-efficient electromagnetic interference shielding and anti-dripping. *Chem. Eng. J.* 425, <https://doi.org/10.1016/j.cej.2021.131699> 131699.
- Miao, P. et al, 2022. A two-dimensional semiconductive metal-organic framework for highly efficient microwave absorption. *Chin. J. Chem.* 40 (4), 467–474. <https://doi.org/10.1002/cjoc.202100660>.
- M. Miao et al., “Silver nanowires intercalating Ti3C2Tx MXene composite films with excellent flexibility for electromagnetic interference shielding,” *Journal of Materials Chemistry C*, 10.1039/C9TC06361G vol. 8, no. 9, pp. 3120–3126, 2020, doi: 10.1039/C9TC06361G.
- A. Nazir et al., “Recent progress in the modification of carbon materials and their application in composites for electromagnetic interference shielding,” *Journal of Materials Science*, vol. 53, no. 12, pp. 8699–8719, 2018, doi: DOI:10.1007/s10853-018-2122-x.
- Nepal, D., Kennedy, W.J., Pachter, R., Vaia, R.A., 2021. Toward architected nanocomposites: MXenes and beyond. *ACS Nano* 15 (1), 21–28. <https://doi.org/10.1021/acsnano.0c09834>.
- Oliveira, F.M., Gusmão, R., 2020. Recent advances in the electromagnetic interference shielding of 2D materials beyond graphene. *ACS Appl. Electron. Mater.* 2 (10), 3048–3071. <https://doi.org/10.1021/acsaelm.0c00545>.
- J. Pan, H. Hu, Z. Li, J. Mu, Y. Cai, and H. Zhu, “Recent progress in two-dimensional materials for terahertz protection,” *Nanoscale Advances*, 10.1039/D0NA01046D vol. 3, no. 6, pp. 1515–1531, 2021, doi: 10.1039/D0NA01046D.
- Qing, Y., Zhou, W., Luo, F., Zhu, D., 2016. Titanium carbide (MXene) nanosheets as promising microwave absorbers. *Ceram. Int.* 42 (14), 16412–16416. <https://doi.org/10.1016/j.ceramint.2016.07.150>.
- Qu, B., Zhu, C., Li, C., Zhang, X., Chen, Y., 2016. Coupling hollow Fe3O4-Fe nanoparticles with graphene sheets for high-performance electromagnetic wave absorbing material. *ACS Appl Mater Interfaces* 8 (6), 3730–3735. <https://doi.org/10.1021/acsami.5b12789>.
- Quan, B. et al, 2018. Laminated graphene oxide-supported high-efficiency microwave absorber fabricated by an in situ growth approach. *Carbon* 129, 310–320. <https://doi.org/10.1016/j.carbon.2017.12.026>.
- K. Raagulan, B. M. Kim, and K. Y. Chai, “Recent Advancement of Electromagnetic Interference (EMI) Shielding of Two Dimensional (2D) MXene and Graphene Aerogel Composites,” *Nanomaterials*, vol. 10, no. 4, p. 702, 2020. [Online]. Available: <https://www.mdpi.com/2079-4991/10/4/702>.
- K. Raagulan et al., “An effective utilization of MXene and its effect on electromagnetic interference shielding: flexible, free-standing and thermally conductive composite from MXene–PAT–poly(p-aminophenol)–polyaniline co-polymer,” *RSC Advances*, 10.1039/C9RA09522E vol. 10, no. 3, pp. 1613–1633, 2020, doi: 10.1039/C9RA09522E.

- Rajavel, K. et al, 2020. 2D Ti3C2Tx MXene/polyvinylidene fluoride (PVDF) nanocomposites for attenuation of electromagnetic radiation with excellent heat dissipation. *Compos. A Appl. Sci. Manuf.* 129,. <https://doi.org/10.1016/j.compositesa.2019.105693> 105693.
- Rajavel, K., Yu, X., Zhu, P., Hu, Y., Sun, R., Wong, C., 2020. Exfoliation and defect control of two-dimensional few-layer MXene Ti3C2Tx for electromagnetic interference shielding coatings. *ACS Appl. Mater. Interfaces* 12 (44), 49737–49747. <https://doi.org/10.1021/acsami.0c12835>.
- Rajavel, K., Hu, Y., Zhu, P., Sun, R., Wong, C., 2020. MXene/metal oxides-Ag ternary nanostructures for electromagnetic interference shielding. *Chem. Eng. J.* 399,. <https://doi.org/10.1016/j.cej.2020.125791> 125791.
- Razaq, A., Khan, A.A., Shakir, U., Arshad, A., 2018. Next generation flexible antennas for radio frequency applications. *Trans. Electr. Electron. Mater.* 19 (5), 311–318. <https://doi.org/10.1007/s42341-018-0051-7>.
- Ren, H. et al, 2021. Broadband electromagnetic absorption of Ti3C2Tx MXene/WS2 composite via constructing two-dimensional heterostructure. *J. Am. Ceram. Soc.* 104 (11), 5537–5546. <https://doi.org/10.1111/jace.17959>.
- Rizwan, M., Khan, M.W.A., Sydänheimo, L., Virkki, J., Ukkonen, L., 2017. Flexible and stretchable brush-painted wearable antenna on a three-dimensional (3-D) printed substrate. *IEEE Antennas Wirel. Propag. Lett.* 16, 3108–3112. <https://doi.org/10.1109/LAWP.2017.2763743>.
- Russell, C.L., 2018. 5 G wireless telecommunications expansion: public health and environmental implications. *Environ. Res.* 165, 484–495. <https://doi.org/10.1016/j.envres.2018.01.016>.
- Ryu, S.H. et al, 2022. Millimeter-scale percolated polyethylene/graphene composites for 5G electromagnetic shielding. *ACS Appl. Nano Mater.* 5 (6), 8429–8439. <https://doi.org/10.1021/acsanm.2c01544>.
- Saghlatoon, H., Sydänheimo, L., Ukkonen, L., Tentzeris, M., 2014. Optimization of inkjet printing of patch antennas on low-cost fibrous substrates. *IEEE Antennas Wirel. Propag. Lett.* 13, 915–918. <https://doi.org/10.1109/LAWP.2014.2322572>.
- Saini, P., Aror, M., 2012. Microwave absorption and EMI shielding behavior of nanocomposites based on intrinsically conducting polymers, graphene and carbon nanotubes. *New Polym. Special App. ch. Chapter 3*.
- Sambyal, P. et al, 2019. Ultralight and mechanically robust Ti3C2Tx hybrid aerogel reinforced by carbon nanotubes for electromagnetic interference shielding. *ACS Appl. Mater. Interfaces* 11 (41), 38046–38054. <https://doi.org/10.1021/acsami.9b12550>.
- Sang, G. et al, 2022. Ni@CNTs/Al2O3 ceramic composites with interfacial solder strengthen the segregated network for high toughness and excellent electromagnetic interference shielding. *ACS Appl. Mater. Interfaces* 14 (3), 4443–4455. <https://doi.org/10.1021/acsami.1c21630>.
- Sankaran, S., Deshmukh, K., Ahamed, M.B., Khadheer Pasha, S.K., 2018. Recent advances in electromagnetic interference shielding properties of metal and carbon filler reinforced flexible polymer composites: a review. *Compos. A Appl. Sci. Manuf.* 114, 49–71. <https://doi.org/10.1016/j.compositesa.2018.08.006>.
- A. Sarycheva, A. Polemi, Y. Liu, K. Dandekar, B. Anasori, and Y. Gogotsi, “2D titanium carbide (MXene) for wireless communication,” *Science Advances*, vol. 4, no. 9, p. eaau0920, 2018, doi:10.1126/sciadv.aau0920.
- Shahzad, F. et al, 2016. Electromagnetic interference shielding with 2D transition metal carbides (MXenes). *Science* 353 (6304), 1137–1140. <https://doi.org/10.1126/science.aag2421>.
- Sharma, A. et al, 2022. “Enhanced electromagnetic interference shielding properties of phenolic resin derived lightweight carbon foam decorated with electrospon zinc oxide nanofibers”. *Mater. Today Commun.* 30,. <https://doi.org/10.1016/j.mtcomm.2021.103055> 103055.
- Shayesteh Zeraati, A., Mirkhani, S.A., Sharif, F., Akbari, A., Roberts, E.P.L., Sundararaj, U., 2021. Electrochemically exfoliated graphite nanosheet films for electromagnetic interference shields. *ACS Appl. Nano Mater.* 4 (7), 7221–7233. <https://doi.org/10.1021/acsanm.1c01172>.
- Shi, Y. et al, 2022. Multi-interface assembled N-doped MXene/HCFG/AgNW films for wearable electromagnetic shielding devices with multimodal energy conversion and healthcare monitoring performances. *ACS Nano* 16 (5), 7816–7833. <https://doi.org/10.1021/acs.nano.2c00448>.
- Shi, Y.-D., Lei, M., Chen, Y.-F., Zhang, K., Zeng, J.-B., Wang, M., 2017. Ultralow percolation threshold in poly(l-lactide)/poly( $\epsilon$ -caprolactone)/multiwall carbon nanotubes composites with a segregated electrically conductive network. *J. Phys. Chem. C* 121 (5), 3087–3098. <https://doi.org/10.1021/acs.jpcc.6b11351>.
- Shi, H.-G., Zhao, H.-B., Liu, B.-W., Wang, Y.-Z., 2021. Multifunctional flame-retardant melamine-based hybrid foam for infrared stealth, thermal insulation, and electromagnetic interference shielding. *ACS Appl. Mater. Interfaces* 13 (22), 26505–26514. <https://doi.org/10.1021/acsami.1c07363>.
- Shu, J.-C. et al, 2020. Molecular patching engineering to drive energy conversion as efficient and environment-friendly cell toward wireless power transmission. *Adv. Funct. Mater.* 30 (10), 1908299. <https://doi.org/10.1002/adfm.201908299>.
- Shu, J.-C., Cao, W.-Q., Cao, M.-S., 2021. Diverse metal-organic framework architectures for electromagnetic absorbers and shielding. *Adv. Funct. Mater.* 31 (23), 2100470. <https://doi.org/10.1002/adfm.202100470>.
- Simorangkir, R.B.V.B., Yang, Y., Matekovits, L., Esselle, K.P., 2017. Dual-band dual-mode textile antenna on PDMS substrate for body-centric communications. *IEEE Antennas Wirel. Propag. Lett.* 16, 677–680. <https://doi.org/10.1109/LAWP.2016.2598729>.
- Song, C. et al, 2017. Three-dimensional reduced graphene oxide foam modified with ZnO nanowires for enhanced microwave absorption properties. *Carbon* 116, 50–58. <https://doi.org/10.1016/j.carbon.2017.01.077>.
- Song, P. et al, 2020. “Honeycomb structural rGO-MXene/epoxy nanocomposites for superior electromagnetic interference shielding performance”. *Sustain. Mater. Technol.* 24, e00153.
- Song, P. et al, 2021. Lightweight, flexible cellulose-derived carbon aerogel@reduced graphene oxide/PDMS composites with outstanding EMI shielding performances and excellent thermal conductivities. *Nano-Micro Lett.* 13 (1), 91. <https://doi.org/10.1007/s40820-021-00624-4>.
- S. K. Srivastava and K. Manna, “Recent advancements in the electromagnetic interference shielding performance of nanostructured materials and their nanocomposites: a review,” *Journal of Materials Chemistry A*, 10.1039/D1TA09522F vol. 10, no. 14, pp. 7431-7496, 2022, doi: 10.1039/D1TA09522F.
- Sun, R. et al, 2017. Highly conductive transition metal carbide/carbonitride(MXene)@polystyrene nanocomposites fabricated by electrostatic assembly for highly efficient electromagnetic interference shielding. *Adv. Funct. Mater.* 27 (45), 1702807. <https://doi.org/10.1002/adfm.201702807>.
- Sun, B. et al, 2021. Asymmetric layered structural design with segregated conductive network for absorption-dominated high-performance electromagnetic interference shielding. *Chem. Eng. J.* 416,. <https://doi.org/10.1016/j.cej.2021.129083> 129083.
- Sun, K. et al, 2021. Flexible conductive polyimide fiber/MXene composite film for electromagnetic interference shielding and Joule heating with excellent harsh environment tolerance. *ACS Appl. Mater. Interfaces* 13 (42), 50368–50380. <https://doi.org/10.1021/acsami.1c15467>.
- A. Thadathil, J. Kaval, G. R. Kovummal, C. P. Jijil, and P. Periyat, “Facile Synthesis of Polyindole/Ni1-xZnxFe2O4 (x = 0, 0.5, 1) Nanocomposites and Their Enhanced Microwave Absorption and Shielding Properties,” *ACS Omega*, vol. 7, no. 13, pp. 11473-11490, 2022, doi: 10.1021/acsomega.2c00824.

- Tong, Z. et al, 2021. Hierarchical Fe<sub>3</sub>O<sub>4</sub>/Fe@C@MoS<sub>2</sub> core-shell nanofibers for efficient microwave absorption. *Carbon* 179, 646–654. <https://doi.org/10.1016/j.carbon.2021.04.051>.
- Verger, L., Xu, C., Natu, V., Cheng, H.M., Ren, W., Barsoum, M. W., 2019. Overview of the synthesis of MXenes and other ultrathin 2D transition metal carbides and nitrides. *Curr. Opin. Solid State Mater. Sci.*
- Vural, M. et al, 2018. Inkjet printing of self-assembled 2D titanium carbide and protein electrodes for stimuli-responsive electromagnetic shielding. *Adv. Funct. Mater.* 28 (32), 1801972. <https://doi.org/10.1002/adfm.201801972>.
- Wan, Y.-J., Zhu, P.-L., Yu, S.-H., Sun, R., Wong, C.-P., Liao, W.-H., 2018. Anticorrosive, ultralight, and flexible carbon-wrapped metallic nanowire hybrid sponges for highly efficient electromagnetic interference shielding. *Small* 14 (27), 1800534. <https://doi.org/10.1002/sml.201800534>.
- Wan, Y. et al, 2021. "Ultrathin, strong and highly flexible Ti<sub>3</sub>C<sub>2</sub>T<sub>x</sub> MXene/bacterial cellulose composite films for high-performance electromagnetic interference shielding". *ACS Nano* 15 (5), 8439–8449. <https://doi.org/10.1021/acs.nano.0c10666>.
- D. Wanasinghe, F. Aslani, G. Ma, and D. Habibi, "Review of Polymer Composites with Diverse Nanofillers for Electromagnetic Interference Shielding," *Nanomaterials*, vol. 10, no. 3, p. 541, 2020. [Online]. Available: <https://www.mdpi.com/2079-4991/10/3/541>.
- Wang, L. et al, 2019. Fabrication on the annealed Ti<sub>3</sub>C<sub>2</sub>T<sub>x</sub> MXene/Epoxy nanocomposites for electromagnetic interference shielding application. *Compos. B Eng.* 171, 111–118. <https://doi.org/10.1016/j.compositesb.2019.04.050>.
- Wang, Q.-W. et al, 2019. Multifunctional and water-resistant MXene-decorated polyester textiles with outstanding electromagnetic interference shielding and joule heating performances. *Adv. Funct. Mater.* 29 (7), 1806819. <https://doi.org/10.1002/adfm.201806819>.
- Wang, L. et al, 2019. 3D Ti<sub>3</sub>C<sub>2</sub>T<sub>x</sub> MXene/C hybrid foam/epoxy nanocomposites with superior electromagnetic interference shielding performances and robust mechanical properties. *Compos. A Appl. Sci. Manuf.* 123, 293–300. <https://doi.org/10.1016/j.compositesa.2019.05.030>.
- Wang, Y. et al, 2021. 3D-printing of segregated carbon nanotube/polylactic acid composite with enhanced electromagnetic interference shielding and mechanical performance. *Mat. Des.* 197, <https://doi.org/10.1016/j.matdes.2020.109222> 109222.
- Wang, TingWei-Wei Kong, Wan-Cheng Yu, Jie-Feng Gao, Kun Dai, Ding-Xiang Yan & Zhong-Ming Li, 2021. A Healable and Mechanically Enhanced Composite with Segregated Conductive Network Structure for High-Efficient Electromagnetic Interference Shielding. *Nano-Micro Letters* 13 (162). <https://doi.org/10.1007/s40820-021-00693-5>.
- Wang, Z., Cheng, Z., Fang, C., Hou, X., Xie, L., 2020. Recent advances in MXenes composites for electromagnetic interference shielding and microwave absorption. *Compos. A Appl. Sci. Manuf.* 136, <https://doi.org/10.1016/j.compositesa.2020.105956> 105956.
- G. Wang, S. J. H. Ong, Y. Zhao, Z. J. Xu, and G. Ji, "Integrated multifunctional macrostructures for electromagnetic wave absorption and shielding," *Journal of Materials Chemistry A*, 10.1039/D0TA08515D vol. 8, no. 46, pp. 24368–24387, 2020, doi: 10.1039/D0TA08515D.
- Wang, S.-J., Li, D.-S., Jiang, L., 2019. Synergistic effects between MXenes and Ni chains in flexible and ultrathin electromagnetic interference shielding films. *Adv. Mater.* *Interfaces* 6 (19), 1900961. <https://doi.org/10.1002/admi.201900961>.
- Wang, L., Ma, Z., Zhang, Y., Chen, L., Cao, D., Gu, J., 2021. Polymer-based EMI shielding composites with 3D conductive networks: a mini-review. *SusMat.* 1 (3), 413–431. <https://doi.org/10.1002/sus2.21>.
- Wang, Y.-Y., Sun, W.-J., Yan, D.-X., Dai, K., Li, Z.-M., 2021. Ultralight carbon nanotube/graphene/polyimide foam with heterogeneous interfaces for efficient electromagnetic interference shielding and electromagnetic wave absorption. *Carbon* 176, 118–125. <https://doi.org/10.1016/j.carbon.2020.12.028>.
- Wang, M., Tang, X.-H., Cai, J.-H., Wu, H., Shen, J.-B., Guo, S.-Y., 2021. Construction, mechanism and prospective of conductive polymer composites with multiple interfaces for electromagnetic interference shielding: a review. *Carbon* 177, 377–402. <https://doi.org/10.1016/j.carbon.2021.02.047>.
- Wang, X.-X., Zhang, M., Shu, J.-C., Wen, B., Cao, W.-Q., Cao, M.-S., 2021. Thermally-tailoring dielectric "genes" in graphene-based heterostructure to manipulate electromagnetic response. *Carbon* 184, 136–145. <https://doi.org/10.1016/j.carbon.2021.07.099>.
- Wang, J.-G., Zhou, R., Jin, D., Xie, K., Wei, B., 2017. Uniform growth of MoS<sub>2</sub> nanosheets on carbon nanofibers with enhanced electrochemical utilization for Li-ion batteries. *Electrochim. Acta* 231, 396–402. <https://doi.org/10.1016/j.electacta.2017.01.108>.
- L. Wang et al., "Recent progress of microwave absorption microspheres by magnetic-dielectric synergy," *Nanoscale*, 10.1039/D0NR06267G vol. 13, no. 4, pp. 2136–2156, 2021, doi: 10.1039/D0NR06267G.
- D.-T. Wang, X.-C. Wang, X. Zhang, H.-R. Yuan, and Y.-J. Chen, "Tunable Dielectric Properties of Carbon Nanotube@Polypyrrole Core-Shell Hybrids by the Shell Thickness for Electromagnetic Wave Absorption \*," *Chinese Physics Letters*, vol. 37, no. 4, 2020, doi: 10.1088/0256-307x/37/4/045201.
- Wei, J. et al, 2022. Lightweight and highly compressible expandable polymer microsphere/silver nanowire composites for wideband electromagnetic interference shielding. *ACS Appl. Mater. Interfaces* 14 (4), 5940–5950. <https://doi.org/10.1021/acsami.1c20593>.
- Wei, B. et al, 2022. Bimetallic nanoarrays embedded in three-dimensional carbon foam as lightweight and efficient microwave absorbers. *Carbon* 191, 486–501. <https://doi.org/10.1016/j.carbon.2022.02.020>.
- Wei, H., Wang, M., Zheng, W., Jiang, Z., Huang, Y., 2020. 2D Ti<sub>3</sub>C<sub>2</sub>T<sub>x</sub> MXene/aramid nanofibers composite films prepared via a simple filtration method with excellent mechanical and electromagnetic interference shielding properties. *Ceram. Int.* 46 (5), 6199–6204. <https://doi.org/10.1016/j.ceramint.2019.11.087>.
- Wen, B. et al, 2013. Temperature dependent microwave attenuation behavior for carbon-nanotube/silica composites. *Carbon* 65, 124–139. <https://doi.org/10.1016/j.carbon.2013.07.110>.
- Weng, G.-M. et al, 2018. Layer-by-layer assembly of cross-functional semi-transparent MXene-carbon nanotubes composite films for next-generation electromagnetic interference shielding. *Adv. Funct. Mater.* 28 (44), 1803360. <https://doi.org/10.1002/adfm.201803360>.
- Weng, C. et al, 2020. Mechanically robust ANF/MXene composite films with tunable electromagnetic interference shielding performance. *Compos. A Appl. Sci. Manuf.* 135, <https://doi.org/10.1016/j.compositesa.2020.105927> 105927.
- Wu, X. et al, 2020. Compressible, durable and conductive polydimethylsiloxane-coated MXene foams for high-performance electromagnetic interference shielding. *Chem. Eng. J.* 381, <https://doi.org/10.1016/j.cej.2019.122622> 122622.
- Wu, Z. et al, 2022. Dimensional design and core-shell engineering of nanomaterials for electromagnetic wave absorption. *Adv. Mater.* 34 (11), 2107538. <https://doi.org/10.1002/adma.202107538>.
- Wu, Z., Shang, T., Deng, Y., Tao, Y., Yang, Q.-H., 2020. The assembly of MXenes from 2D to 3D. *Adv. Sci.* 7 (7), 1903077. <https://doi.org/10.1002/advs.201903077>.
- Wu, H., Yin, R., Zhang, Y., Wang, Z., Xie, P., Qian, L., 2017. Synergistic effects of carbon nanotubes on negative dielectric properties of graphene-phenolic resin composites. *J. Phys. Chem. C* 121 (22), 12037–12045. <https://doi.org/10.1021/acs.jpcc.7b02858>.
- Xiang, C. et al, 2019. Lightweight and ultrathin TiO<sub>2</sub>-Ti<sub>3</sub>C<sub>2</sub>T<sub>x</sub>/graphene film with electromagnetic interference shielding. *Chem. Eng. J.* 360, 1158–1166. <https://doi.org/10.1016/j.cej.2018.10.174>.
- Xie, C. et al, 2021. Macroscopic-scale preparation of aramid nanofiber aerogel by modified freezing-drying method. *ACS Nano* 15 (6), 10000–10009. <https://doi.org/10.1021/acs.nano.1c01551>.

- F. Xie *et al.*, "Ultrathin MXene/aramid nanofiber composite paper with excellent mechanical properties for efficient electromagnetic interference shielding," *Nanoscale*, 10.1039/C9NR07331K vol. 11, no. 48, pp. 23382–23391, 2019, doi: 10.1039/C9NR07331K.
- Xin, W., Ma, M.-G., Chen, F., 2021. Silicone-coated MXene/cellulose nanofiber aerogel films with photothermal and Joule heating performances for electromagnetic interference shielding. *ACS Appl. Nano Mater.* 4 (7), 7234–7243. <https://doi.org/10.1021/acsnm.1c01185>.
- W. Xin *et al.*, "Lightweight and flexible MXene/CNF/silver composite membranes with a brick-like structure and high-performance electromagnetic-interference shielding," *RSC Advances*, 10.1039/C9RA06399D vol. 9, no. 51, pp. 29636–29644, 2019, doi: 10.1039/C9RA06399D.
- Xu, H. *et al.*, 2019. Lightweight Ti<sub>2</sub>CTx MXene/poly(vinyl alcohol) composite foams for electromagnetic wave shielding with absorption-dominated feature. *ACS Appl. Mater. Interfaces* 11 (10), 10198–10207. <https://doi.org/10.1021/acsnm.8b21671>.
- Xu, X. *et al.*, 2019. In situ confined bimetallic metal-organic framework derived nanostructure within 3D interconnected bamboo-like carbon nanotube networks for boosting electromagnetic wave absorbing performances. *ACS Appl. Mater. Interfaces* 11 (39), 35999–36009. <https://doi.org/10.1021/acsnm.9b14754>.
- Xu, J. *et al.*, 2020. N-doped reduced graphene oxide aerogels containing pod-like N-doped carbon nanotubes and FeNi nanoparticles for electromagnetic wave absorption. *Carbon* 159, 357–365. <https://doi.org/10.1016/j.carbon.2019.12.020>.
- Xu, J. *et al.*, 2020. General strategy for fabrication of N-doped carbon nanotube/reduced graphene oxide aerogels for dissipation and conversion of electromagnetic energy. *J. Mater. Chem. C* 8 (23), 7847–7857. <https://doi.org/10.1039/d0tc01236j>.
- Xu, M.-K. *et al.*, 2021. Electrically conductive Ti<sub>3</sub>C<sub>2</sub>Tx MXene/polypropylene nanocomposites with an ultralow percolation threshold for efficient electromagnetic interference shielding. *Indus. Eng. Chem. Res.* 60 (11), 4342–4350. <https://doi.org/10.1021/acs.iecr.1c00320>.
- Xu, J. *et al.*, 2021. Tailoring electronic properties and polarization relaxation behavior of MoS<sub>2</sub> monolayers for electromagnetic energy dissipation and wireless pressure micro-sensor. *Chem. Eng. J.* 425. <https://doi.org/10.1016/j.cej.2021.131700>.
- Xu, J. *et al.*, 2021. Lightweight, fire-retardant, and anti-compressed honeycombed-like carbon aerogels for thermal management and high-efficiency electromagnetic absorbing properties. *Small* 17 (33), e2102032.
- Xu, J. *et al.*, 2021. Multifunctional graphene microstructures inspired by honeycomb for ultrahigh performance electromagnetic interference shielding and wearable applications. *ACS Nano* 15 (5), 8907–8918. <https://doi.org/10.1021/acsnano.1c01552>.
- Xu, L., Wang, L., Zhang, W., Xue, J., Hou, S., 2022. "The reinforced electromagnetic interference shielding performance of thermal reduced graphene oxide films via polyimide pyrolysis". *ACS Omega* 7 (13), 10955–10962. <https://doi.org/10.1021/acsomega.1c06767>.
- J. Xu *et al.*, "Recent advances in 2D MXenes: preparation, intercalation and applications in flexible devices," *Journal of Materials Chemistry A*, 10.1039/D1TA03070A vol. 9, no. 25, pp. 14147–14171, 2021, doi: 10.1039/D1TA03070A.
- Yan, F. *et al.*, 2018. Growth of CoFe<sub>2</sub>O<sub>4</sub> hollow nanoparticles on graphene sheets for high-performance electromagnetic wave absorbers. *J. Mater. Chem. C* 6 (47), 12781–12787. <https://doi.org/10.1039/c8tc04222e>.
- Yan, F. *et al.*, 2018. An ultra-small NiFe<sub>2</sub>O<sub>4</sub> hollow particle/graphene hybrid: fabrication and electromagnetic wave absorption property. *Nanoscale* 10 (6), 2697–2703. <https://doi.org/10.1039/c7nr08305j>.
- Yan, F. *et al.*, 2018. Enhanced electromagnetic wave absorption induced by void spaces in hollow nanoparticles. *Nanoscale* 10 (39), 18742–18748. <https://doi.org/10.1039/c8nr07338d>.
- Yang, J. *et al.*, 2013. Two-dimensional hybrid nanosheets of tungsten disulfide and reduced graphene oxide as catalysts for enhanced hydrogen evolution. *Angew. Chem. Int. Ed.* 52 (51), 13751–13754. <https://doi.org/10.1002/anie.201307475>.
- Yang, Y. *et al.*, 2018. Fe<sub>3</sub>O<sub>4</sub>@LAS/RGO composites with a multiple transmission-absorption mechanism and enhanced electromagnetic wave absorption performance. *Chem. Eng. J.* 352, 510–518. <https://doi.org/10.1016/j.cej.2018.07.064>.
- Yang, R. *et al.*, 2021. Ultrathin, lightweight, and flexible CNT buckypaper enhanced using MXenes for electromagnetic interference shielding. *Nano-Micro Lett.* 13 (1), 66. <https://doi.org/10.1007/s40820-021-00597-4>.
- Yang, W., Zhao, Q., Zhou, Y., Cui, Z., Liu, Y., 2022. Research progress of metal organic frameworks/carbon-based composites for microwave absorption. *Adv. Eng. Mater.* 24 (4), 2100964. <https://doi.org/10.1002/adem.202100964>.
- Yin, H. *et al.*, 2020. "2D foaming of ultrathin MXene sheets with highly conductive silver nanowires for wearable electromagnetic interference shielding applications owing to multiple reflections within created free space". *Nano Futures* 4, (3). <https://doi.org/10.1088/2399-1984/ab92f5> 035002.
- Yin, G., Wang, Y., Wang, W., Yu, D., 2020. Multilayer structured PANI/MXene/CF fabric for electromagnetic interference shielding constructed by layer-by-layer strategy. *Colloids Surf., A: Physicochem. Eng. Asp.* 601,. <https://doi.org/10.1016/j.colsurfa.2020.125047> 125047.
- Yu, J., Li, Y., Xu, X., Duan, G., Li, Y., Zhou, W., 2021. Rambutan-like Nb<sub>2</sub>O<sub>5</sub>@SHCs microspheres for improved microwave absorption performance. *Compos. Commun.* 24. <https://doi.org/10.1016/j.coco.2021.100643>.
- Yu, J., Li, Y., Duan, G., Wen, P., Zhou, W., 2022. Bio-templated fabrication of chain-spherical V<sub>2</sub>O<sub>5</sub>/C composites from dandelion fiber for high-efficiency electromagnetic wave absorption. *Vacuum* 195. <https://doi.org/10.1016/j.vacuum.2021.110683>.
- Yuan, H., Yan, F., Li, C., Zhu, C., Zhang, X., Chen, Y., 2018. Nickel nanoparticle encapsulated in few-layer nitrogen-doped graphene supported by nitrogen-doped graphite sheets as a high-performance electromagnetic wave absorbing material. *ACS Appl Mater Interfaces* 10 (1), 1399–1407. <https://doi.org/10.1021/acsnm.7b15559>.
- Yun, T. *et al.*, 2020. Electromagnetic shielding of monolayer MXene assemblies. *Adv. Mater.* 32 (9), 1906769. <https://doi.org/10.1002/adma.201906769>.
- A. Zamanian, "Electromagnetic Radiation and Human Health : A Review of Sources and Effects By," 2005
- Zang, Y. *et al.*, 2015. Microwave absorption enhancement of rectangular activated carbon fibers screen composites. *Compos. B Eng.* 77, 371–378. <https://doi.org/10.1016/j.compositesb.2015.03.059>.
- Zeng, Z. *et al.*, 2020. Nanocellulose-MXene biomimetic aerogels with orientation-tunable electromagnetic interference shielding performance. *Adv. Sci.* 7 (15), 2000979. <https://doi.org/10.1002/advs.202000979>.
- Zeng, Z.-H. *et al.*, 2022. Porous and ultra-flexible crosslinked MXene/polyimide composites for multifunctional electromagnetic interference shielding. *Nano-Micro Lett.* 14 (1), 59. <https://doi.org/10.1007/s40820-022-00800-0>.
- Zhan, Y. *et al.*, 2021. Superhydrophobic and flexible silver nanowire-coated cellulose filter papers with sputter-deposited nickel nanoparticles for ultrahigh electromagnetic interference shielding. *ACS Appl. Mater. Interfaces* 13 (12), 14623–14633. <https://doi.org/10.1021/acsnm.1c03692>.
- Zhan, Y. *et al.*, 2021. Lightweight and self-healing carbon nanotube/acrylic copolymer foams: toward the simultaneous enhancement of electromagnetic interference shielding and thermal insulation. *Chem. Eng. J.* 417,. <https://doi.org/10.1016/j.cej.2021.129339> 129339.
- Zhang, X. *et al.*, 2018. Hollow N-doped carbon polyhedron containing CoNi alloy nanoparticles embedded within few-layer N-doped

- graphene as high-performance electromagnetic wave absorbing material. *ACS Appl Mater Interfaces* 10 (29), 24920–24929. <https://doi.org/10.1021/acsami.8b07107>.
- Zhang, X. et al, 2019. Novel solvothermal preparation and enhanced microwave absorption properties of Ti<sub>3</sub>C<sub>2</sub>T<sub>x</sub> MXene modified by in situ coated Fe<sub>3</sub>O<sub>4</sub> nanoparticles. *Appl. Surf. Sci.* 484, 383–391. <https://doi.org/10.1016/j.apsusc.2019.03.264>.
- Zhang, X. et al, 2019. Three dimensional graphene-supported nitrogen-doped carbon nanotube architectures for attenuation of electromagnetic energy. *J. Mater. Chem. C* 7 (38), 11868–11878. <https://doi.org/10.1039/c9tc04191e>.
- Zhang, X. et al, 2019. Large-scale synthesis of three-dimensional reduced graphene oxide/nitrogen-doped carbon nanotube hetero-nanostructures as highly efficient electromagnetic wave absorbing materials. *ACS Appl. Mater. Interfaces* 11 (42), 39100–39108. <https://doi.org/10.1021/acsami.9b13751>.
- Zhang, X. et al, 2019. Metal organic framework-derived three-dimensional graphene-supported nitrogen-doped carbon nanotube spheres for electromagnetic wave absorption with ultralow filler mass loading. *Carbon* 155, 233–242. <https://doi.org/10.1016/j.carbon.2019.08.074>.
- Zhang, X. et al, 2019. Interface-induced enhanced electromagnetic wave absorption property of metal-organic frameworks wrapped by graphene sheets. *J. Alloy. Compd.* 780, 718–726. <https://doi.org/10.1016/j.jallcom.2018.11.411>.
- Zhang, Y. et al, 2020. Nacre-inspired tunable electromagnetic interference shielding sandwich films with superior mechanical and fire-resistant protective performance. *ACS Appl. Mater. Interfaces* 12 (5), 6371–6382. <https://doi.org/10.1021/acsami.9b18750>.
- Zhang, X. et al, 2020. Flexible MXene-decorated fabric with interwoven conductive networks for integrated Joule heating, electromagnetic interference shielding, and strain sensing performances. *ACS Appl. Mater. Interfaces* 12 (12), 14459–14467. <https://doi.org/10.1021/acsami.0c01182>.
- Zhang, X. et al, 2020. CoNi nanoparticles encapsulated by nitrogen-doped carbon nanotube arrays on reduced graphene oxide sheets for electromagnetic wave absorption. *Chem. Eng. J.* 383. <https://doi.org/10.1016/j.cej.2019.123208>.
- Zhang, C. et al, 2020. Two-dimensional transition metal carbides and nitrides (MXenes): synthesis, properties, and electrochemical energy storage applications. *Energy Environ. Mater.* 3 (1), 29–55. <https://doi.org/10.1002/eeem2.12058>.
- Zhang, J. et al, 2021. Design and synthesis strategies: 2D materials for electromagnetic shielding/absorbing. *Chem. –Asian J.* 16 (23), 3817–3832. <https://doi.org/10.1002/asia.202100979>.
- Zhang, X. et al, 2021. N-doped carbon nanotube arrays on reduced graphene oxide as multifunctional materials for energy devices and absorption of electromagnetic wave. *Carbon* 177, 216–225. <https://doi.org/10.1016/j.carbon.2021.02.085>.
- Zhang, Y. et al, 2021. Ti<sub>3</sub>C<sub>2</sub>T<sub>x</sub>/rGO porous composite films with superior electromagnetic interference shielding performances. *Carbon* 175, 271–280. <https://doi.org/10.1016/j.carbon.2020.12.084>.
- Zhang, Z. et al, 2021. The recent progress of MXene-based microwave absorption materials. *Carbon* 174, 484–499. <https://doi.org/10.1016/j.carbon.2020.12.060>.
- Zhang, Y. et al, 2022. rGO/MXene sandwich-structured film at spunlace non-woven fabric substrate: application to EMI shielding and electrical heating. *J. Colloid Interface Sci.* 614, 194–204. <https://doi.org/10.1016/j.jcis.2022.01.030>.
- Zhang, Y. et al, 2022. Strong and conductive reduced graphene oxide-MXene porous films for efficient electromagnetic interference shielding. *Nano Res.* 15 (6), 4916–4924. <https://doi.org/10.1007/s12274-022-4311-9>.
- Zhang, X. et al, 2022. Flexible and waterproof nitrogen-doped carbon nanotube arrays on cotton-derived carbon fiber for electromagnetic wave absorption and electric-thermal conversion. *Chem. Eng. J.* 433. <https://doi.org/10.1016/j.cej.2021.133794>.
- Zhang, S. et al, 2022. Two-dimensional nanomaterials for high-efficiency electromagnetic wave absorption: an overview of recent advances and prospects. *J. Alloy. Compd.* 893. <https://doi.org/10.1016/j.jallcom.2021.162343>.
- Zhang, M., Cao, M.-S., Shu, J.-C., Cao, W.-Q., Li, L., Yuan, J., 2021. Electromagnetic absorber converting radiation for multi-function. *Mater. Sci. Eng.: R: Rep.* 145. <https://doi.org/10.1016/j.mser.2021.100627>.
- Zhang, Y., Gu, J., 2022. A perspective for developing polymer-based electromagnetic interference shielding composites. *Nano-Micro Lett.* 14 (1), 89. <https://doi.org/10.1007/s40820-022-00843-3>.
- Zhang, L., Mei, S., Huang, K., Qiu, C.-W., 2016. Advances in full control of electromagnetic waves with metasurfaces. *Adv. Opt. Mater.* 4 (6), 818–833. <https://doi.org/10.1002/adom.201500690>.
- Zhang, M., Wang, X.-X., Cao, W.-Q., Yuan, J., Cao, M.-S., 2019. Electromagnetic functions of patterned 2D materials for micro-nano devices covering GHz, THz, and optical frequency. *Adv. Opt. Mater.* 7 (19), 1900689. <https://doi.org/10.1002/adom.201900689>.
- Zhang, Y., Zhou, W., Chen, H., Duan, G., Luo, H., Li, Y., 2021. Facile preparation of CNTs microspheres as improved carbon absorbers for high-efficiency electromagnetic wave absorption. *Ceram. Int.* 47 (7), 10013–10018. <https://doi.org/10.1016/j.ceramint.2020.12.147>.
- Zhang, Y., Zhang, J., Wang, X., Liu, Z.-H., Bi, S., Hou, Z.-L., 2022. Metal-organic frameworks derived carbon nanotube and carbonyl iron composite materials for broadband microwave absorbers with a wide filling range. *J. Magn. Magn. Mater.* 555. <https://doi.org/10.1016/j.jmmm.2022.169391>.
- X. Zhang *et al.*, “Identification of the Intrinsic Dielectric Properties of Metal Single Atoms for Electromagnetic Wave Absorption,” *Nano-Micro Letters*, vol. 14, no. 1, 2021, doi: 10.1007/s40820-021-00773-6.
- Zhao, S. et al, 2018. Highly electrically conductive three-dimensional Ti<sub>3</sub>C<sub>2</sub>T<sub>x</sub> MXene/reduced graphene oxide hybrid aerogels with excellent electromagnetic interference shielding performances. *ACS Nano* 12 (11), 11193–11202.
- Zhao, S. et al, 2018. Highly electrically conductive three-dimensional Ti<sub>3</sub>C<sub>2</sub>T<sub>x</sub> MXene/reduced graphene oxide hybrid aerogels with excellent electromagnetic interference shielding performances. *ACS Nano* 12 (11), 11193–11202. <https://doi.org/10.1021/acsnano.8b05739>.
- Zhao, Y. et al, 2021. Structural engineering of hierarchical aerogels comprised of multi-dimensional gradient carbon nanoarchitectures for highly efficient microwave absorption. *Nano-Micro Lett.* 13 (1), 144. <https://doi.org/10.1007/s40820-021-00667-7>.
- Zhao, B., Zhao, C., Li, R., Hamidinejad, S.M., Park, C.B., 2017. Flexible, ultrathin, and high-efficiency electromagnetic shielding properties of poly(Vinylidene Fluoride)/carbon composite films. *ACS Appl. Mater. Interfaces* 9 (24), 20873–20884. <https://doi.org/10.1021/acsami.7b04935>.
- Zheng, Y. et al, 2021. Reduced graphene oxide-supported boron and nitrogen co-doped carbon nanotubes with embedded cobalt nanoparticles for absorption of electromagnetic wave. *J. Alloy. Compd.* 865. <https://doi.org/10.1016/j.jallcom.2021.158967>.
- Zheng, J. et al, 2022. From waste to wealth: crumb rubber@carbon nanotube/Fe<sub>3</sub>O<sub>4</sub> composites towards highly effective electromagnetic microwave absorption with wide bandwidth. *Diam. Relat. Mater.* 126. <https://doi.org/10.1016/j.diamond.2022.109089>.
- Zhi, W.-J., Wang, L.-F., Hu, X.-J., 2017. Recent advances in the effects of microwave radiation on brains. *Mil. Med. Res.* 4 (1), 29. <https://doi.org/10.1186/s40779-017-0139-0>.
- Zhou, B. et al, 2020. Flexible, robust, and multifunctional electromagnetic interference shielding film with alternating cellulose nanofiber and MXene layers. *ACS Appl. Mater. Interfaces* 12 (4), 4895–4905. <https://doi.org/10.1021/acsami.9b19768>.
- Zhou, Z.-H. et al, 2020. Structuring hierarchically porous architecture in biomass-derived carbon aerogels for simultaneously achieving high electromagnetic interference shielding effectiveness and

- high absorption coefficient. *ACS Appl. Mater. Interfaces* 12 (16), 18840–18849. <https://doi.org/10.1021/acsami.0c01190>.
- Zhou, Z., Liu, J., Zhang, X., Tian, D., Zhan, Z., Lu, C., 2019. Ultrathin MXene/calcium alginate aerogel film for high-performance electromagnetic interference shielding. *Adv. Mater. Interfaces* 6 (6), 1802040. <https://doi.org/10.1002/admi.201802040>.
- Zhou, Q., Qian, K., Fang, J., Miao, M., Cao, S., Feng, X., 2020. UV-light modulated Ti<sub>3</sub>C<sub>2</sub>T<sub>x</sub> MXene/g-C<sub>3</sub>N<sub>4</sub> heterojunction film for electromagnetic interference shielding. *Compos. A Appl. Sci. Manuf.* 134. <https://doi.org/10.1016/j.compositesa.2020.105899> 105899.
- M. Zhou *et al.*, “Sustainable wood-based composites for microwave absorption and electromagnetic interference shielding,” *Journal of Materials Chemistry A*, 10.1039/D0TA08372K vol. 8, no. 46, pp. 24267–24283, 2020, doi: 10.1039/D0TA08372K.
- Zhu, Y., Bai, B., Ding, E., Bi, S., Liu, W., Zhang, L., 2022. Enhanced electromagnetic interference shielding performance of geopolymer nanocomposites by incorporating carbon nanotubes with controllable silica shell. *Ceram. Int.* 48 (8), 11103–11110. <https://doi.org/10.1016/j.ceramint.2021.12.330>.
- Zhu, H., Yang, Y., Sheng, A., Duan, H., Zhao, G., Liu, Y., 2019. Layered structural design of flexible waterborne polyurethane conductive film for excellent electromagnetic interference shielding and low microwave reflectivity. *Appl. Surf. Sci.* 469, 1–9. <https://doi.org/10.1016/j.apsusc.2018.11.007>.
- Zhu, C., Zhang, S., Sun, Y., Chen, Y., 2017. Incorporation of CoO@Co yolk-shell nanoparticles and ZnO nanoparticles with graphene sheets as lightweight and high-performance electromagnetic wave absorbing material. *J. Alloy. Compd.* 711, 552–559. <https://doi.org/10.1016/j.jallcom.2017.04.061>.